Alma Mater Studiorum – Università di Bologna

DOTTORATO DI RICERCA

MODELLISTICA FISICA PER LA PROTEZIONE
DELL'AMBIENTE

Ciclo XXI

Settore scientific disciplinare GEO/10

Assessment of Tsunami Hazard in Central America

Presentata da: BEATRIZ BRIZUELA REYES

Coordinatore Dottorato **Relatore**

Prof. Ezio Todini **Prof. Stefano Tinti**

Esame finale anno 2009

ABSTRACT

Tsunamis are not considered a major hazard in Central America, people are not aware of that risk and recent tsunami events recorded in the area have been forgotten. Despite this, recent studies have established that Central America is a moderately tsunamigenic zone and that is affected mainly by tsunamis triggered by earthquakes, especially at the Pacific coast where the Middle American Trench runs parallel to the coast. The most recent event occurred on the 2nd of September 1992 offshore the Nicaraguan coast, the run-up values measured at that time varied between 2 and 6 metres. This event has led to several studies including the compilation of a tsunami catalogue for the region, some empirical, statistical and deterministic studies. In this thesis, a statistical and deterministic analysis is followed. The statistical approach aimed to estimate the Gutenberg-Richter coefficient of the region in order to know the annual rate of occurrence of tsunamigenic earthquakes and their corresponding return period. A hybrid analysis, probabilistic and deterministic, has been use to compute the run-up distribution along the coast corresponding to a given annual rate of occurrence of a tsunamigenic earthquake. A further scenario-based analysis has been undertaken consisting in the numerical simulations of six historical earthquakes that were carried out by means of the UBO-TSUFE MODEL.

ASSESSMENT OF TSUNAMI HAZARD IN CENTRAL AMERICA

INDEX

1. INTRODUCTION

1.1. MOTIVATION FOR THE STUDY

Central America is located at the southernmost isthmian portion of the North American continent, its main land lays on the North American Plate and on the Caribbean Plate whereas its Pacific coast runs parallel to the Middle American Trench, where the Cocos Plate subducts beneath the Caribbean Plate and the Nazca Plate subducts beneath the South American Plate.

The region covers an area of approximately 524,000 km² and its population is about 40.5 million people. The countries belonging to the region are: Guatemala, Belice, El Salvador, Honduras, Nicaragua, Costa Rica and Panama. See figure 1.1.

Figure 1.1: Map of Central America.

Earthquakes, landslides, mudslides and hurricanes are among the most known natural hazards. Tsunamis, on the other hand, are not considered a major hazard in Central America, people are not aware that they could be at risk and even recent tsunami events that occurred in the area have been forgotten. Despite this, recent studies have established that Central America is a moderately tsunamigenic zone.

The most recent event occurred on the 2nd of September 1992 offshore the Nicaraguan coast, the run-up values measured at that time varied between 2 and 6 metres, leaving about 170 fatalities and 13,000 homeless, see figure 1.2. This event has led to several studies including the compilation of a tsunami catalogue for the region and some empirical, statistical and deterministic tsunami assessments, and has also increase the tsunami awareness of the authorities. The studies performed after 1992 revealed that the Pacific coast of Central America is prone to be hit by tsunami waves triggered mainly by earthquakes; nevertheless, no tsunami warning system has been implemented in the region. The need of setting tsunami early warning systems to save lives in case of tsunami has been recently reaffirmed by the disastrous 26 December 2004 Asian event.

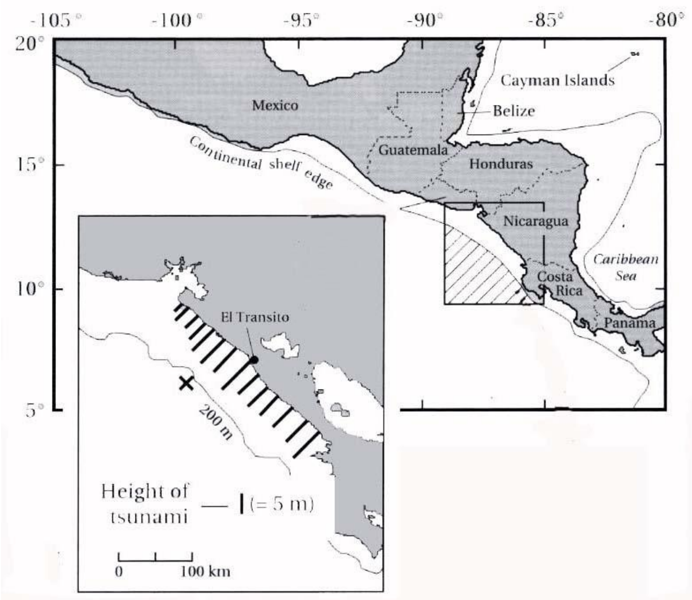

Figure 1.2: Run-up heights of the 1992 Nicaraguan Tsunami.

(Bryant, E., [2000])

The aim of this thesis is to estimate the wave height values expected at the coast, given an earthquake with magnitude and epicentral coordinates, using a combination of statistic and deterministic approaches. The statistical approach estimates the probability of occurrence per year of earthquakes, then the number of expected tsunamis can be estimated, considering that tsunamis in the region are mainly triggered by earthquakes exceeding a threshold magnitude and with epicentres near the coast. The magnitude is used as input value in empirical relations in order to define the characteristics of the rupture mechanism, the seismic moment and the maximum dislocation of the seafloor. These values are used as initial conditions for the deterministic part of the study, which aims at estimating the wave height values expected at the coast. This procedure allows us to make an estimation of the minimum magnitude capable to trigger a threshold wave height at the coast, and when this value is associated to the number of earthquakes likely to occur per year, then the number of tsunamigenic earthquakes expected per year that could trigger tsunamis with wave heights exceeding the threshold value can be estimated.

1.2. DISSERTATION OUTLINE

This thesis can be divided in seven main chapters. The first chapter contains the introduction and dissertation outline of the study.

The second chapter of the document contains some general terminology and causes of tsunamis. Chapter 3 contains the geological setting, tectonics, bathymetry and tsunamigenic sources of Central America. Historical information and the tsunami catalogue of Central America is presented in Chapter 4.

A detailed description of the tsunami hazard approach adopted in this thesis is presented in Chapter 5, followed by the results of the analysis and the conclusions presented in Chapter 6 and 7, respectively.

2. TSUNAMIS

2.1. GENERAL CONCEPTS AND DEFINITIONS

In general terms, tsunamis[1] are train waves that are sinusoidal shaped in deep water but become peak shaped in shallower water. The amplitude of each wave increase when it approaches the shoreline; for example, in the open sea a tsunami wave reaches about 0.3 to 0.6 meters (UNESCO, [1991]), whereas near the coastline can reach several meters depending on the coastline configuration and the bathymetry. In deep waters tsunami waves can reach velocities higher than 700 km/h and their wavelength values can be higher than 750 km (González, F. [1999]). The velocity of the waves decreases as the tsunami approaches shallow waters taking values as low as 36km/h near shore (Bryant, E., [2001]).

Tsunamis are water waves generated by displacement of the seafloor (Fernández, M., et al, [2004]). The displacement is usually triggered by earthquakes, submarine or terrestrial landslides, volcanic eruptions or meteorite impacts. Tsunami waves can be generated in oceans, seas, bays, fiords, lakes or reservoirs (Bryant, E. [2001]).

The term tsunami was adopted by the scientific community in 1963; previously, these phenomena were called “tidal waves”, a term not accurate, given that tides are not related to tsunamis, even if the impact of tsunami waves on the coast depends on the water level at the arriving time. Another term used before 1963 was “seismic sea waves”, again, another not accurate name given that tsunamis are not only triggered by seismic events.

Tsunami waves usually flood coastal areas, the flooding extent depends on the amplitude of the waves near the shore, coastal configuration and use of coastal land. The main parameters that describe tsunamis are *run-up* and *inland penetration* which describe the wave height at furthermost dry lands and determine the inundation area, respectively. The run-up is the distance between the elevation of water penetration and the tidal level at the arriving time (see figure 2.1) whereas the inland penetration is the distance from the shoreline to the furthermost flooded point. Run-up and inland penetration values vary from point to point along the coast, the values measured are usually shown in the so-called run-up distribution maps (see figure 2.2). *Travel time* is another tsunami parameter and it is “ the time required for the first tsunami wave to propagate from its source to a given point on a coastline” (ITIC/UNESCO, [http://www.shoa.cl/oceano/itic/frontpage.html]). Travel time is shown in maps containing *isochrones,* that are lines of equal tsunami travel time starting from the source to distant points, as shown in Fig. 2.3.

---

[1] From the Japanese (tsu) harbour (nami) wave.

Tsunami run-up is measured using tidal gauges at different points of the coast (see figure 2.4), whereas inland penetration is measured through field survey some time after the tsunami occurred by the observation of water traces in buildings, or vegetation destroyed by salty water.

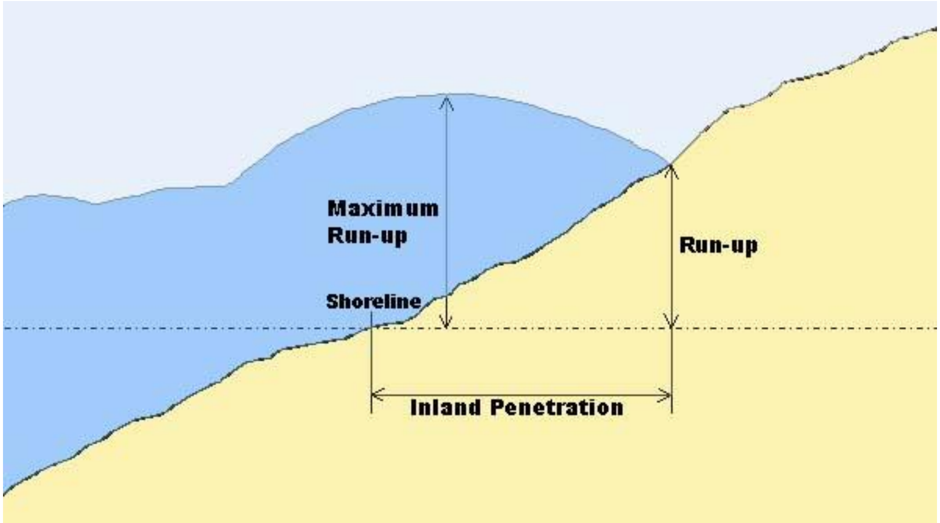

Figure 2.1: Tsunami Run-up and Inland Penetration.

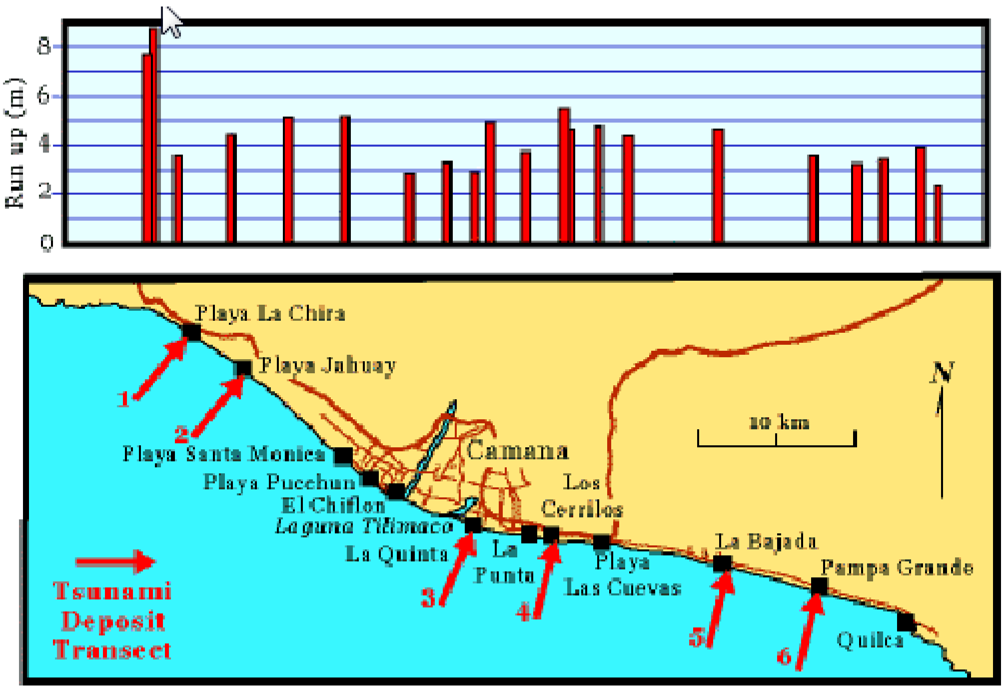

Figure 2.2: Distribution of Tsunami Run-up.

[http://walrus.wr.usgs.gov/peru2/images/transect.map.2.gif]

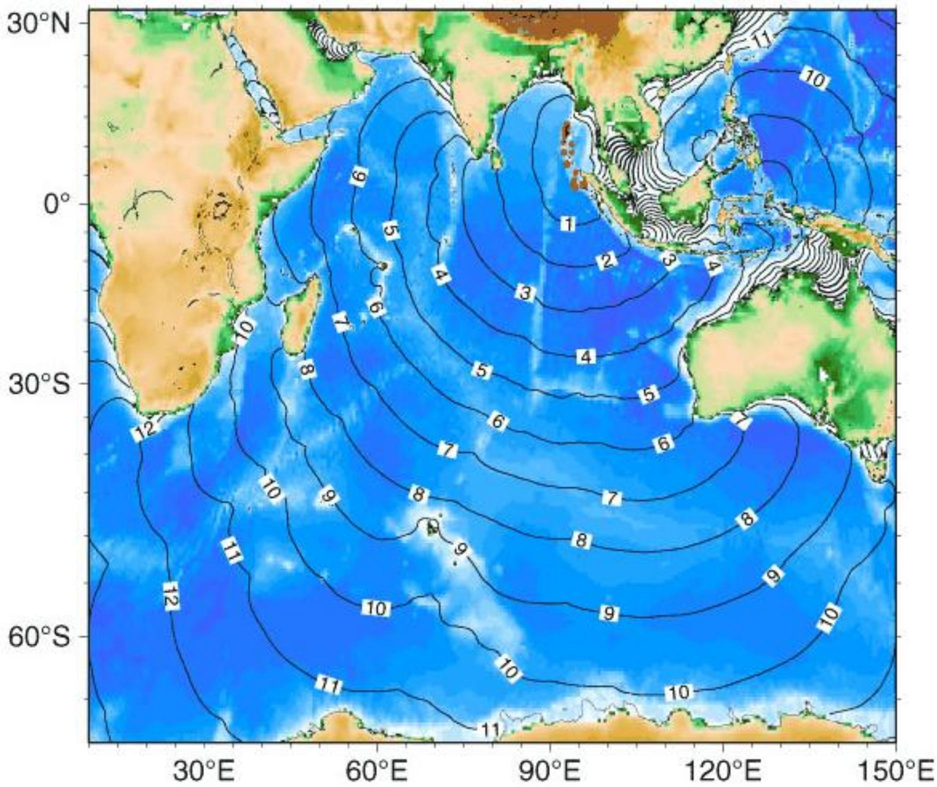

Figure 2.3: Travel time tsunami maps.

[http://www.indiana.edu/~pepp/earthquakes/images/sumatra12_26_04/tsunami_traveltime_region.jpeg]

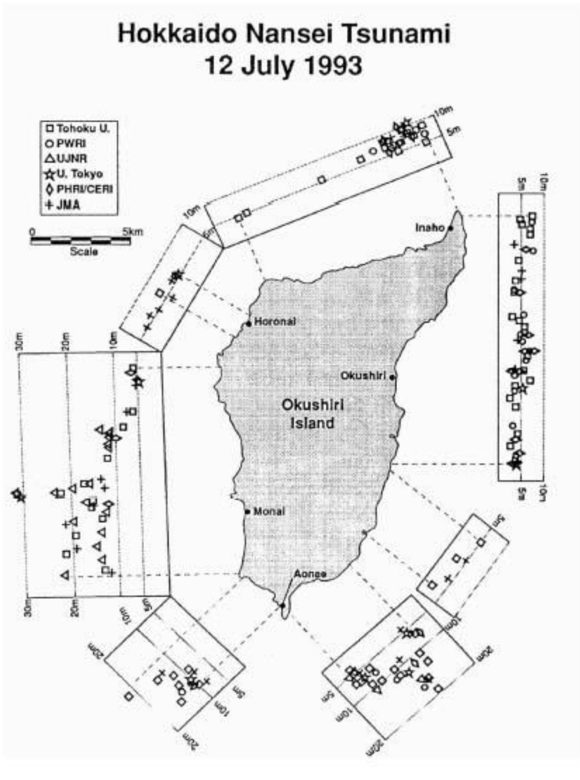

Figure 2.4: Vertical run-up measures map of the 12 July 1993 Hokkaido Nansei (Japan) Tsunami.

[http://www.shoa.cl/oceano/itic/frontpage.html]

There are several factors that have influence on the run-up and inland penetration distribution. The run-up values depend on the bathymetry, coastal topography and the volume of water involved on the seafloor displacement. The inland penetration depends on the factors listed before as well as the coastal surface roughness and the use of land of the coast affected.

Tsunamis are generally sized using the Imamura-Iida scale (see table 2.1), the magnitude of an event under this scale depends on the observed run-up values and on the damaged caused. The tsunami magnitude (m) takes values between -1 and 4, and it follows the relation $m = \log_2 H$, where H is the maximum run up value registered in a coastline near the tsunami generating area (ITIC/UNESCO, [http://www.shoa.cl/oceano/itic/frontpage.html]).

Table 2.1 Tsunami Magnitude Scale Imamura-Iida.

(Molina, [1997])

m	Hmax	Hmin	Damage
4	30	30	Considerable damage along more than 500 km of coastline
3	20	10	Considerable damage along more than 400 km of coastline
2	6	4	Damage and lives lost in certain landward areas
1	2	2	Coastal and ship damage
0	1	1	Very small damage
-1	0.5	0.5	None

There are several scales to estimate the tsunami intensity. One of this scales is the Sieberg-Ambraseys Tsunami Intensity scale (see table 2.2), which is a six-point intensity scale. The original scale was proposed by August Sieberg 1927 and then modified by Nicolas Ambraseys in 1962 [http://geology.about.com/library/bl/bltsunamiscaleold.htm]. A new 12-point tsunami intensity scale was proposed in 2001 by Gerassimos Papadopoulos and Fumihiko Imamura (see table 2.3), The tsunami intensity is established based on the effects of tsunamis on humans, objects including boats, and damage to buildings [http://geology.about.com/library/bl/bltsunamiscalenew.htm].

Table 2.2 Sieberg-Ambraseys Tsunami Intensity Scale.

[ITIC/UNESCO, Tsunami Glossary [http://www.shoa.cl/oceano/itic/frontpage.html]

Intensity		Damage description
1	Very light	Wave so weak as to be perceptible only on tide-gauge records.
2	Light	Wave noticed by those living along the shore and familiar with the sea.
3	Rather strong	Generally noticed. Flooding of gently sloping coasts. Light sailing vessels carried away on shore. Slight damage to light structures situated near the coasts. In estuaries reversal of the river flow some distance upstream.
4	Strong	Flooding of the shore to some depth. Light scouring on man-made ground. Embankments and dikes damaged. Light structures on the coast injured. Bid sailing and small ships drifted inland or carried out to the sea. Coasts littered with floating debris.
5	Very strong	General flooding of the shore to some depth. Quay-walls and solid structures near the sea damaged. Light structures destroyed. Severe scouring of cultivated land and littering of the coast with floating items and sea animals. With exception of big ships all other type of vessels carried inland or out to sea. Big bores in estuary rivers. Harbor works damaged. People drowned. Wave accompanied by strong roar.
6	Disastrous	Partial or complete destruction of made structures for some distance from the shore. Flooding of coasts to great depths. Big ships severely damaged. Trees uprooted or broken. Many casualties.

Tsunamis are also classified as local, regional and distant regarding to their propagation distance from their source. Local tsunami waves can propagate up to 100 km, whereas regional tsunami waves travel up to 700 km and distant tsunami waves more than 700km (Fernández, M. and Rojas, W., [2000]). Locally triggered tsunamis generally have shorter arrival times than regional and distant tsunamis and that could make them more dangerous, given that people usually cannot be warned on time; nowadays some countries are able to issue tsunami warnings within few minutes from their generation (Fernández, M., et al., [2004]).

Table 2.2 Papadopoulos-Imamura Tsunami Intensity Scale.

Intensity		Effects
I	Not felt	
II	Scarcely felt	a. Felt by few people onboard small vessels. Not observed on the coast. b. No effect. c. No damage.
III	Weak	a. Felt by most people onboard small vessels. Observed by a few people on the coast. b. No effect. c. No damage.
IV	Largely observed	a. Felt by all onboard small vessels and by few people onboard large vessels. Observed by most people on the coast. b. Few small vessels move slightly onshore. c. No damage.
V	Strong	a. Felt by all onboard large vessels and observed by all on the coast. Few people are frightened and run to higher ground. b. Many small vessels move strongly onshore, few of them crash into each other or overturn. Traces of sand layer are left behind on ground with favorable circumstances. Limited flooding of cultivated land. c. Limited flooding of outdoor facilities (such as gardens) of near-shore structures.
VI	Slightly damaging	a. Many people are frightened and run to higher ground. b. Most small vessels move violently onshore, crash strongly into each other, or overturn. c. Damage and flooding in a few wooden structures. Most masonry buildings withstand.
VII	Damaging	a. Many people are frightened and try to run to higher ground. b. Many small vessels damaged. Few large vessels oscillate violently. Objects of variable size and stability overturn and drift. Sand layer and accumulations of pebbles are left behind. Few aquaculture rafts washed away. c. Many wooden structures damaged, few are demolished or washed away. Damage of grade 1 and flooding in a few masonry buildings.
VIII	Heavily damaging	a. All people escape to higher ground, a few are washed away. b. Most of the small vessels are damaged, many are washed away. Few large vessels are moved ashore or crash into each other. Big objects are drifted away. Erosion and littering of the beach. Extensive flooding. Slight damage in tsunami-control forests and stop drifts. Many aquaculture rafts washed away, few partially damaged. c. Most wooden structures are washed away or demolished. Damage of grade 2 in a few masonry buildings. Most reinforced-concrete buildings sustain damage, in a few damage of grade 1 and flooding is observed.
IX	Destructive	a. Many people are washed away. b. Most small vessels are destroyed or washed away. Many large vessels are moved violently ashore, few are destroyed. Extensive erosion and littering of the beach. Local ground subsidence. Partial destruction in tsunami-control forests and stop drifts. Most aquaculture rafts washed away, many partially damaged. c. Damage of grade 3 in many masonry buildings, few reinforced-concrete buildings suffer from damage grade 2.
X	Very destructive	a. General panic. Most people are washed away. b. Most large vessels are moved violently ashore, many are destroyed or collide with buildings. Small boulders from the sea bottom are moved inland. Cars overturned and drifted. Oil spills, fires start. Extensive ground subsidence. c. Damage of grade 4 in many masonry buildings, few reinforced-concrete buildings suffer from damage grade 3. Artificial embankments collapse, port breakwaters damaged.
XI	Devastanting	b. Lifelines interrupted. Extensive fires. Water backwash drifts cars and other objects into the sea. Big boulders from sea bottom are moved inland. c. Damage of grade 5 in many masonry buildings. Few reinforced-concrete buildings suffer from damage grade 4, many suffer from damage grade 3.
XII	Completely devastating	c. Practically all masonry buildings demolished. Most reinforced-concrete buildings suffer from at least damage grade 3.

Tsunamis are events with long return periods. Despite this in the last decades the number of events observed and recorded has increased sharply. This could be due to the increase of instrumental measurement and also to the fact that coastal areas nowadays are populated and developed as residential or touristic areas. Tsunamis can be extremely devastating events, as the Sumatra 2004 event has shown. They cannot be avoided, but their impact could be diminished through tsunami hazard assessment, the setting of adequate tsunami warning systems and evacuation plans.

Following tsunami hazard assessment approaches, one should be able first to establish if a region is likely to be hit by tsunamis and which are the potential tsunamigenic sources, second to estimate the value of the tsunami parameters that could be reached, and third to indicate different levels of hazard within the region of study. There are two tsunami hazard assessment approaches; one is the statistical approach, which finds the tsunami probability occurrence law that governs a region and the other is the deterministic approach, which uses numerical modelling to estimate the tsunami parameters that a hypothetical event would produce in a scenario. As stated above, in this work we will use a hybrid probabilistic-deterministic approach. Tsunami warning systems and evacuation plans should be set once the results of the hazard assessment have established that the region is prone to tsunamis.

2.2. CAUSES OF TSUNAMIS

Tsunamis have occurred since remote times, however, not all of them have been recorded or reported. Tsunamis that have been recorded are called *historical tsunamis*, tsunamis that have not been recorded but there is geological evidence of their occurrence are called *paleotsunamis*. Compilations of paleotsunami and historical tsunami data are called *tsunami catalogues*. The catalogues are generally compiled for specific regions and they usually contain information regarding the places affected by tsunamis, run-up values, date, tsunami triggering mechanisms and sometimes descriptions of the damage caused by these events.

According to Bryant, E. [2001], the most tsunami-affected region world-wide has been the Pacific Ocean where more than 25 % of tsunamis have been recorded, closely followed by the East Indies at 20.3 % and the Japanese and Russian coasts at 18.6%. Taking the tsunamis recorded in the Pacific Ocean; earthquakes, volcanic eruptions and submarine landslides can be cited as the main causes of tsunami. Around 8% of these tsunamis have not been associated to any triggered mechanism. See in this regard information illustrated in figure 2.5 and table 2.4.

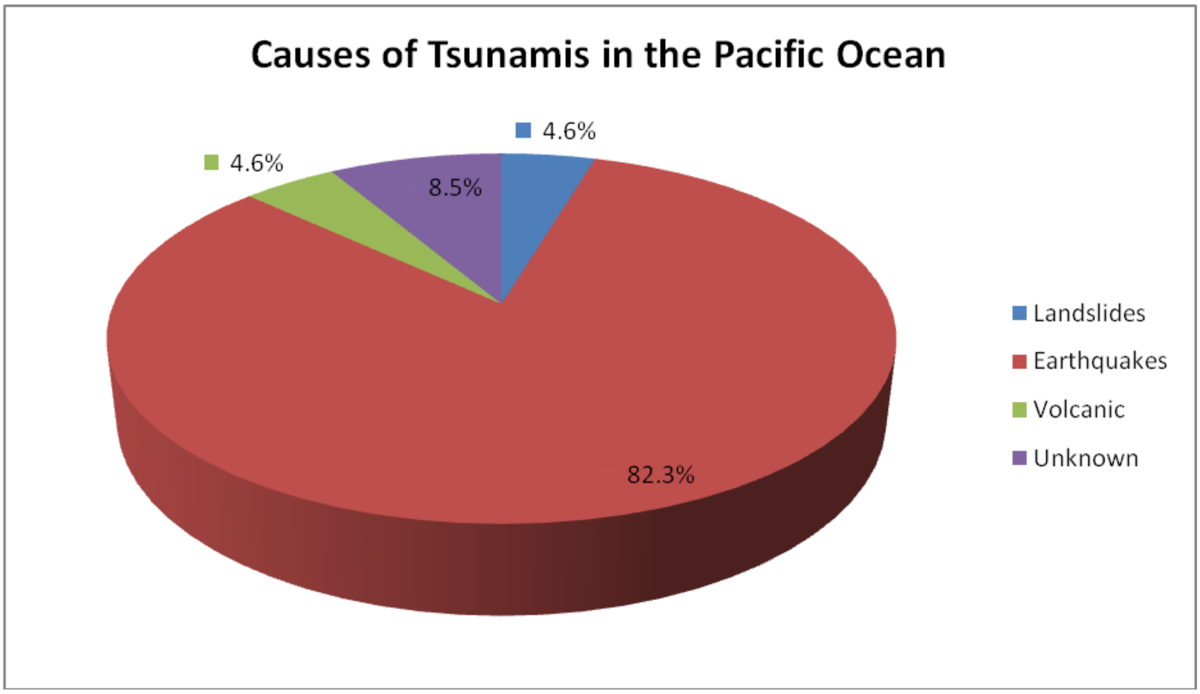

Figure 2.5: Generatioon mechanism of tsunamis in the Pacific Ocean.

(Data taken from: Bryant, E. [2001])

Table 2.4: Causes of Tsunami in the Pacific Ocean Region over the last 2,000 years

(Bryant, E. [2001])

Cause	Number of events	%	Number of deaths	%
Landslides	65	4.6	14,661	3.2
Earthquakes	1171	82.3	390,929	84.5
Volcanic	65	4.6	51,643	11.2
Unknown	121	8.5	5,364	1.1
	1422	100	462,597	100

Table 2.4 shows that in the Pacific Ocean earthquakes have been the most common cause of tsunamis at 82.3%, whereas volcanic eruptions and landslides have each triggered 4.6 %. The same pattern is observed when it comes to the number of deaths[2]: tsunamis triggered by earthquakes have caused around 84.5% of the total deaths, while tsunamis due to volcanic eruptions and landslides have caused around 11% and 3% of the deaths, respectively.

2.2.1 Tsunamigenic earthquakes.

Earthquakes are the most common tsunami-triggering mechanism world-wide. T*sunamigenic earthquakes* and *tsunami earthquakes* have caused around 82% of the total tsunamis registered in the Pacific Ocean (see table 2.4). Based on the statistics on tsunami occurrence in the Pacific basin shown in table 2.4 and on the cause associated to the events compiled in the Central American tsunami catalogue (see chapter 4), earthquakes will be the main tsunami triggering mechanism

[2] This information is based on data gathered before the 26 December 2004 Asian Tsunami.

considered for this study. The characteristics of tsunamigenic and tsunami earthquakes are described below.

Tsunamigenic earthquakes are all those earthquakes that generate tsunamis (Satake, et al, [1992]). These seismic events are usually located offshore or inland at small distances from the coast. Surface wave magnitudes (M_s) of tsunamigenic earthquakes generally exceed 6.5, their focal depth is commonly less than 100 km and their seismic mechanisms can be strike-slip, normal and thrust faulting (Bryant, E. [2001]), see [Fig. 2.6], though the efficiency of tsunami generation varies greatly from one mechanism to the other.

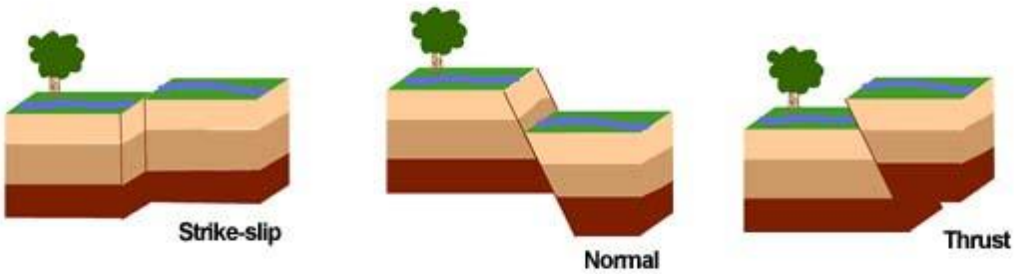

Figure 2.6: Main Fault Types.

(USGS [http://earthquake.usgs.gov/image_glossary/fault.html])

Tsunami earthquakes are offshore earthquakes that cause slow rupture along faults lines (Bryant, E. [2001]) and generate a large tsunami relative to its magnitude (ITC/UNESCO [http://www.shoa.cl/oceano/itic/frontpage.html]). Those earthquakes have very shallow foci, fault dislocations that reach several meters and fault surfaces smaller than for normal earthquakes. Tsunami earthquakes are slow earthquakes and their slippages occur more slowly than for normal earthquakes (ITC/UNESCO [http://www.shoa.cl/oceano/itic/frontpage.html]).

The main characteristics of the *tsunami earthquakes* are that first their surface wave magnitude M_s and their moment magnitude M_w differ considerably (about half a unit or more), being the latter generally higher than 7; second, tsunami earthquakes frequencies are low and their periods are usually greater than 100 seconds; and third, their seismic force describes a smooth curve along the time in contrast with the fast rupture earthquakes whose force peaks several times while the earthquake occurs. In some cases tsunami earthquakes are barely felt by the coastal inhabitants (Bryant, E., [2001]).

The 2 September 1992 Nicaraguan tsunami can be cited as an example of tsunami earthquake event. The earthquake was barely felt by coastal inhabitants although the surface wave magnitude was very high. Long waves reached coastal land (shaking the ground gently), whereas short waves dissipated quickly from the epicentre and did not reach the coast. Standard non-broadband seismometers did not record the long waves, that led to the conclusion that the waves had very long periods since that kind of equipment are able to record periods less than 20 seconds. The earthquake triggered waves whose run up reached between 2 and 6 meters (Bryant, E. [2001], Satake et al, [1993] and Gonzalez, F. [1999]).

Some earthquake parameters have been related to tsunami generation: the seismic moment, the earthquake mechanism and the depth. The seismic moment is computed as the product of the rigidity of the source's soil, the fault area and the average fault slip and it is an indicator of the tsunami size. The earthquake mechanism indicates the orientation of the earthquake and the direction of the fault slip. Events with large vertical slip are usually more effective triggering tsunamis than those with large horizontal slip. Finally, the earthquake's depth is also an important factor to consider in the generation of tsunamis. The shallower the event, the greater are the chances to trigger a big tsunami since a larger slip is likely to being produced at the sea floor (Bryant, E., [2001]).

2.2.2 Landslides.

Tsunamis caused purely by landslides have not been recorded directly, however, there are some historical events related to landslides for example the 9 July 1958 Lituya Bay (Alaska) event and the Grand Banks (Burin Peninsula, Canada) tsunami in 1929 (Bryant, E. [2001]).

Landslides are displacements of soil in coherent blocks that generally occur in steep slopes (see Fig. 2.7). These events may be due to earthquakes, soil instability or gravity effects due to the water saturation of the soil that occurs during raining seasons or flooding. If these events occur at the seafloor they are called submarine landslides.

Submarine landslides usually occur at slopes less steep than 1° at the seafloor (Ward, S. and Day S., [2002]). There are several causes of submarine landslides, among them the most common are earthquakes. The other causes found are: loading-unloading processes (over steep slopes) due to big tidal waves generated by meteorological phenomena, failure of non-consolidated or weak soil layers that lie beneath heavier layers of material, and finally, failure of soil due to the accumulation of gasses in voids when decomposition of organic sediments occurs (Bryant, E., [2001], Ward N. and Day S., [2002]).

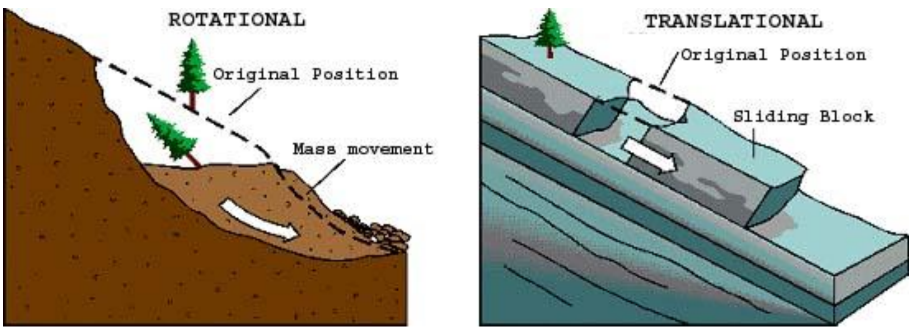

Figure 2.7: Rotational and translational landslides.

[www.milarium.com]

There are three processes related to landslides that are able to generate tsunami waves: first the sliding of soil blocks on steep slopes, second the disintegration of soil blocks that generates debris flows (see Fig. 2.8) and third the generation of turbidity currents that occur when water is involved in a debris flow. If the volume of material involved in any of those three processes is large enough, a tsunami is triggered. The size of tsunamis generated by landslides depends on the volume of material involved, the depth at which the landslides occurs and the sliding velocity of the material (Bryant, E., [2001]).

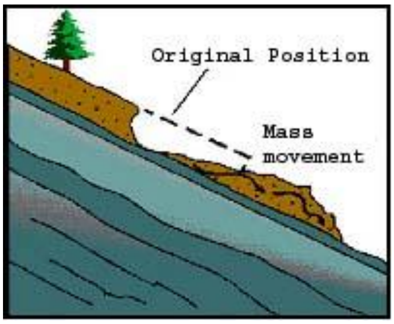

Figure 2.8: Terrestrial Debris flow.

[www.millanium.com]

2.2.3 Volcanic eruptions

Volcanic eruptions are also considered a cause of tsunami. They can trigger tsunamis depending on the location of the volcano with respect to the ocean, generally speaking, submarine volcanoes are more likely to cause tsunamis than those inland located in the vicinity of the ocean. Submarine volcanic eruptions can cause big tsunamis if the volcano lies up to 500 meters below the sea level. Eruptions of deeper volcanoes cause small tsunami waves that generally travel no more than 150 kilometres (Bryant, E., [2001]). However, the formation of a deep underwater volcanic caldera could trigger a large tsunami depending on the size of the caldera (Fernández, M. [written communication]).

Tsunamis due to volcanic eruptions can be triggered if underwater explosions occur when water penetrates into the volcano magma chamber becoming vapour, or also, when these explosions are big enough to generate a caldera, which is a large approximately circular, steep-walled basin of several kilometres in diameter (Skinner, B. and Porter, S. [1992]). The depression is then filled with water and that could propitiate the generation of waves due to the water displaced (Bryant, E., [2001]).

Tsunamis generated by surface volcanic eruptions are due to explosions and debris avalanches or lahars[3]. Inland volcanic explosions can generate tsunamis if they are close enough to large amounts of solid material in the ocean, for example if the volcano is located at about 20km from the coast (Fernández, M. [written communication]). If that is the case, pyroclastic flows can hit the ocean transferring energy or displacing water depending on the ash density. If the ash density is low, energy is transferred as the ash floats on the ocean generating a small wave. On the contrary, if the density is high, the ash submerges displacing water that can trigger a tsunami depending on the volume of material involved (Bryant, E., [2001]). Debris flows or lahars produced by inland volcanic eruptions can trigger tsunamis when large amount of transported material reaches the ocean. These avalanches can travel about 100km from the volcano and their speeds can reach 200km/h (Tarbuck, E. and Lutgens F., [2003]).

[3] Lahars are debris flows and/or mudflows produced by loose soil and rock flowing down the sides of a volcano.

3. GEOLOGICAL SETTING OF CENTRAL AMERICA

3.1. OVERVIEW

Geologically speaking, Central America can be divided in northern and southern Central America. Guatemala, Honduras, El Salvador and northern Nicaragua can be included in the northern portion, whereas southern Nicaragua, Costa Rica and Panama are considered the southern portion. Northern Central America has a continental style crust and it contains Palaeozoic or older rocks and sediments from the upper Palaeozoic, the Mesozoic and the Tertiary. A Cretaceous type crust composes the southern portion, and it has on top thick marine and tertiary volcanic sediments. This portion is, at the moment, a transition zone from pure oceanic to continental crust (Bommer, J. and Rodriguez, C., [2002]).

3.2. TECTONIC FEATURES

The Pacific coast of Central America runs parallel to the Middle America Trench, which is the zone where the Cocos plate subducts beneath the Caribbean plate. It has been established that the incoming plate along the Middle America trench was formed at similar ages although its morphology changes dramatically along the strike. The region is characterised by a smooth slope at the Nicaraguan coast, a very steep slope in Guatemala and a transition zone along the Salvadoran coast. The smooth slope is built of en-echelon terraces, whereas the steep slope contains several canyons and gullies. The transition zone can be described as rough terrain variable in width (Ranero, C., et al [2004]). Figure 3.1 shows approximate locations of tectonic plate boundaries in Central America.

There are basically three seismogenic sources at northern Central America. First the Cocos-Caribbean subduction zone, that produces the largest earthquakes in the region, and the Cocos-North American convergence zone. Second the North America-Caribbean interaction zone and third the upper crust seismicity along the quaternary volcanoes, as shown in Fig. 3.2. Southern Central America's seismicity is due to the interaction of four main tectonic plates and several microplates at their boundaries (See Fig. 3.1).

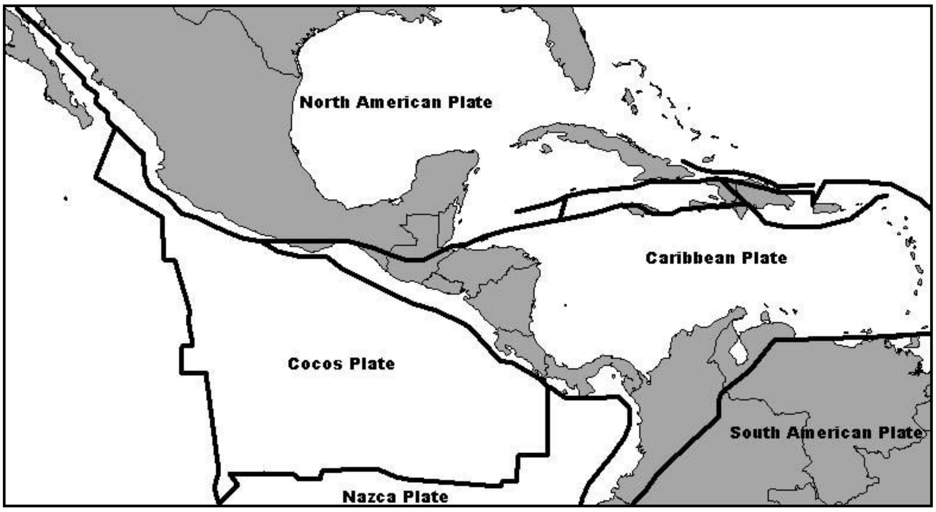

Figure 3.1: Tectonic Plates of Central America.

The subduction zone of Central America can be classified as intermediate, if compared with the *Mariana* and *Chilean* style. The Mariana subduction zone is characterised for having a very sharp dip with a highly extensional overriding zone (see Fig. 3.3) whereas the Chilean subduction zone presents a shallow dip and highly compressional overriding zone (see Fig. 3.2). The Central American trench is considered an intermediate stage between those subduction zones. It has a steep dip that shallows from south Nicaragua to north Guatemala and the overriding zone (the Caribbean Plate) is slightly extensional (Dewey, et al. [2004]).

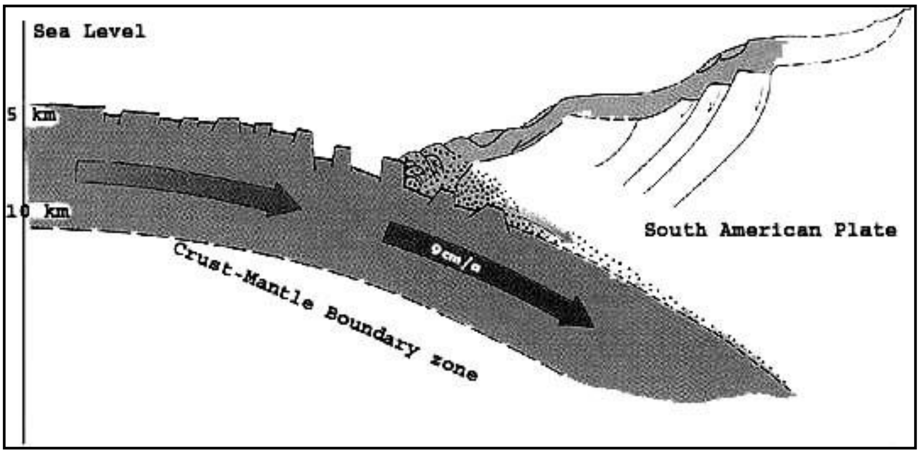

Figure 3.2: Chilean type Subduction Zone.

[http://www.margins.wustl.edu/Eugene.html]

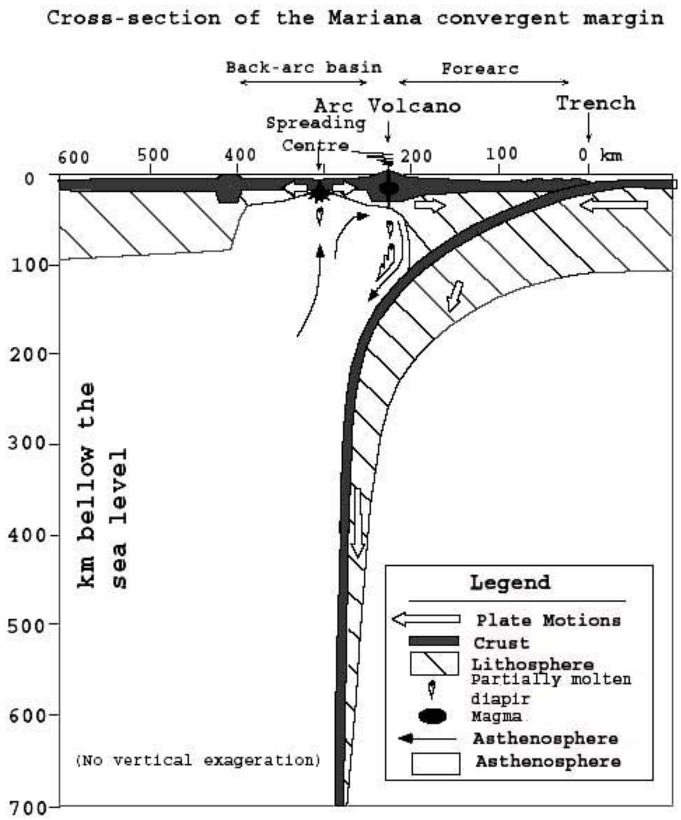

Figure 3.3: Mariana type Subduction Zone.

[http://www.margins.wustl.edu/Eugene.html]

Recent research have established the plate kinematics schemes of Central America through the use of GPS observations. The estimated velocity of motion of the plates is shown in figure 3.4. The North American plate moves to the south west at rates of about 21mm/yr, whereas the Caribbean plate moves at about 9mm/yr to the south east and the Cocos plates moves north east at approximately 70mm/yr. If the Cocos-Caribbean and North American junction were an ideal stable triple junction, the Cocos plate would tear as shown in figure 3.5a. The previous situation is not happening, since the Cocos plate seems to be mechanically stronger than the North American and Caribbean plates, which have to accommodate as shown in figure 3.5b. The implication of the situation described previously, is that the roll-back of Cocos plate's slab will be continuous along the Middle American Thrench, which also means that the forearc motion must be also continuous along the junction (Phipps Morgan, J., et al, [2008]).

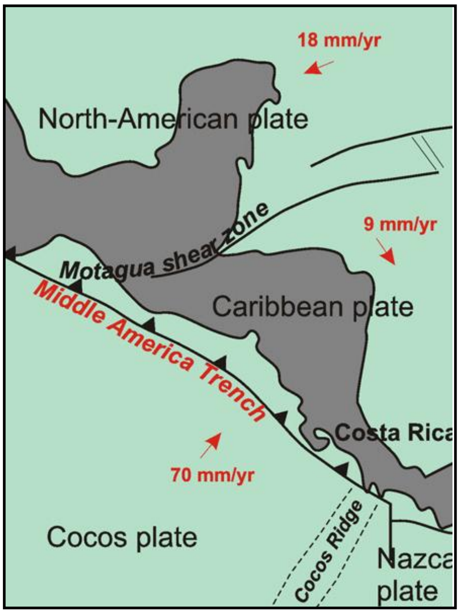

Figure 3.4: Velocity Rates of the Tectonic Plates of Central America
(Morgan, J., et al, [2008])

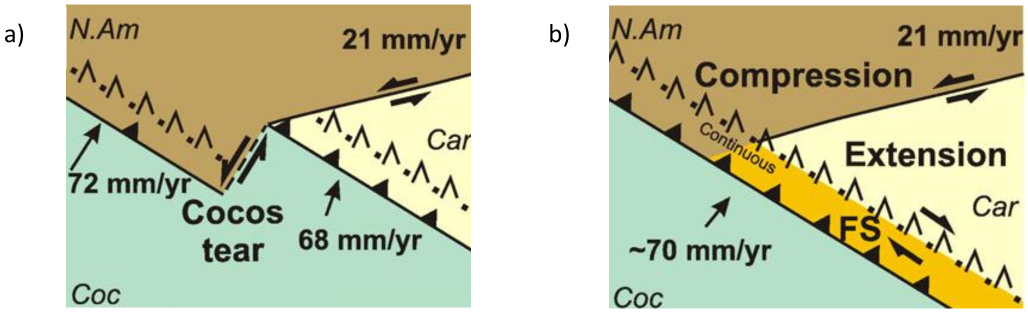

Figure 3.5: Junction of the Tectonic Plates of Central America. (a) Ideal situation: weak Cocos plate.
(b) Roll-back of the Cocos plate slab: Strong Cocos plate.
(Phipps Morgan, J., et al, [2008])

There is evidence that the tearing of the Cocos plate is being accommodated by deformation of the North American and Caribbean. There are some consequences of this deformation process, the first is that the North American plate will present compressive stress at the junction zone on its southern boundary with the Caribbean and Cocos plates (see figures 3.1). The second consequence is that segments of the arc within the Caribbean plate would be under arc-normal extension and depending on the rates of slab roll-back and the changing of azimuth, arc-normal extension values will differ from region to region: for example, the values will be larger in Nicaragua than in El Salvador; along the arc, shear will be slower in Nicaragua than in El Salvador. Guatemala, being located at the end of the strike-slip fault boundary of the North American and the Caribbean plates, is characterised by a more complex mechanism, which presents shear along the arc, while the extension zone seems to be accommodating by the formation of rifts at the forearc on the Caribbean plate (Phipps Morgan, J., et al, [2008]).

At the Caribbean coast, Northern Central America's geomorphology is characterised by sierras formed of several sub-parallel ranges, composed of metamorphosed deposits, separated by faults and grabens. At the Pacific coast, volcanic ranges and plateaus are located in Nicaragua, El Salvador and parts of Honduras and southwest Guatemala (Bommer, J. and Rodriguez, C., [2002]).

3.3. BATHYMETRY OF CENTRAL AMERICA

Bathymetry is crucial when tsunami modelling is implemented since the run-ups and velocity of the tsunami waves depend on the shape of the seafloor. When numerical simulation is implemented, a very precise description of the seafloor is needed to get accurate results. Some organisations such as the General Bathymetric Chart of the Oceans (GEBCO), the National Oceanic and Atmospheric Administration (NOAA) and The United States Geological Survey (USGS) provide worldwide bathymetric information at different levels of resolution. For more details see the GEBCO website http://www.gebco.net/USGS, the USGS website http://walrus.wr.usgs.gov/infobank/gazette/html/bathymetry/cam.html, and the NOAA website http://www.ngdc.noaa.gov/mgg/bathymetry/multibeam.html. The bathymetry data used in this study were taken from the GEBCO website, see figure 3.6. This data was also used to create the finite element grid that will be used for the deterministic analysis (see Chapter 5, section 5.4).

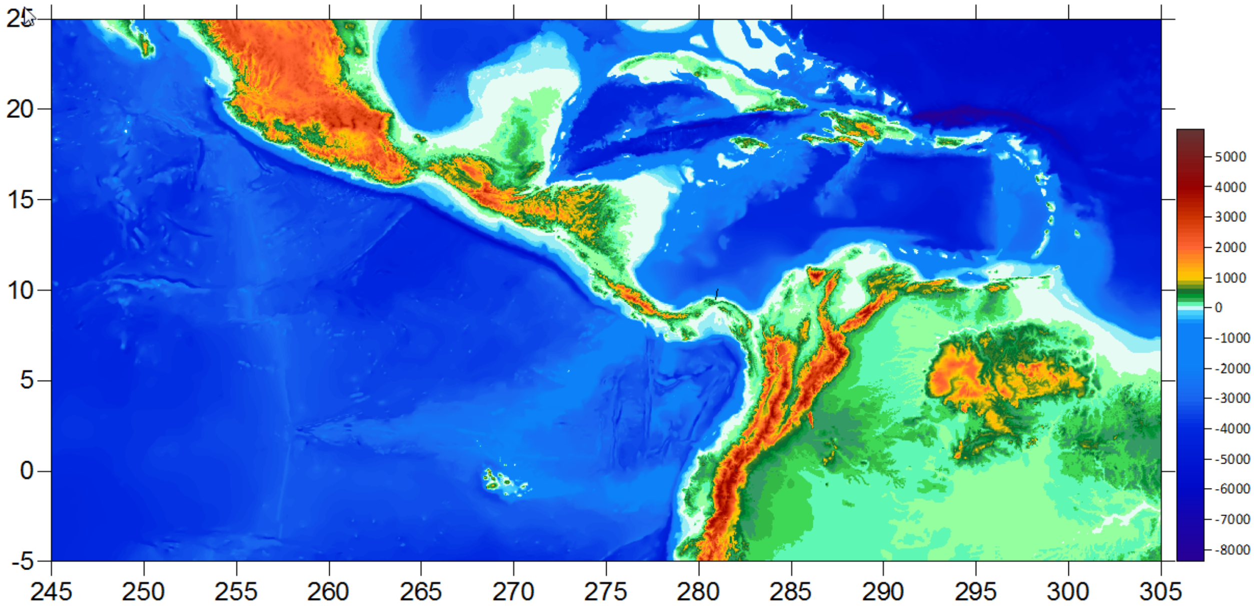

Figure 3.6: Bathymetry of Central America.

The Middle America Trench is continuous at depths greater than 4400 m, it is deeper than 5500 m off the Guatemala Deep, see figure 3.7. It widens and deepens abruptly to a maximum 6400 m off western Guatemala, then shoals gradually to merge into the sea floor off Costa Rica. The southeast segment is asymmetrical in cross section, V-shaped with irregular bottom (Fisher, R., [1961]).

4. THE CENTRAL AMERICAN TSUNAMI CATALOGUE

4.1. INTRODUCTION

Tsunami catalogues started to emerge worldwide since 1947. Before then, tsunamis were considered as secondary effects that accompanied earthquakes, volcanic eruptions or natural catastrophes. The first tsunami catalogues included parameters like observed run-up and tsunami intensities at the affected sites. Starting from the 1980's a description of tsunamigenic historical sources was included. Around 1990, reliability of the events was also introduced in the tsunami catalogues. Compiling tsunami catalogues is useful when computing the tsunamicity, tsunami hazard or tsunami risk of a specific region and also when defining the tsunamigenic sources and studying tsunami propagation (Tinti, S., et al., [2001]).

There are two types of tsunami database, according to the type of data compiled: *tsunami event database*, which are more related to the tsunami magnitude, intensity, cause and source location and *tsunami run-up database* that describe run-up values and their measurement procedures at a specific location. Generally speaking, both types of database contain run-up values and cause of the event, but they are presented in different ways (NOAA, [www.ngdc.noaa.gov/seg/hazard/tsuintro.shtml]).

Tsunami catalogues are more related to run-up databases in the sense that they describe the tsunami effects occurred at different locations. They are a compilation of tsunami magnitude and maximum height values registered or estimated at a specific location. These datasets are generally ordered by date. Generally speaking, catalogues also include the tsunami triggering mechanism, and sometimes a brief description of damage.

4.2. THE CENTRAL AMERICAN TSUNAMI CATALOGUE

The 1992 Nicaraguan tsunami put in evidence the need of studying these phenomena in the Central American area. Several studies have been conducted with the aim of establishing the tsunamicity in the region. The 1992 event was very destructive along the Pacific Nicaraguan coast, but caused no damage in the rest of the Central American countries. This might have contributed to the little awareness of the rest of the Central American population regarding to tsunami hazard.

Several studies established that Central America is a tsunamigenic region where (very) destructive tsunamis have been reported and that all countries are likely to be hit by tsunami waves in the future. The studies have also shown that the Caribbean coast is less tsunamigenic than the Pacific coast. At the Pacific coast, *empirical tsunami hazard estimation*[4] has found that Nicaragua, El Salvador, and Honduras are the most prone coasts to be hit by tsunamis. *Numerical simulations*[5] have also been performed, in order to study historical tsunamis. The need of implementing a *tsunami warning system* that matches the region characteristics has been also suggested.

The Central American tsunami catalogue was built in order to define the frequency, spatial distribution, characteristics and hazard of tsunamis in the region. The catalogue is a compilation of tsunamis occurred since the XVI century in the Pacific and the Caribbean coasts of Central America, all occurred in a geographical window from 6° to 18° N and 93° to 77° W. The document was prepared[6] in 1997 as the second phase of the program called "Reduction of Natural Disasters in Central America" at the Institute of Solid Earth Physics at Bergen University. Having found that 49 tsunamis occurred in that area, studies regarding to tsunami hazard mitigation and tsunami warning systems started to emerge (Molina, E., [1997]).

The catalogue contains forty-nine events that occurred between 1539 and 1996, information for each event includes source parameters (which is related to earthquakes in almost all of the cases), tsunami magnitude and its reliability, region affected, brief description of damage and sometimes figures that show the tsunami front waves. Earthquakes triggered almost all of those tsunamis except two of them that were supposed to be s*eiches*[7] in the Nicaraguan lake and a tsunami caused by volcanic *lahars* at northern Nicaraguan coast.

The catalogue was divided in three main time periods that correspond to the XVI-XVIII, the XIX and the XX centuries. Only 4 tsunamis were reported in the first period, whereas 11 and 35 events were reported in the XIX and XX centuries. The events compiled in the catalogue have magnitudes varying between 0 and 2.5 (in the Imamura-Iida scale) and the damage reports described destruction of small ships, coastal infrastructure and sometimes destruction of small villages.

Information for each event include date, earthquake source parameters, tsunami parameters and tectonic region of the source. The date is related to the earthquake, rather than the tsunami arrival time. Earthquake source parameters include the latitude, longitude and magnitude (usually surface wave magnitude M_s). Tsunami source parameters specify the type of tsunami (local, regional or distant), the affected region and the tsunami magnitude under the Imamura-Iida scale. Information concerning the tectonic region indicates the tectonic context of the event, for example if it was due to an earthquake belonging to the Cocos-Caribbean subduction zone, the boundary between the North American and the Caribbean plates, at the North Panama Deformed

[4] Empirical approaches of tsunami hazard were implemented in 2000 by Centro de Investigaciones Geofísicas (CIGEFI) de la Universidad de Costa Rica, the Red Sismológica Nacional (RSN: ICE-UCR), the Instituto de Sismología, Vulcanología, Hidrogeología y Meteorología de Guatemala and the Institute of Solid Earth of the University of Bergen, Norway.

[5] Tsunami numerical simulations were implemented in 2004 by the Central American Seismological Centre (CASC), the Centro de Investigación Cientifica y Educación Superior de Ensenada (CICESE) and the Escuela Centroamericana de Geología de la Universidad de Costa Rica.

[6] The Central American Tsunami Catalogue was presented in 1997 as the second phase of the "Reduction of Natural Disasters in Central America" of the Institute of Solid Earth Physics of the University of Bergen, Norway and the Instituto de Sismología, Vulcanología, Hidrogeología y Meteorología de Guatemala (INSIVUMEH).

[7] Seiche is the oscillation of water in enclosed lagoons or bays due to a disturbance (meteorological conditions, earthquakes, etc.) that sets "waves" that are not tidal. The "wave" will bounce back and forth until its energy is dissipated through friction. (UNESCO, [1991]).

Belt or at the Panama Channel Discontinuity. Maps of the region struck by the tsunami and the triggering earthquake epicentres are commonly shown, and in some cases, figures regarding macroseismicity are also included.

The list of tsunamis included in the Central American tsunami catalogue is shown in table 4.1 and in figure 4.1

Table 4.1: Tsunami Catalogue of Central America
(Molina, E. [1997])

No	DATE	TIME	EARTHQUAKE SOURCE PARAMETRES			TSUNAMI PARAMETERS			TECTONIC REGION	OCEAN
			Lat	Lon	Ms/I	T	Region	m		
			(N)	(N)						
1	1539-1124	---	---	---	---	L	Honduras Gulf, HON	---	NO-CA	C
2	1579-0316	---	---	---	---	L	Cano Island, CR	---	CO-CA	P
3	1621-0502	---	8.97	79.5	5.6-6.0	L	Panama la Vieja, PAN	---	CANAL DISCONTINUITY	P
4	1798-0222	---	10.2	82.9	VI-VI+	L	Matina, CR	-1	NPDB	C
5	1822-0507	---	9.5	83.0	7.6	L	Matina, CR	-1	NPDB	C
6	1825-02--	---	---	---	5-5.5	L	Roatan Island, Honduras Gulf, HON	---	NO-CA	C
7	1844-05--	---	11.2	84.8	7.0-7.9	S?	Nicaragua Lake, NIC	---	CO-CA	N-L
8	1854-0805	5.30	8.5	83.0	7.25	L	Golfo Dulce, CR	1.5	CO-CA	P
9	1855-0925	---	---	---	6-6.5	L	Trujillo Bay, Honduraas Gulf, HON	---	NO-CA	C
10	1856-0804	---	---	---	7-8	L	Omoa, Honduras Gulf, HON	2	NO-CA	C
11	1859-0826	---	13	87.5	6-6.5	L	Amapala, Fonseca Gulf, HON	1.5	CO-CA	P
12	1859-1209	---	13.7	89.8	7-7.9	L	Acajutla Bay, SAL	1.5	CO-CA	P
13	1873-1014	0.05	10.2	80.0	V	L	Colon & Panama Harbors, PAN	---	NPDB	C
14	1882-0907	9.18	10.0	79.0	7.9	L	San Blas Coast, PAN	2	NPDB	C
15	1884-1105	---	4.0	76.0	---	L?	Acandi, Colombia	---	Colombia	P
17	1902-0118	23.23	14.7	91.6	6.3	L?	Ocos, GUA	---	CO-CA	P
18	1902-0226	---	13.0	89.0	7.0	?L	Pacific Coast GUA-SAL	2		P
19	1902-0419	2.24	14.9	91.5	7.5	L?	Ocos, GUA	-1	CO-CA	P
20	1904-0120	14.50	7.0	82.0	5.0	L?		---		P
21	1904-1220	5.42	9.2	82.8	7.45	L	Bocas del Toro, PAN	---	NPDB	C
22	1905-0120	18.23	9.85	84.68	6.8	L?	Coco Island, CR	---	CO-CA	P
23	1906-0131	15.36	1.0	81.3	8.2	R	Tumaco, Euador, San Carlos, PAN,Potrero Bay, CR	---	Ecuador	P
24	1906-----	---	---	---	---	T	El Salvador Coast, SAL	---		P
25	1913-1002	4.23	7.1	80.6	6.7	L	Azuero Peninsula, San Miguel Gulf, PAN	-1	Azuero-Torio F. Z.	P
26	1915-0907	1.20	13.9	89.6	7.7	L?	El Salvador Coast, SAL	0.5	CO-CA	P
27	1916-0131	---	---	---	---	T	Panama Canal, PAN	---		P

Table 4.1 (cont): Tsunami Catalogue of Central America

(Molina, E. [1997])

No	DATE	TIME	EARTHQUAKE SOURCE PARAMETRES			TSUNAMI PARAMETRES			TECTONIC REGION	OCEAN
			Lat	Lon	Ms/I	T	Region	m		
			(N)	(N)						
28	1916-0426	2.21	9.2	83.1	6.9	L	Bocas del Toro, PAN	0	NPDB	C
29	1916-0525	---	12.0	90.0	7.5	?L?	El Salvador	---		P
30	1919-0629	23.14	13.5	87.5	6.7	L	Corinto, NIC	---	CO-CA	P
31	1919-1212	---	---	---	---	L	El Ostial, NIC	---	CO-CA	P
32	1920-1209	---	---	---	---	L	Fonseca Gulf	---		P
33	1926-1105	7.55	12.3	85.8	7.0	L	Offshore, NIC	---	CO-CA	P
34	1934-0718	1.36	8.1	82.6	7.5	L	Chiquiri Gulf, PAN	1.5	PFZ	P
35	1941-1205	20.46	8.7	83.2	7.6	L	Pta. Dominical, CR	-1	CO-CA	P
36	1941-1206	---	10.0	85.2	6.9	L	Nicoya Gulf, CR	-2	CO-CA	P
37	1950-1005	16.09	10.0	85.7	7.9	L	Coasts CR-NIC-SAL	-1	CO-CA	P
38	1950-1023	16.13	14.3	91.8	7.3	L	Coasts GUA-SAL	-1	CO-CA	P
39	1951-0803	0.24	13.0	87.5	6.0	LH	Potosi, Fonseca Gulf, HON	---	CO-CA	P
40	1952-0513	19.31	10.3	85.3	6.9	L	Puntarenas, CR	-3	CO-CA	P
41	1956-1024	14.42	11.5	86.5	7.2	L?	San Juan del Sur, NIC	---	CO-CA	P
42	1957-0310	14.42	51.63	175.41	8.1	D	Acajutla, SAL	---	Auletian	P
43	1960-0522	19.11	-38.2	73.5	8.5	R?	La Union, Fonseca Gulf, SAL	---	Chile	P
44	1962-0312	11.40	8.0	89.9	6.7	L	Armuelles, Chiquiri G., PAN	-1	CO-CA	P
45	1968-0925	10.38	15.6	92.5	6.0		Pacific Coast	---		P
46	1976-0204	9.01	15.2	89.2	7.5	L	Cortes, Honduras G, HON	-0.5	C	
47	1976-0711	16.54	7.43	78.12	7.0	L	Jaque, Darien, PAN	-1	P	
48	1990-0325	13.16	9.8	84.8	7.0	L	Puntarenas & Quepos, CR	0	P	
49	1991-0422	21.56	9.6	83.2	7.6	L	Bocas del Toro, PAN	1	C	
50	1992-0902	0.16	11.7	87.4	7.2	L	Nicaragua Coast, Bahia de Salinas & Papagayo G., CR	2.5	P	

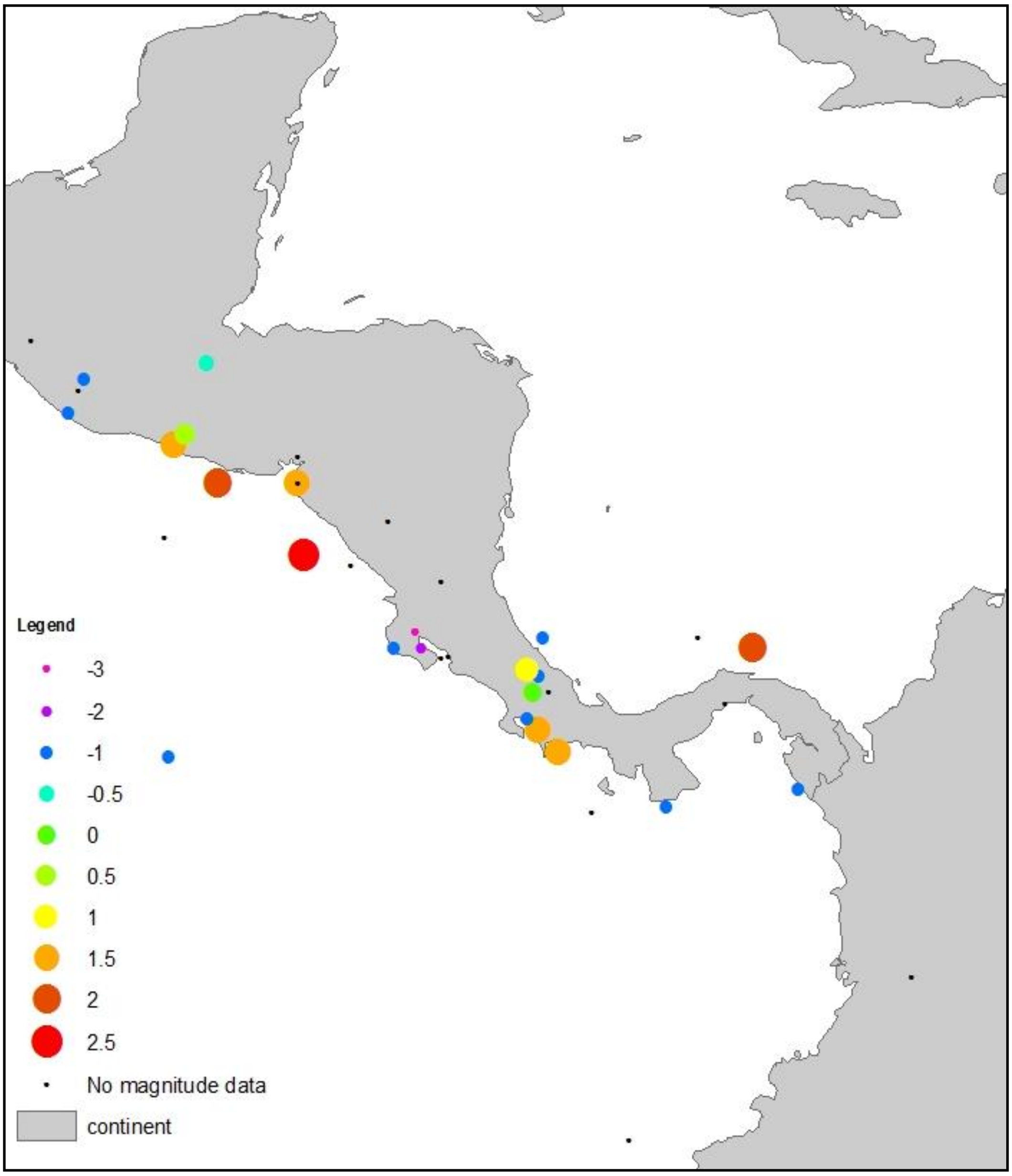

Figure 4.1:The Central American Tsunami Catalogue.

Thirty-seven of the events occurred in the Pacific coast whereas 12 were reported in the Caribbean coast (Molina, E., [1997]). Six of the tsunamis registered at the Pacific coast where associated to an unknown cause, the rest were associated to earthquakes that occurred at the Cocos-Caribbean subduction zone, Panama fracture zone, North American-South American plates boundary or due to shallow faults. All of the tsunamis registered at the Caribbean coast were associated to earthquakes (Fernandez, M. [2000]). Tsunamis associated with submarine landslides, terrestrial landslides or volcanic eruptions have not been reported in the area. Submarine eruptions are not a possible tsunamigenic source in the region, given the fact that there are no active submarine volcanoes in the area. However, it is possible that one of the inland volcanoes located in Nicaragua (The Cosigüina Volcano) triggered tsunamis (Fernández, M. [written communication]).

An important aspect of a tsunami catalogue is the reliability and accuracy of its data. The term reliability may be defined as the probability that the expected value of a measurement determined with a certain technique is equal to the true value. Reliability may be affected by bias and systematic errors. Accuracy is also called precision and represents an estimate of the dispersion or scatter of the measurement around its expected value (Harr, M., [1996]).

The Central America tsunami catalogue is a compilation of tsunami reports from different sources, therefore, each event is characterised by a different level of reliability that depends on the authors who compiled the database and on references used (Molina, E., written communication, [2004]). Textual descriptions from references were included in the Central American tsunami catalogue (no translations of the descriptions were made) in order to avoid the authors' interpretation of the events (Molina, E., [1997]).

Thirty-six out of 50 events compiled in the Central American tsunami catalogue are well documented, whereas according to the author it is likely that 9 events did not occur. The reliability of each event is specified using question marks preceding or following the tsunami type symbol, as shown in table 4.2.

Table 4.2 Data Reliability symbols in the Central America Tsunami Catalogue.

Symbol	Meaning
L?	Not reliable local tsunami, reliable earthquake occurrence.
?L	Not reliable earthquake, reliable tsunami phenomenon occurrence.
?L?	Both earthquake and tsunami occurrence are not reliable

Tsunami catalogues have emerged recently, some of the events that occurred in ancient times are likely to have not been registered due to the lack of measuring equipment (some of them could have passed unnoticed, especially weak events) or due to the fact that they occurred in uninhabited places. This explains the reduced number of events registered in the catalogues some decades ago and their sharply increase in more recent times. In order to account for this fact, the concept of *completeness* has been introduced. A catalogue can be considered complete if it contains a more or less constant number of events registered along constant time intervals (Albarello, D. et al [2001]).

Completeness can be estimated using a graphical method called "visual cumulative method to estimate completeness". The method is originally applied to seismic catalogues to find their *periods of completeness* (Albarello, D. et al [2001]). Having chosen a seismic catalogue of a region, the steps to evaluate its completeness under this method are:

a) Select the homogenising criteria that will be adopted for the analysis (generally magnitude or intensity).
b) Divide the selected criteria in different interval classes. For example, if magnitude is the selected criterion, the smallest magnitude registered is 3 and the greatest is 6; a possible arrange of interval classes could be [0,3], [0,4], [0,5] and [0,6]. In each class there would be included those events whose magnitude is smaller or equal to the upper bound limit of the interval class. Each class interval will be analysed separately.
c) Choose a time interval for the analysis (20 years is commonly used).
d) For each time interval and for each interval class criterion (magnitude), count the number of events that exceed the upper boundary of the interval class considered.

e) Plot the number of events computed in (d) for each time interval.
f) Time intervals that fit a trend defined by a straight line would be considered complete
g) If the trend found can be attributed to a few decades, the catalogue is considered complete.

Given the reduced number of events contained in the Central American tsunami catalogue and also due to the fact that not all of them have a magnitude value associated, the visual cumulative method to estimate completeness has not been applied to establish the completeness of the catalogue. It has been decided that earthquake catalogues are going to be used to perform the analysis, given that tsunamis in Central America are mainly triggered by earthquakes, and given also that earthquake catalogues for the region in study are more populated than the tsunami catalogue. The completeness analysis of the earthquake catalogue is presented in section 4.3

4.3. EARTHQUAKE CATALOGUES

There are several earthquake catalogues that contain events registered in Central America (see table 4.3). Some of these catalogues cover small areas of Central America, some others contain only recent events or only events with high magnitude. The catalogues that were available have been plotted in figure 4.2.

Table 4.3 Seismic Catalogues of Central America.

number	Author	area covered	date covered	type
1	Leeds	Nicaragua	1520-1973	all
2	NEIC	Mexico, CA and SA	1973-1979	no mag
3	Ambraseys	central america	1898-1995	all
4	Peraldo and Montero	not available	1500-1899	
5	Rojas	not available	1502-1992	
6	Singh, Rodriguez and Espinoza	Southern Mexico, Pacific	1900-1981	shallow
7	NOAA	Mexico, CA and SA	1471-2008	all
8	CERESIS	South America	1530-1991	all
9	Mexico-noticeable earthquakes	Mexico	1900-1999	m>6.5
10	Mexico SSN	Mexico	1998-2008	all

Brief descriptions of some of the catalogues contained in table 4.3 are presented as follows. The catalogue compiled by Leeds (Leeds, J.[1974]) contains 399 events, that occurred between 1520 and 1973, with magnitude varying from 3.7 to 7.7, the catalogue covers Nicaragua only. The catalogue compiled by the "National Earthquake Information Center" (NEIC, USGS) was not plotted given that no magnitude value was available. The Ambraseys catalogue contains about 1800 events, occurred in Central America from 1898 to 1995, the magnitude values (Ms) vary from 3 to 7.9 (Ambraseys, N., Adams R., [1996]). The catalogue proposed by Singh, Rodriguez and Espinoza (Singh, K. et al, [1984]) contains 31 shallow events with magnitudes between 7 and 8.4. The "National Oceanic and Atmospheric Administration" (NOAA) catalogue contains about 1400 events occurred from 1471 and 2008, the magnitude range goes from 1.6 to 9.5 and covers the whole American continent. The catalogue compiled by the "Centro Regional de Sismologia para America del Sur" (CERESIS) contains more than 1000 events, that have occurred in South America. The Mexico noticeable earthquake catalogue contains 181 events, whose magnitude varies between 6.4 and 8.2. Last, but not least, the Mexico "Sevicio

Simologico Nacional" (SSN) catalogue contains about 9400 events from 1998 to 2008, with magnitude range from 2.3 to 7.6.

The earthquake catalogue selected to carry out the analysis is the Ambraseys catalogue, given that it is a specific study of the seismology Central America, it has a large number of events containing their magnitude values and it covers the whole Central American area. As mentioned before, the Ambraseys catalogue has events going from 1898 to 1995 (see figure 4.3).

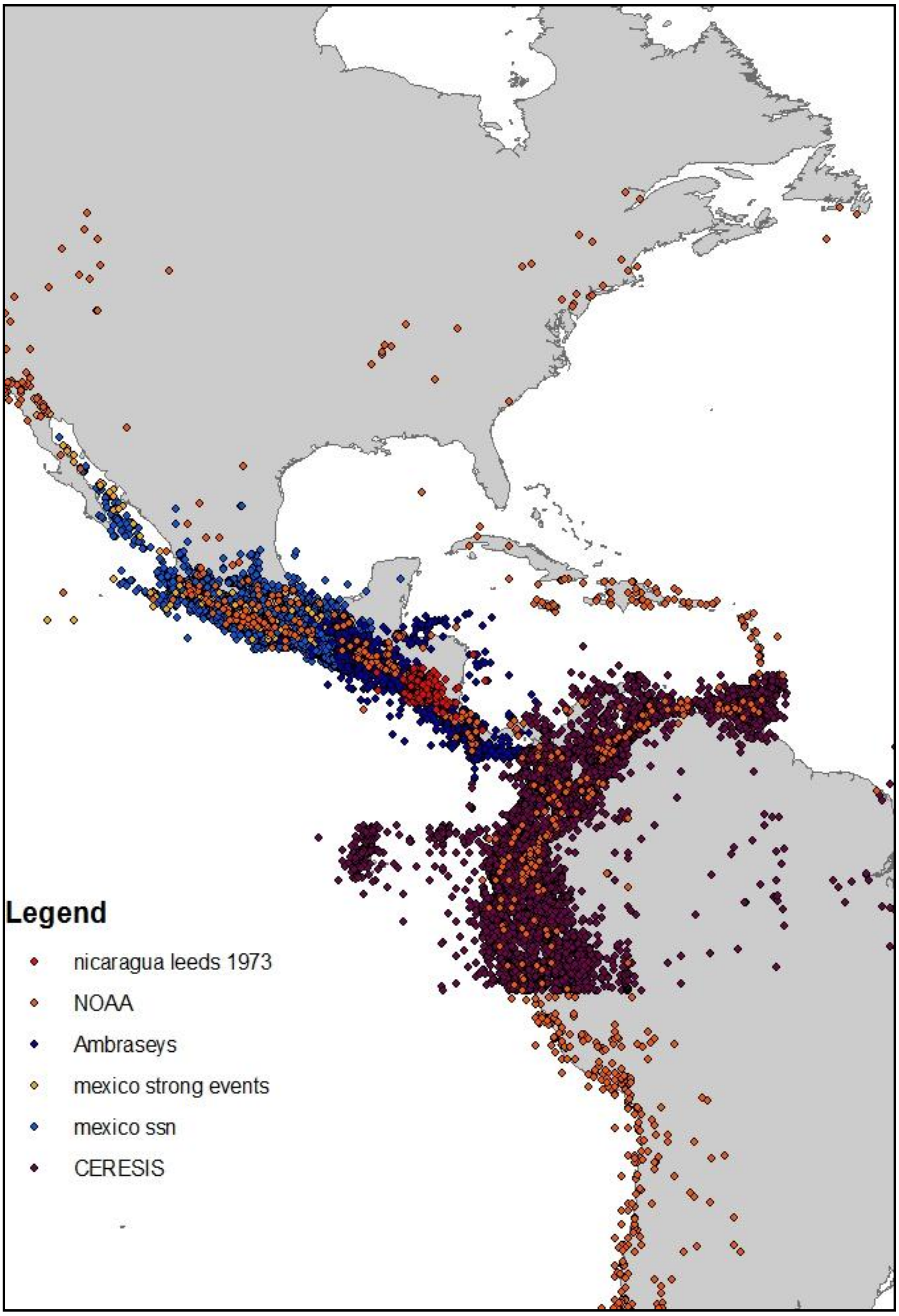

Figure 4.2:Seismic Catalogues of Central America.

The Ambraseys catalogue contains events from 1898 to 1995. In order to increase the number of events and cover a larger temporal window, the NOAA catalogue events were joined to the Ambraseys catalogue, (see figure 4.4). Then the area of study was selected going from 5°S to 25°N and 115°W to 55°W (see figure 4.4). The events within the area of study of the NOAA catalogue were selected using ArcGis, then the events contained in both catalogues were searched and one of them was deleted, generally the one contained in the NOAA catalogue. Following this procedure, a catalogue Ambraseys-NOAA was produced (see figure 4.5) containing 1931 events registered from 1530 to 2008. Events with depth greater than 100km were removed, given that they are unlikely to cause tsunamis. The Ambraseys-NOAA catalogue will be used as the earthquake catalogue to be used in the analysis followed in this thesis.

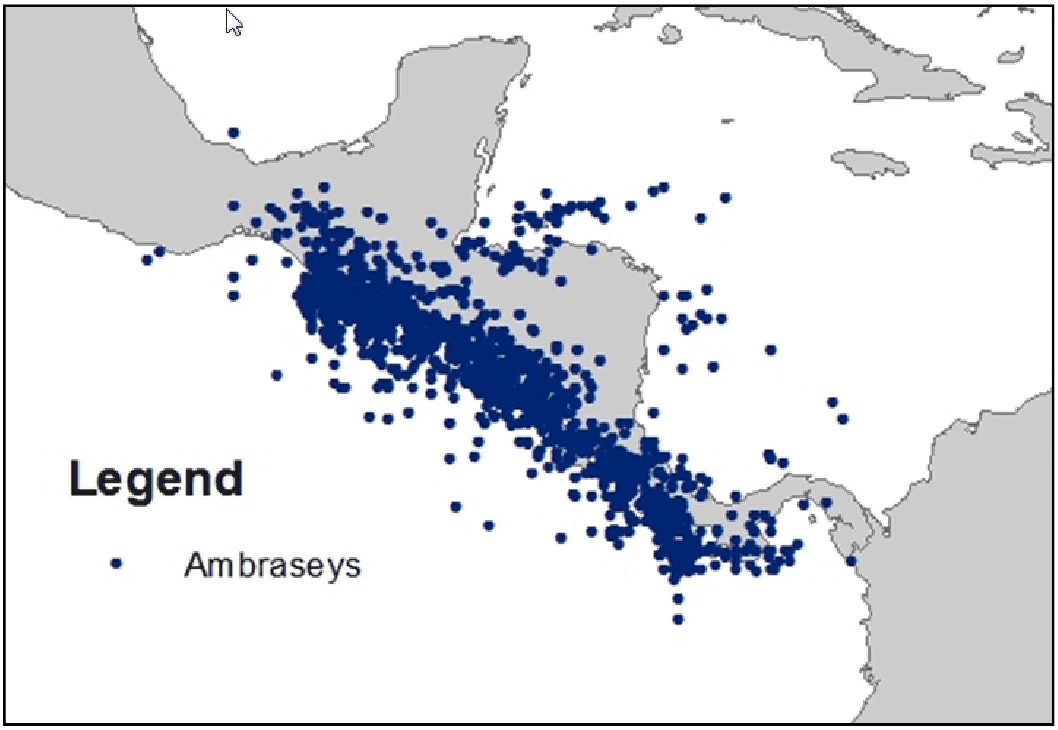

Figure 4.3:Ambraseys Catalogue.

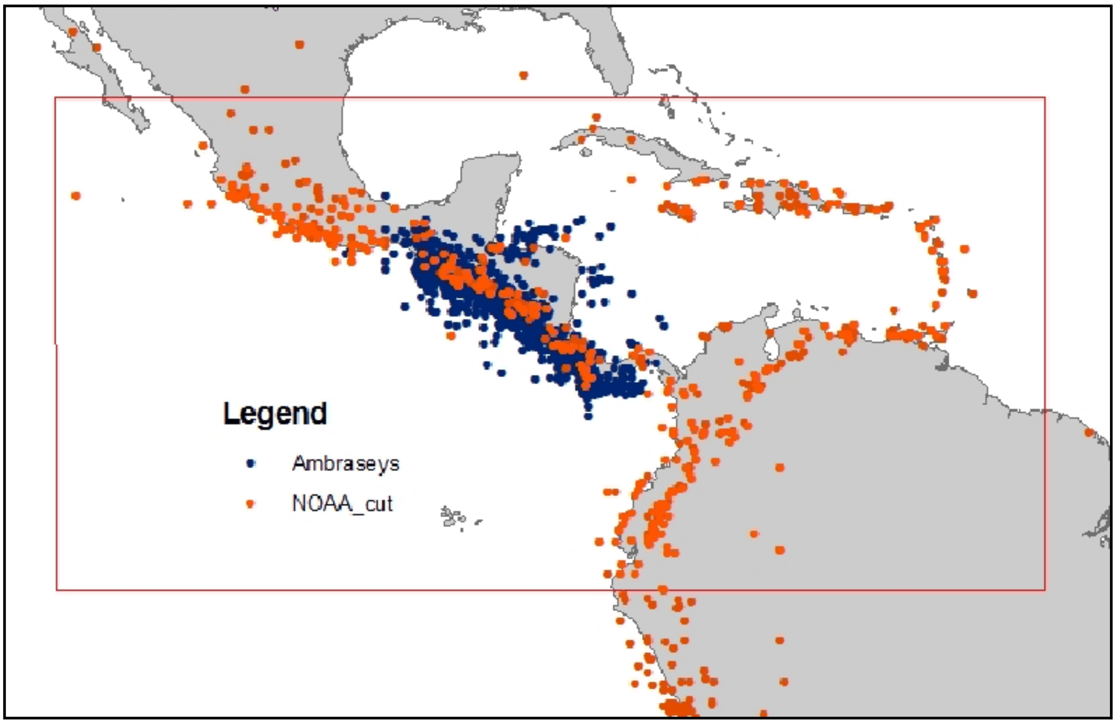

Figure 4.4:Ambraseys and NOAA Catalogue.

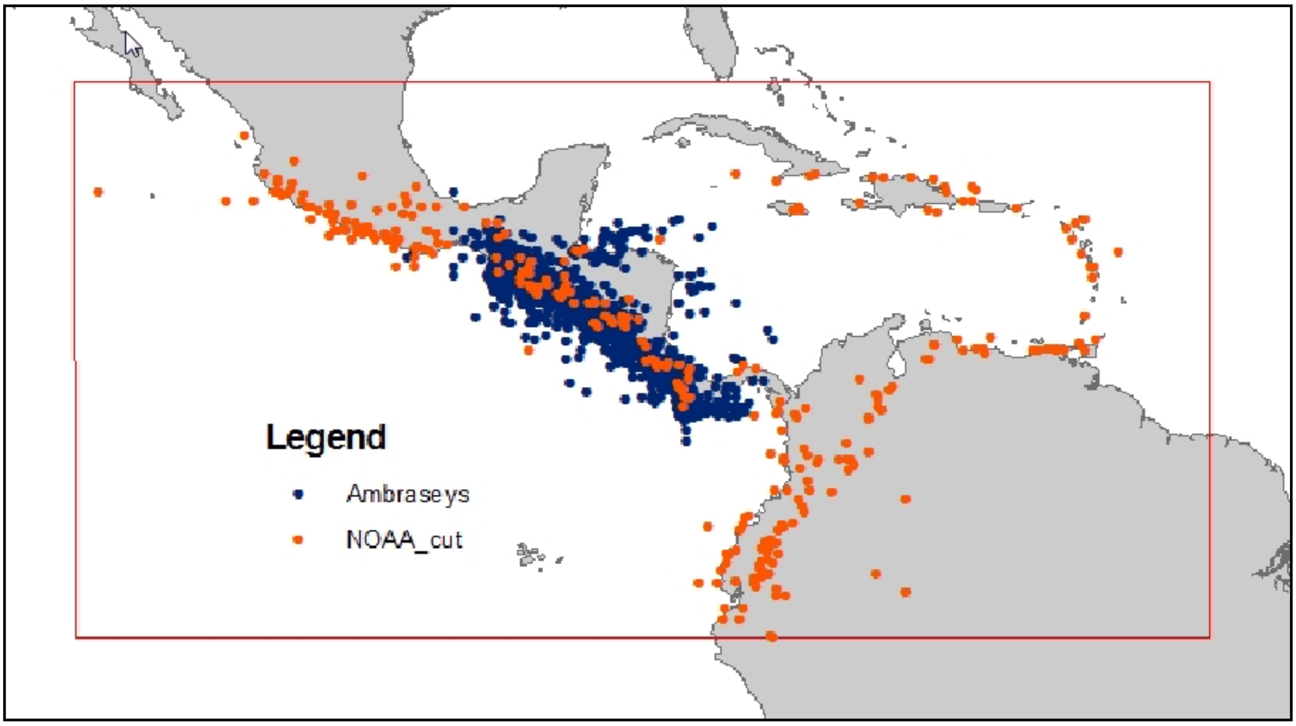

Figure 4.4:Ambraseys-NOAA joined Catalogue.

5. TSUNAMI HAZARD ASSESSMENT

5.1. OVERVIEW

The goal of this study is to perform a tsunami hazard assessment through two approaches, first a statistical approach aiming at establishing the annual rate of occurrence of tsunamis and second a deterministic analysis which will provide estimated extreme water elevation values along the coast.

According to previous studies, the Central American region is a moderate tsunamigenic zone (Fernandez, 2001), and almost all of the tsunamis reported in the area have been related to seismic activity (Molina, 1997). At the Pacific coast, the tsunamigenic earthquakes are generally located at the Middle American Trench. The statistical analysis will be performed on earthquake catalogues. According to us this is appropriated, given that this study is focused on the Pacific coast of Central America, where tsunamis are mainly triggered by earthquakes, and given also that the earthquake catalogues are more populated than the tsunami catalogues.

A hybrid analysis, probabilistic and deterministic, aiming at obtaining run-up distribution along the coast corresponding to a given annual rate of occurrence was performed. This kind of analysis is flexible in the sense that allows one to fix the run-up value and estimate the values of annual rate of occurrence along the coast.

The deterministic approach will be performed using the code UBO-TSUFE MODEL, which is a finite element code developed by the Tsunami Research Team of the University of Bologna. The analysis was performed by choosing historical events as scenarios, with parameters taken from previous studies or estimated according to the tectonics of the region.

5.2. STATISTICAL APPROACH

A statistical analysis of the Ambraseys-NOAA seismic catalogue was performed, the aim of this approach is to estimate the annual rate of occurrence of earthquakes with magnitude higher than a fixed threshold value. The magnitude threshold values were established as the minimum earthquake magnitude able to trigger a tsunami, and these values have been chosen on the basis of historical data.

The following steps were followed in order to estimate the annual occurrence rate of earthquakes with magnitude higher than a fixed value.

a) Choosing an appropriate catalogue:
As explained in chapter 4, the Ambraseys-NOAA catalogue was chosen to perform the statistical analysis for this thesis. The catalogue was obtained by joining two catalogues, the Ambraseys catalogue and the NOAA catalogue. The Ambraseys catalogue is contained in the study "Seismicity in Central America" compiled by Ambraseys and published in 2001.The NOAA catalogue is a catalogue covering the Central America region. Doubled events were deleted, given priority to the events contained in the Ambraseys catalogue.

b) Dividing the catalogue into homogeneous zones.

Seismic events along Central America are related to several tectonic structures, for example, earthquakes with epicentre along the middle American Trench, at the Pacific coast, are related to the subduction of the Cocos plate under the Caribbean plate, whereas those occurring on land inside the Caribbean plate are due to volcanic activity or geological faults. There are also some inland events occurring near the interaction zone between the North American and the Caribbean plate. At the Caribbean coast, events are mainly produced by the interaction between the Caribbean plate and the North American plate and some transition zones as the Deformed belt of Southern Panama and the Deformed Belt of the Southern Caribbean.

The Ambraseys-NOAA catalogue was divided into six zones, considering their geographical location and the probable tectonic unit related to the earthquake. The first zone covers the Pacific coast of southern Mexico, the second zone extends along the Pacific coast from southern Mexico to Panama, the third zone covers the Atlantic coast from southern Mexico to Panama, the forth zone goes from southern Panama to the Pacific coast of Ecuador, the fifth zone covers the Atlantic coast of Venezuela and the lesser Antilles and last but not least, the sixth zone covers Cuba and the Antilles. See figure 5.1.

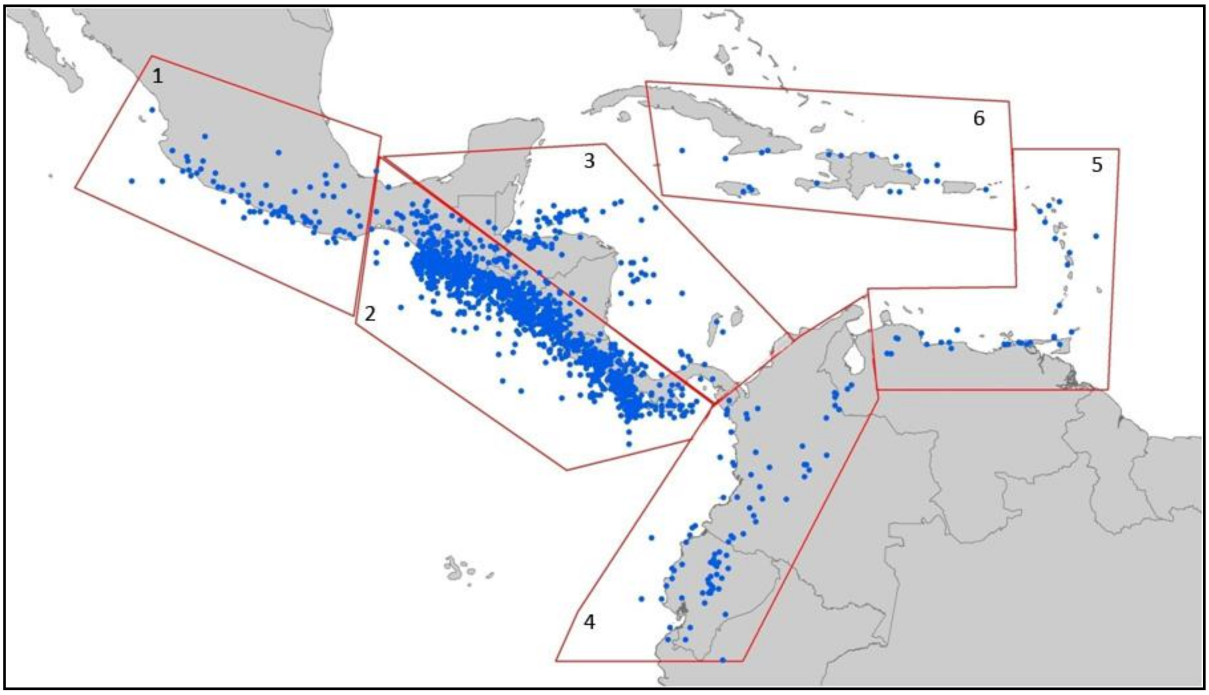

Figure 5.1: Seismic zones in Central America.

The zones were divided considering their geographical location, and their vicinity to major tectonic units. Events within zones 1, 2 and 4 are related to the subduction zone of the Middle American Trench, whereas events within zone 3, 6 and 5 are related to the deformed belt of North Panama or the deformed belt of the southern Caribbean (see figure 5.2).

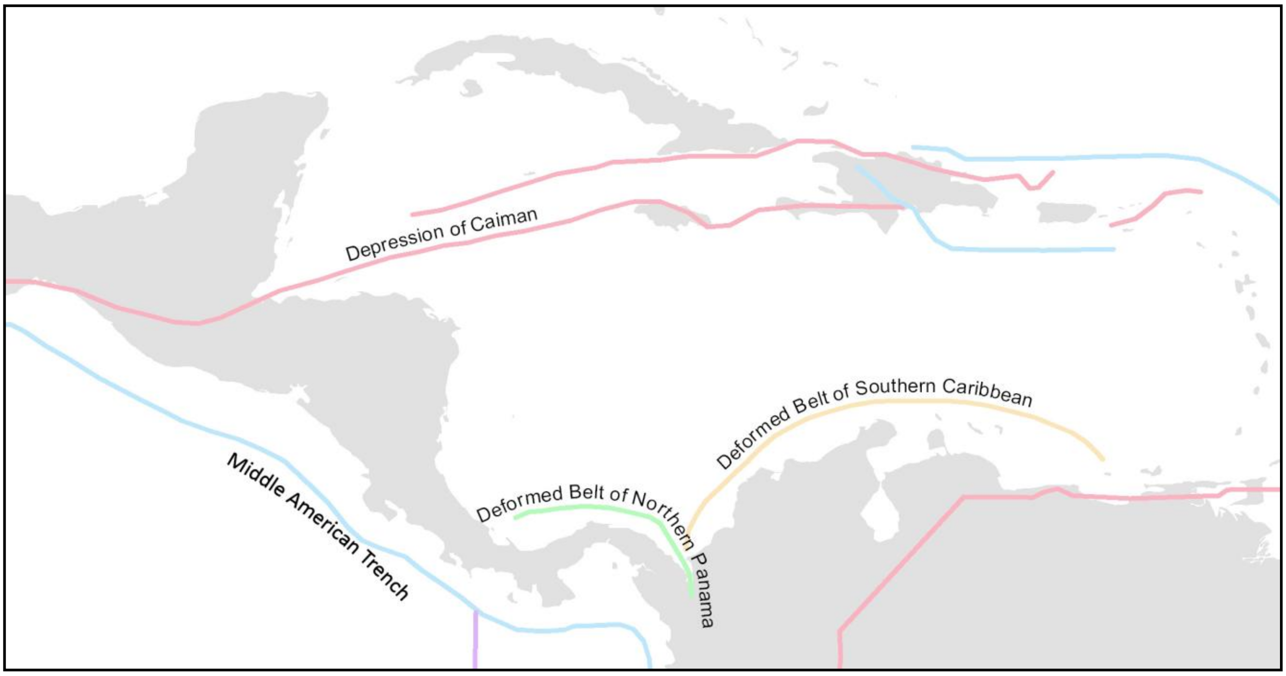

Figure 5.2: Tectonic Units in Central America.

As it can be noticed in figure 5.1, zone 2 has a large number of events, whereas zones 3, 5 and 6 have a reduced number of earthquake registered. The poor number of events that would provide a non reliable statistical analysis, and also the fact that small number of tsunamis have been reported at the Caribbean coast, led us to the decision of not taking into account zones 3, 5 and 6 to perform the statistical analysis.

The following steps of the statistical analysis were performed for zones 1, 2 and 4 of the Ambraseys-NOAA catalogue.

c) Performing the completeness analysis.

The completeness analysis aims at establishing the time period in which a catalogue has a linear decrease of the cumulative number of events vs time within a class of magnitude. The completeness of a catalogue is usually estimated through a graphical method called “visual cumulative method to estimate completeness” (Albarello, D. et al [2001]). The steps followed to estimate the completeness period are:

The homogenising criteria adopted for the analysis is the magnitude, and classes of magnitude were established depending on the magnitude distribution of the historical events. For example, for zone 1, the smallest magnitude registered is 4.7 and the greatest is 8.4; we have chosen the interval classes to be [0,5[, [5,5.5[, [5.5,6[, [6,6.5[, [6.5,7[, [7,7.5[, [7.5,8[, [8, 8.5[and M≥ 8.5. In each class are included those events whose magnitude is within the bound limit of the interval class. Each class interval is analysed separately. Figures 5.3, 5.4 and 5.5 show the magnitude distribution for zones 1, 2 and 4, respectively.

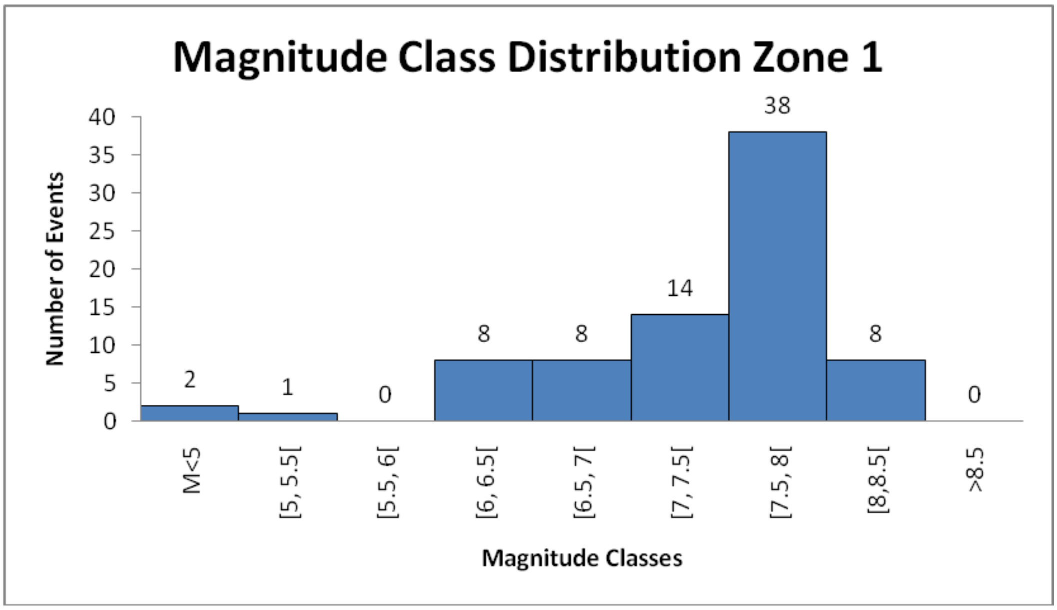

Figure 5.3: Magnitude Class Distribution of Zone 1.

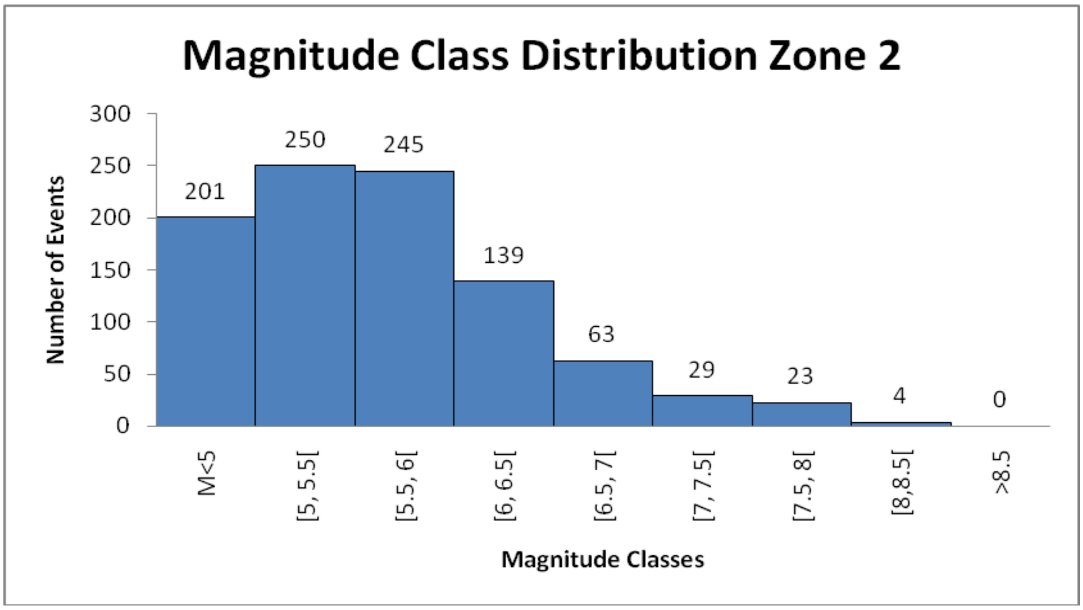

Figure 5.4: Magnitude Class Distribution of Zone 2.

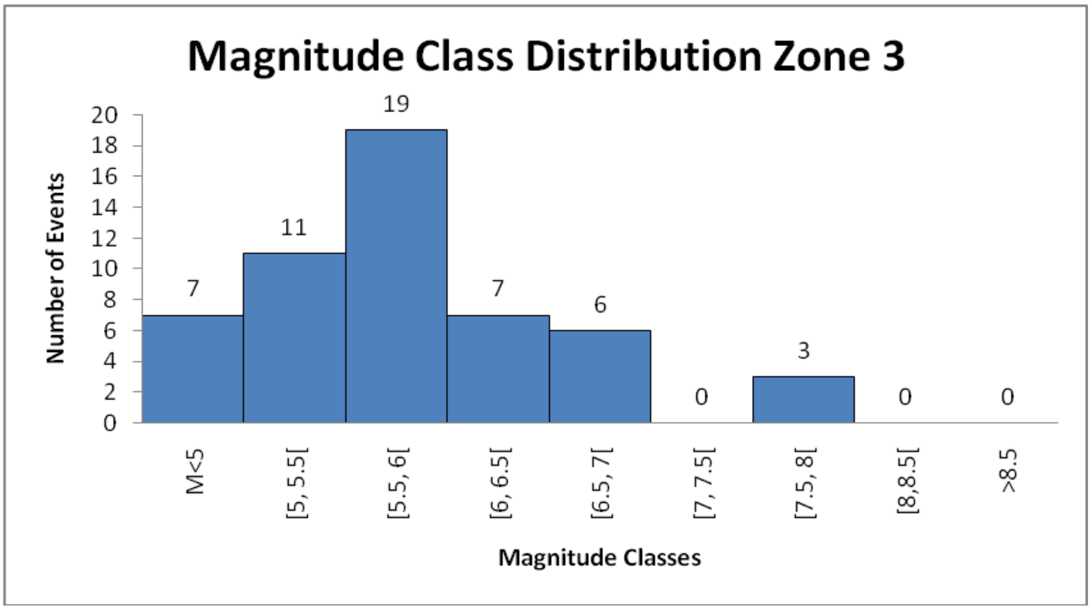

Figure 5.5: Magnitude Class Distribution of Zone 4.

Time interval of 50 or 20 years have been chosen for this analysis, depending on the temporal distribution of each zone. The number of events that were included within the boundary of each magnitude class were plotted for each time interval. Time intervals that fit a trend defined by a straight line were considered complete; for example, if the trend found started at 1800 for the magnitude class [7. 7.5[, then the catalogue would be considered as complete since 1800 for magnitude values superior to 7. The completeness periods for each zone are shown in figures 5.6 to 5.17.

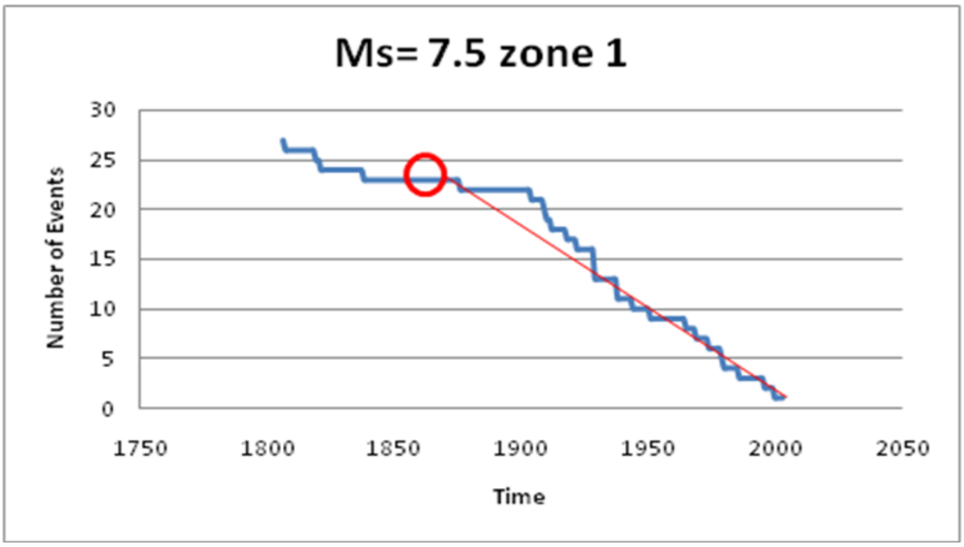

Figure 5.6: Completeness Analysis, Zone 1, Magnitude 7.5.

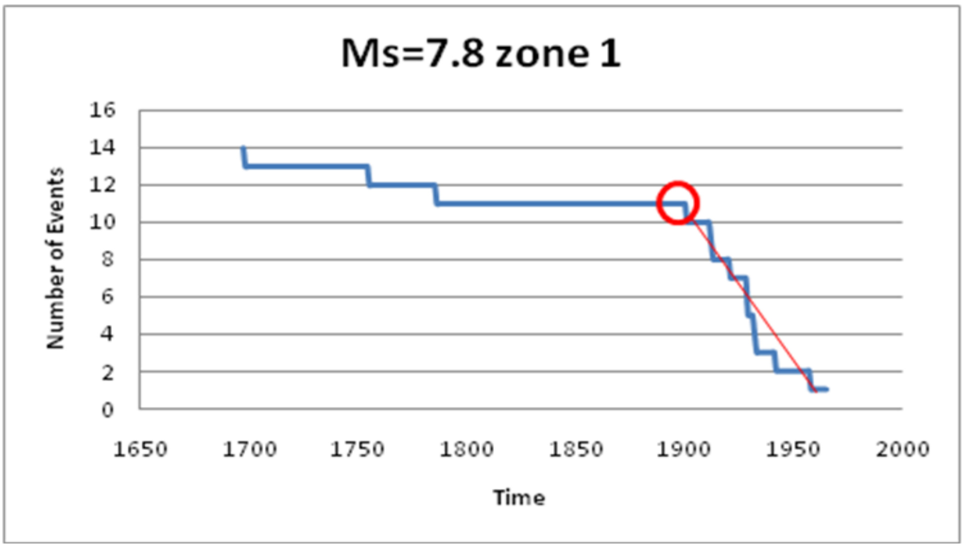

Figure 5.7: Completeness Analysis, Zone 1, Magnitude 7.8.

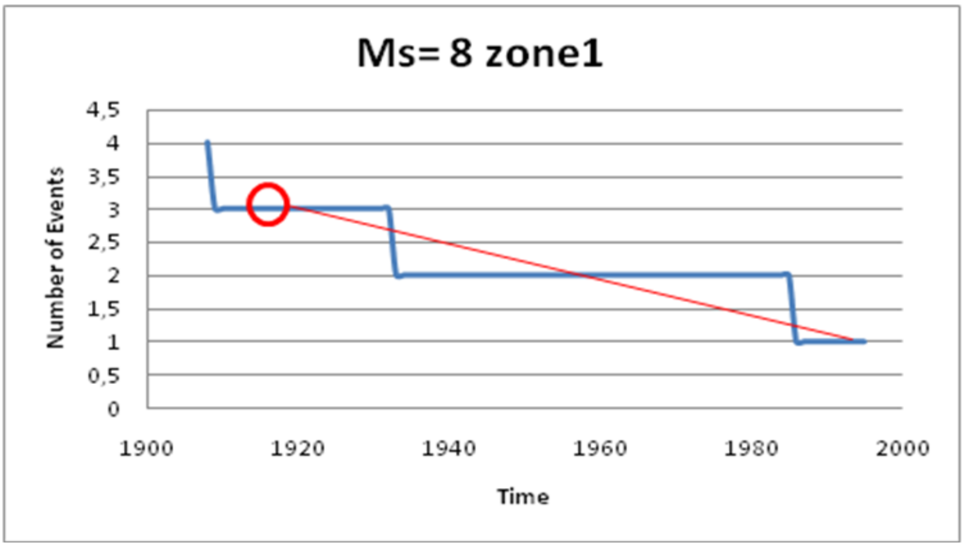

Figure 5.7: Completeness Analysis, Zone 1, Magnitude 8.

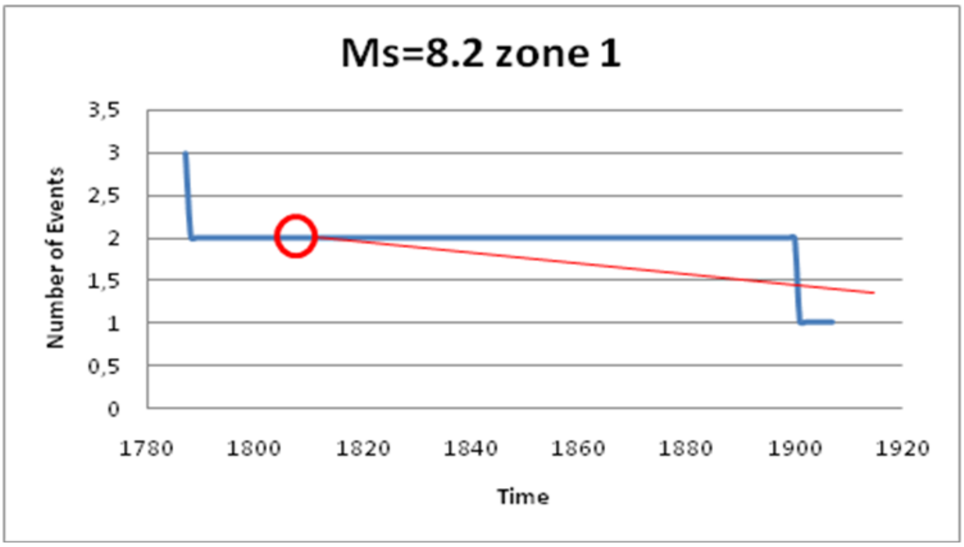

Figure 5.8: Completeness Analysis, Zone 1, Magnitude 8.2.

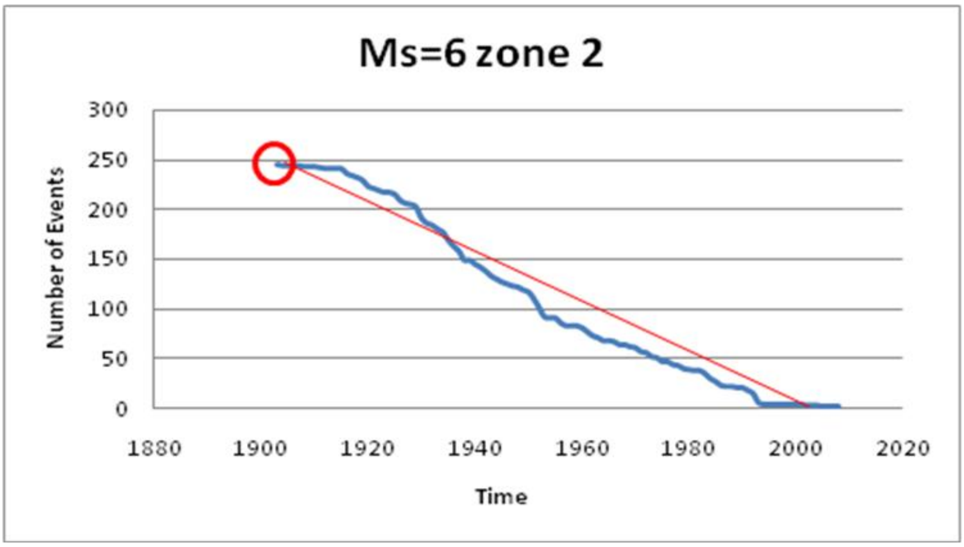

Figure 5.9: Completeness Analysis, Zone 2, Magnitude 6.

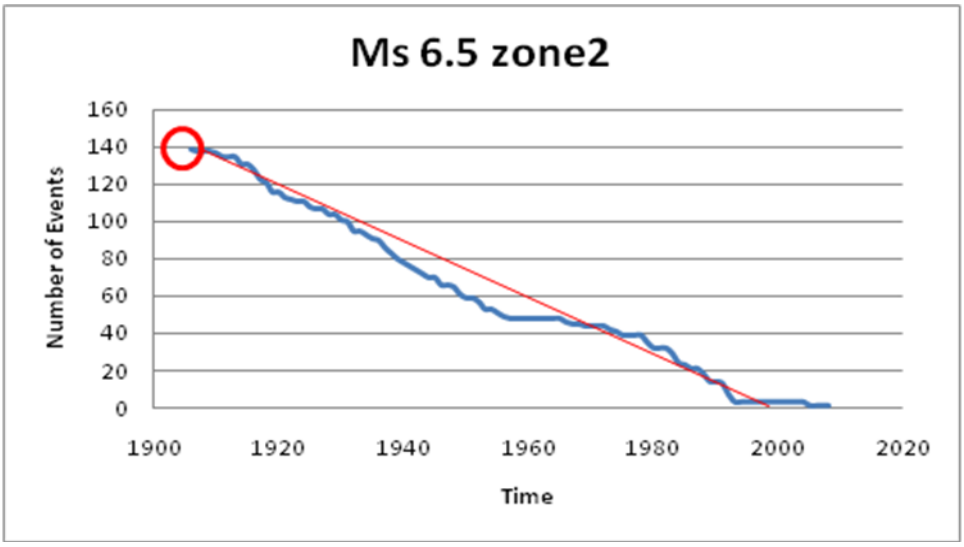

Figure 5.10: Completeness Analysis, Zone 2, Magnitude 6.5.

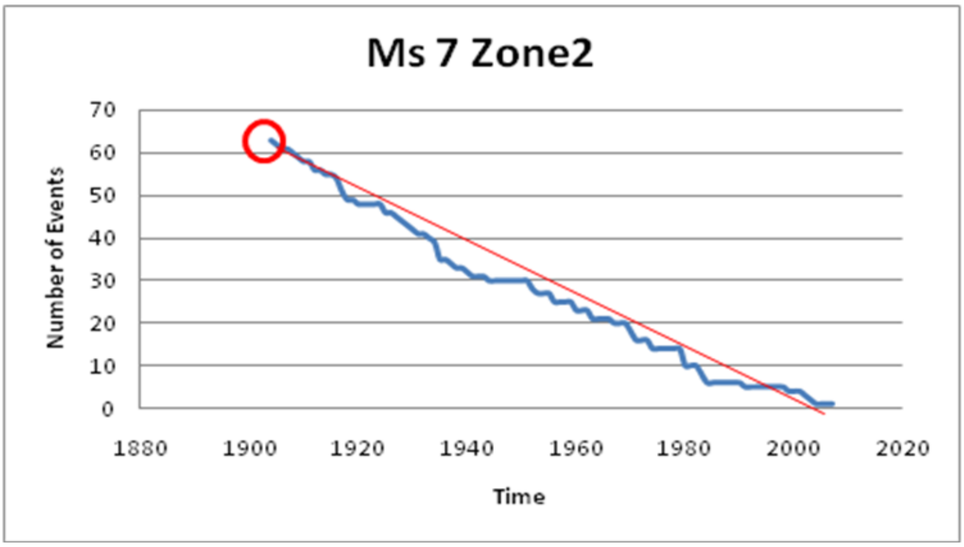

Figure 5.11: Completeness Analysis, Zone 2, Magnitude 7.

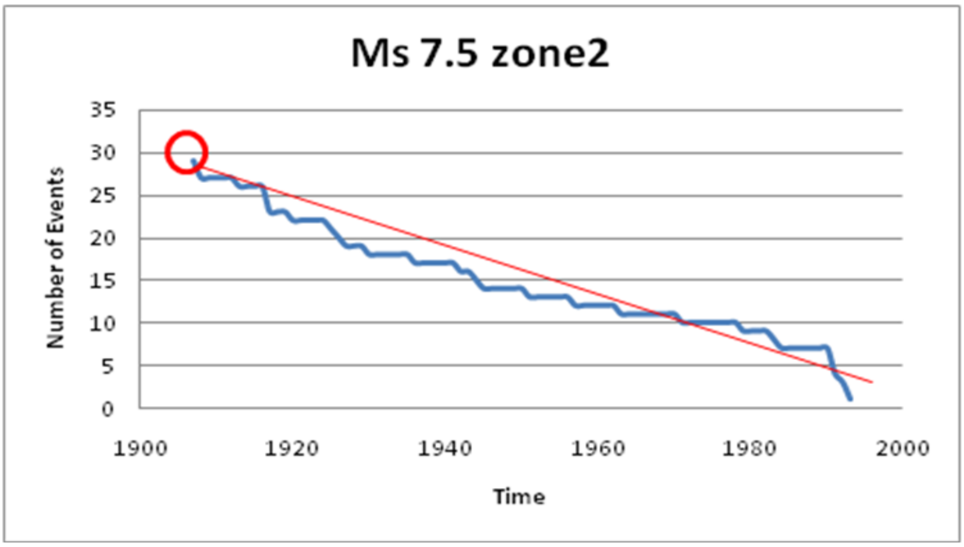

Figure 5.12: Completeness Analysis, Zone 2, Magnitude 7.5.

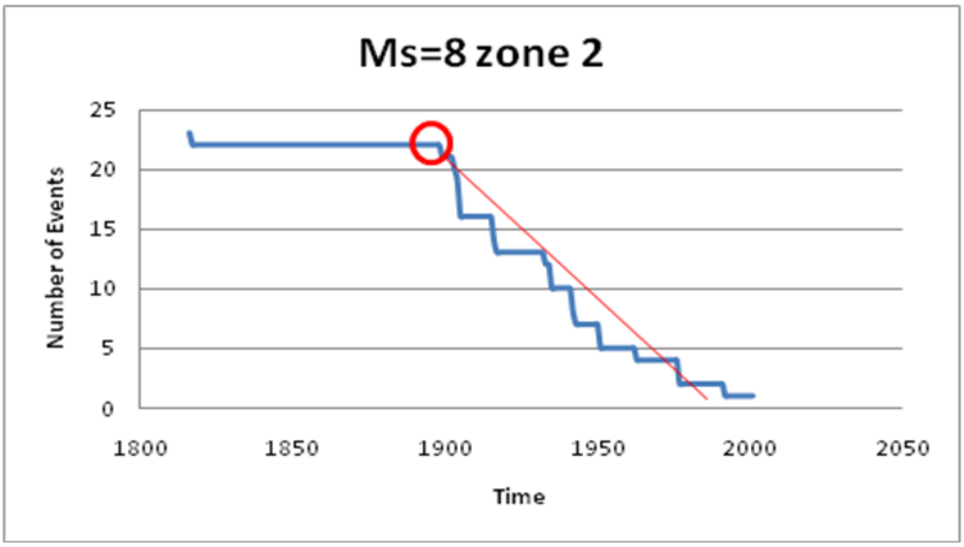

Figure 5.13: Completeness Analysis, Zone 2, Magnitude 8.

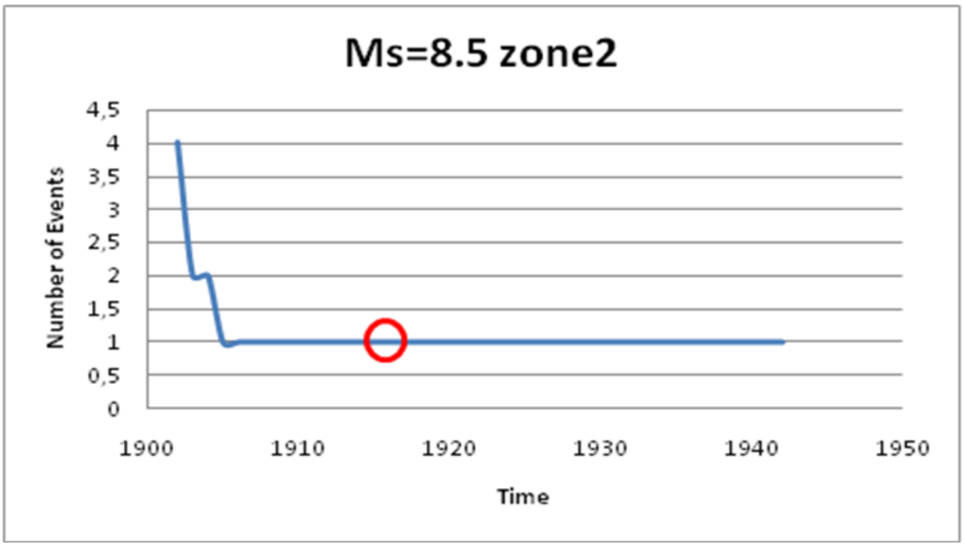

Figure 5.14: Completeness Analysis, Zone 2, Magnitude 8.5.

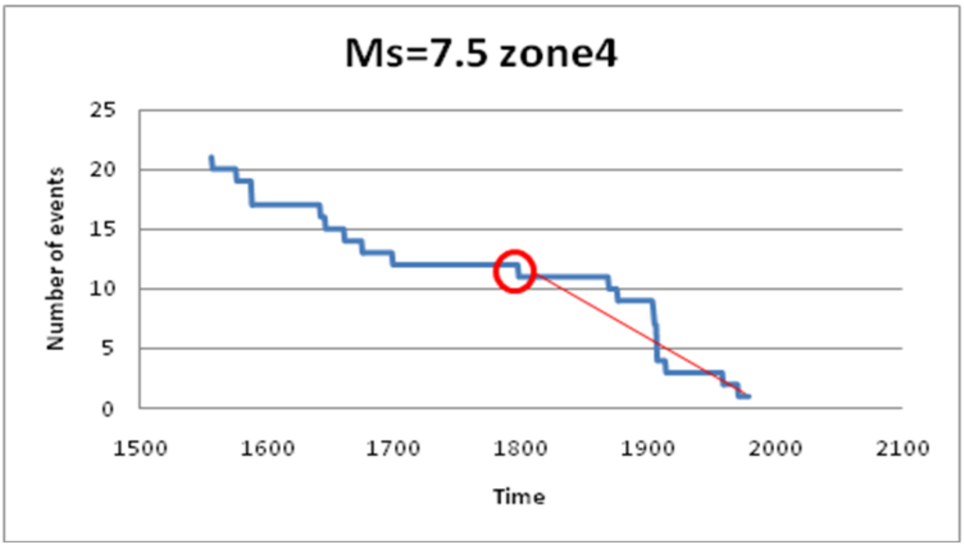

Figure 5.15: Completeness Analysis, Zone 4, Magnitude 7.5.

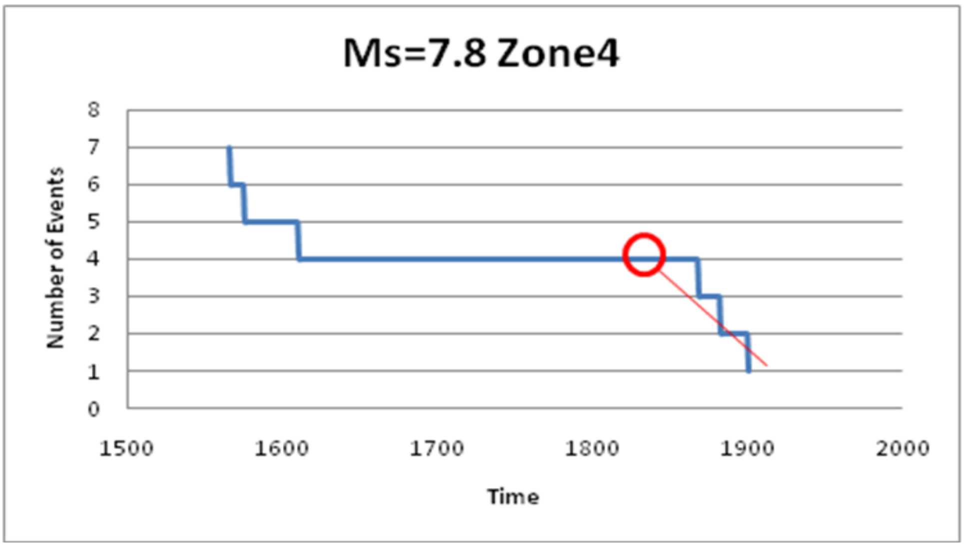

Figure 5.16: Completeness Analysis, Zone 4, Magnitude 7.8.

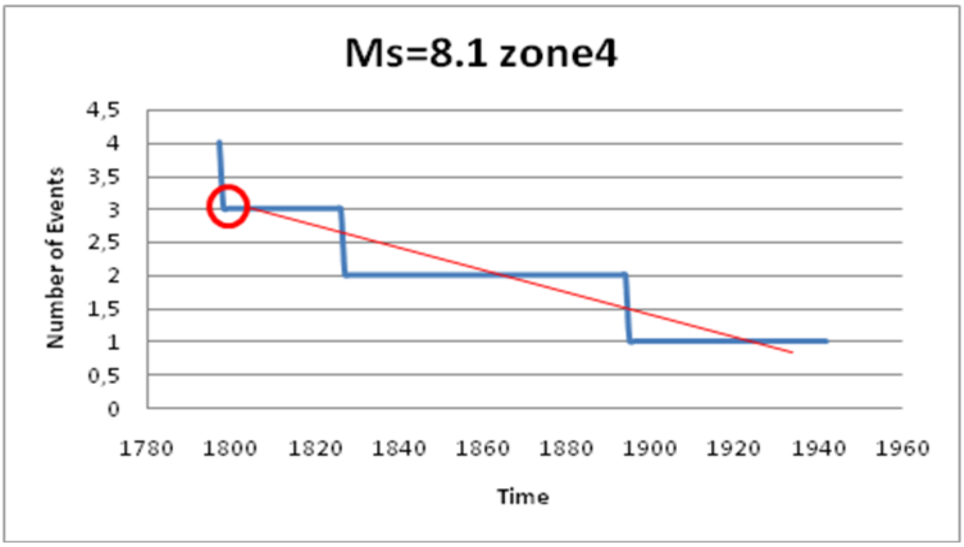

Figure 5.17: Completeness Analysis, Zone 4, Magnitude 8.1.

d) Computing the Gutenberg-Richter coefficients:
Having done the completeness analysis, the next step is to compute the Gutenberg-Richter coefficients for each zone. The cumulative Gutenberg-Richter law relates the magnitude with the number of occurred earthquakes within a region and it is given with the form:

$$Log\ N = a - bM \qquad \text{Eq. 5.1}$$

where N is the expected number of events with magnitude larger than M, a and b are the Gutenberg-Richter coefficients, that are constant for a seismic homogeneous zone. The parameter a is associated with the seismic activity of a particular region, whereas b is the power-law exponent of scaling.

The Gutenberg-Richter Equation has been modified in order to account for the maximum possible magnitude that may occur within the region studied and that is assumed to be larger than the maximum observed magnitude. The modified or truncated cumulative Gutenberg-Richter equation is shown below.

$$\log N = a + \log\left(\frac{e^{-\beta M} - e^{-\beta M_{\max}}}{e^{-\beta M_{\min}} - e^{-\beta M_{\max}}}\right) \quad \text{with} \quad \beta = \frac{\mathrm{b}}{\log \mathrm{e}} \qquad \text{Eq.5.2}$$

where M_{min} is the lower bound of the magnitude interval where the GR coefficients are estimated and M_{max} is the maximum magnitude value expected for the zone studied.

The values of a and b obtained for zone 1,2 and 4 and the magnitude range of validity are shown in table 5.1. The plot of the Gutenberg-Richter relation for the same zones are shown in figures 5.18, 5.19 and 5.20.

Table 5.1 Gutenberg-Richter Coefficients and Boundary values.

Zone	Mmin	Mmax	a	b
1	7.3	8.5	0.001	1.91
2	6	8.7	0.737	0.68
4	7.4	8.7	-0.543	1.28

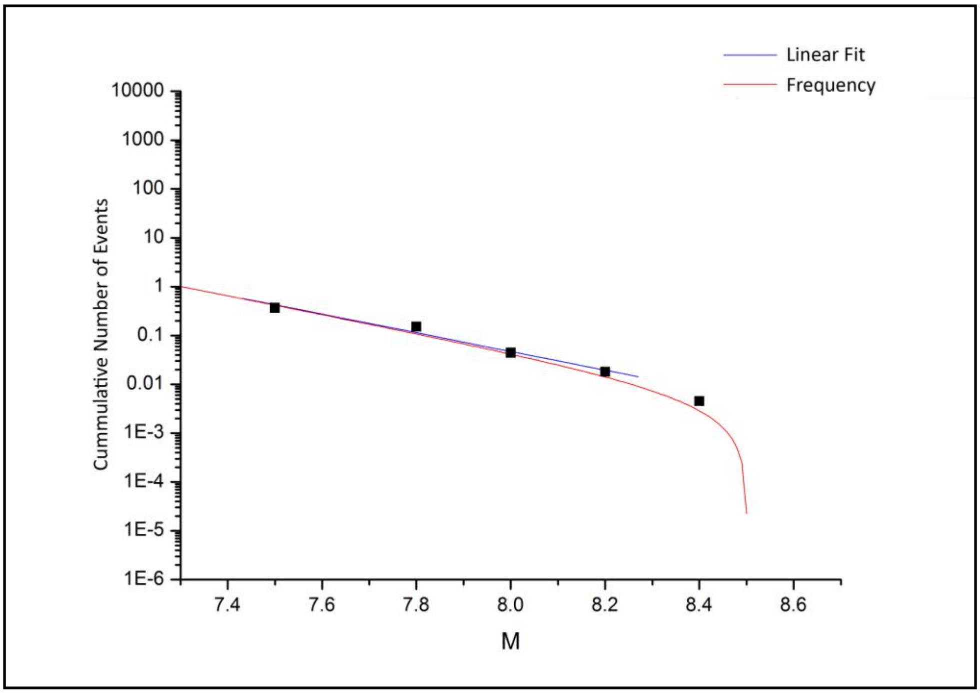

Figure 5.18: Gutenberg-Richter relation, zone 1. Note that by linear fit we mean the fit of the GR law given in Eq.5.1

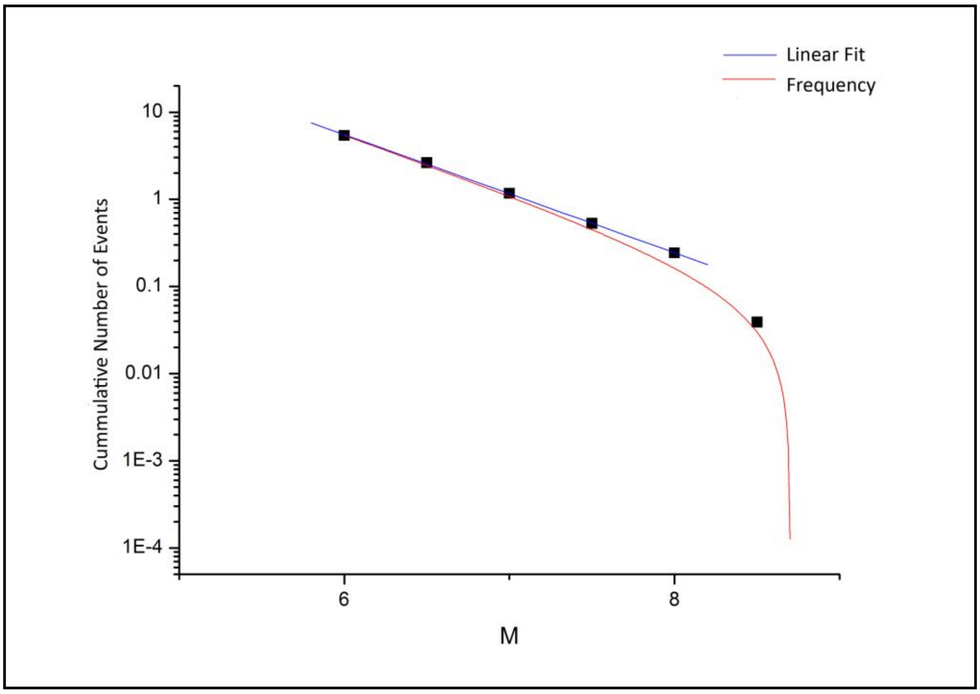

Figure 5.19: Gutenberg-Richter relation, zone 2.

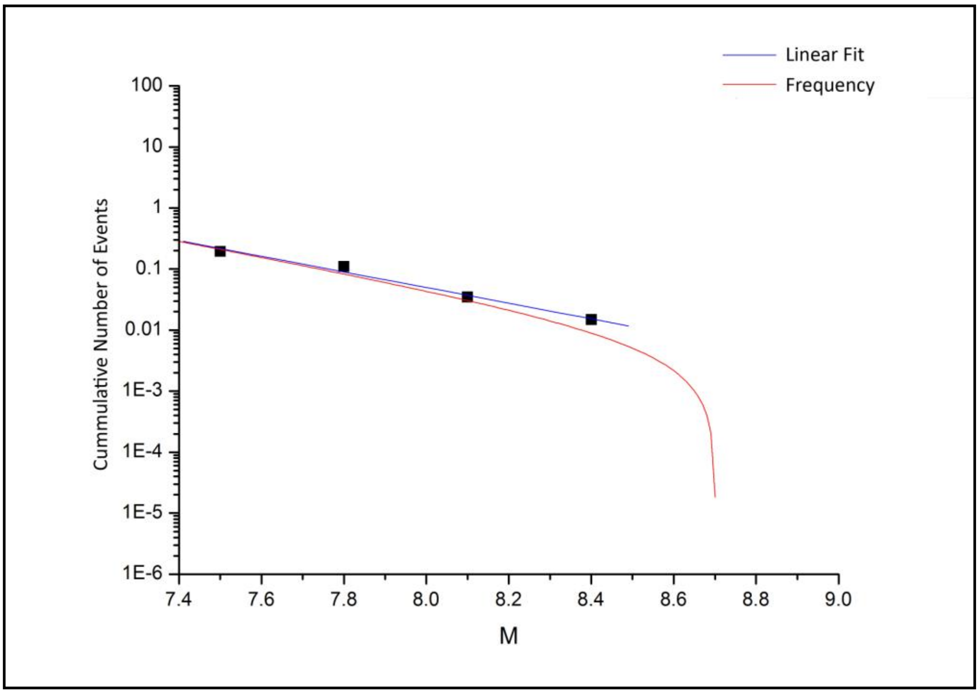

Figure 5.20: Gutenberg-Richter relation, zone 4.

e) Estimating the annual rate of occurrence

From the cumulative Gutenberg-Richter law, one can deduce the corresponding non-cumulative law and hence compute the annual rate of occurrence of an earthquake of any given magnitude (i.e. included within M and M+dM), provided it falls within the validity interval of the law. In this work we have used the cumulative distribution. The annual rate of occurrence is simply N, where N is the number of events, resulting from the application of the cumulative GR law and the corresponding return period is 1/N.

5.3. PROBABILISTIC AND DETERMINISTIC ANALYSIS

A hybrid analysis, probabilistic and deterministic, aiming at obtaining run-up values along the coast corresponding to a given annual rate of occurrence was performed. This analysis allows one to fix a run-up value and to obtain an annual rate of occurrence along the coast. The steps followed to perform the analysis are mentioned below.

a) The first step is to obtain a bathymetry chart of the region of interest, in this case, as described in chapter 3, the GEBCO data was used to build up the bathymetry of Central America. The main tectonic characteristics of the zone were identify, i.e. the Middle American Trench. Bathymetric profiles were plotted in order to gain better insight of the seafloor shape. A typical bathymetrical profile off the Pacific coast of Central America is shown in figure 5.21.

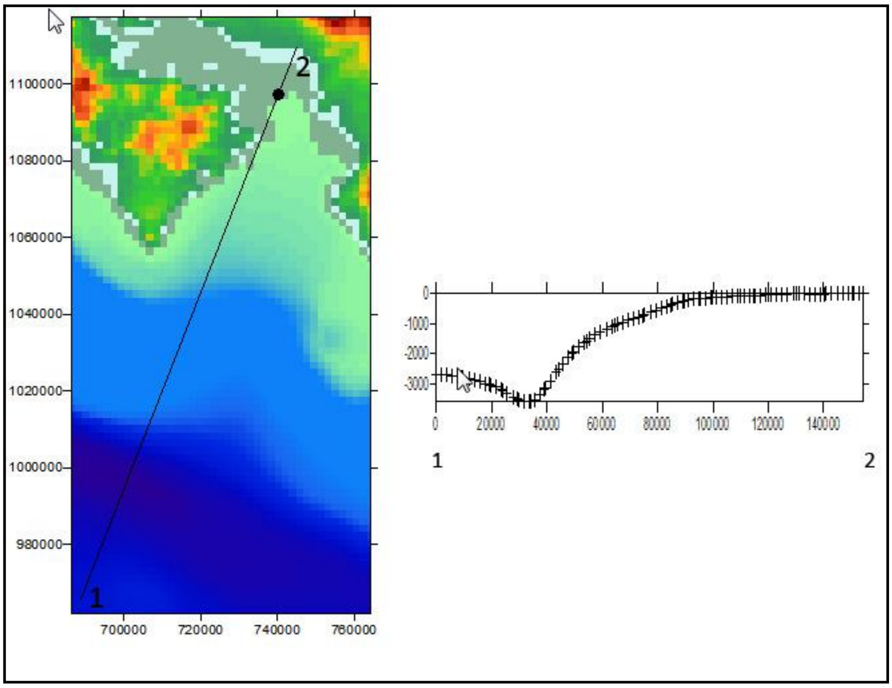

Figure 5.21: Typical bathymetrical profile along the Pacific Coast of Central America.

b) The typical profile of the Central American Pacific seafloor led us to simplify its cross section as shown in figure 5.22, where z3 is the deepest isobath line and depending on the region is 1000m or 3000m, and it is considered the limit where the seafloor reaches its maximum depth. The point shown as z2 is the second major change in the seafloor and this is considered to be 150m or 200m. The coast is located at z1 with elevation equal to zero. See figure 5.22.

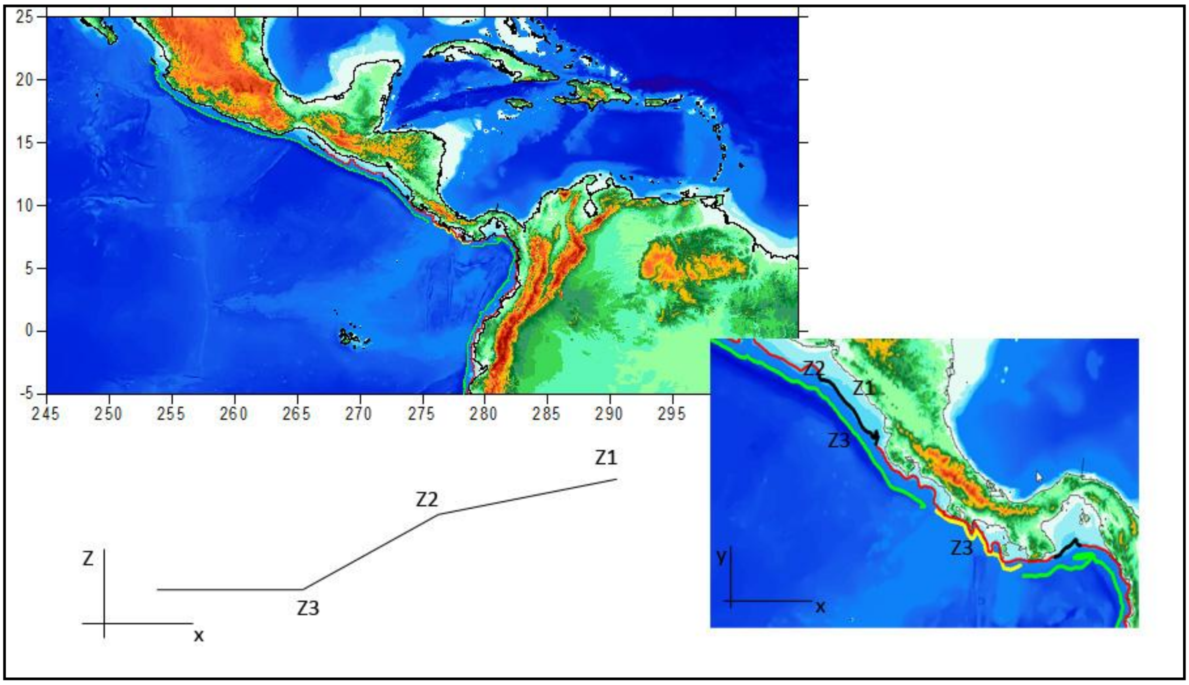

Figure 5.22: Isobaths and seafloor scheme.

c) Once established the geometry of the seafloor the next step is computing the maximum wave height offshore at depth equals to z3. In order to do so, a strike value is fixed for the fault and then a profile line, that is normal to the strike and that passes the middle point of the fault. A range of dip values is also chosen. The geometrical parameters of the fault, length (L) and rupture area (A) are computed using the Wells and Coppersmith (1994) empirical relations (see figure 5.23) for each value of magnitude (varying at steps of 0.1). The width of the fault is then computed as A/L. Using the Hanks and Kanamori (1979) formula (Equation 5.3) it is possible to relate the magnitude M to the seismic moment (Mo).

$$M = \frac{2}{3} Log(M_0) - 10.7 \qquad \text{Eq. 5.3}$$

where M is the magnitude and Mo is the seismic moment in dyne-cm.

Then the average slip (u) at the fault can be estimated through the following formula:

$$Mo = A\mu u$$

where μ is the rigidity of the crust, considered in this case as 3×10^{10} Pa, and u is the average slip of the fault.

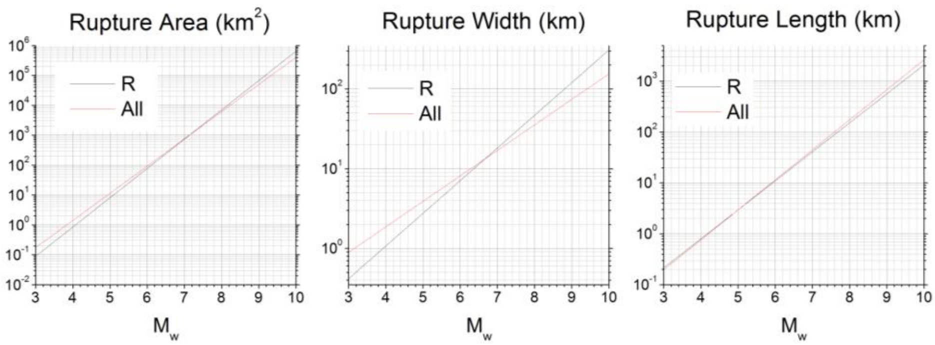

Figure 5.23: Wells& Coppersmith empirical relation.

(Wells and Coppersmith, [1994])

Finally, through the Okada (1992) model (see figure 5.24), one can compute the maximum positive amplitude of the wave u_z^{max} . At the end of this step, values of dip and u_z^{max} are associated to each magnitude value (varying with steps of 0.1).

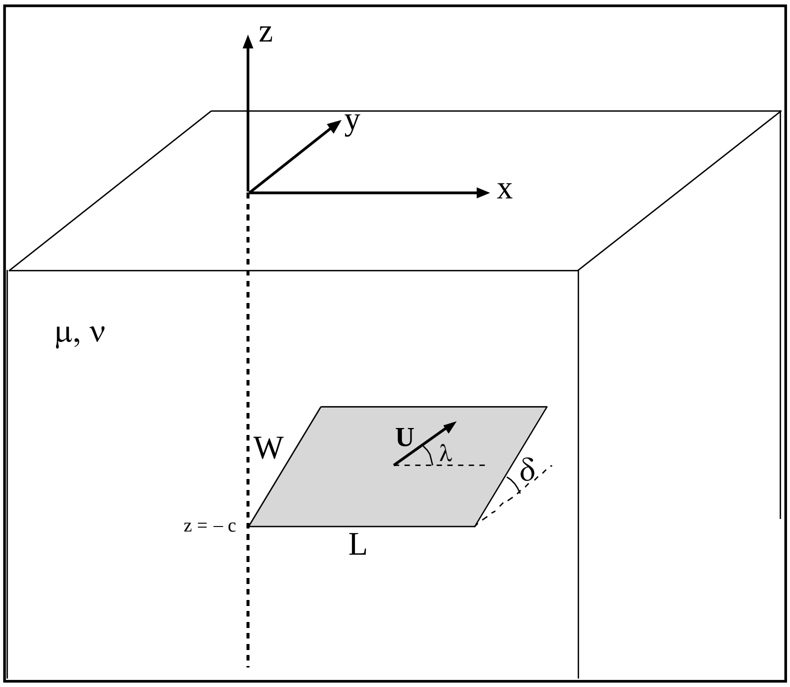

Figure 5.24: Okada Model.

(Okada, [1992])

d) Taking into account the bathymetry data, and considering that the deepest isobath is z3, a series of profiles going from z3, passing z2 and reaching z1 are plotted. See figure 5.25 The isobaths z3, z2 and z1 are interpolated, in order to have the same number of points along them, the profiles are plotted joining the respective points from line z3 to z1. Computing the intersection point between the line z3 to z1 and the isobaths z2, and knowing the value of isobath z2, then the slope from z2 to z1 can be established.
The region is also divided into zones with different values of dip, and also different Gutenberg-Richter coefficients and different maximum magnitude values.

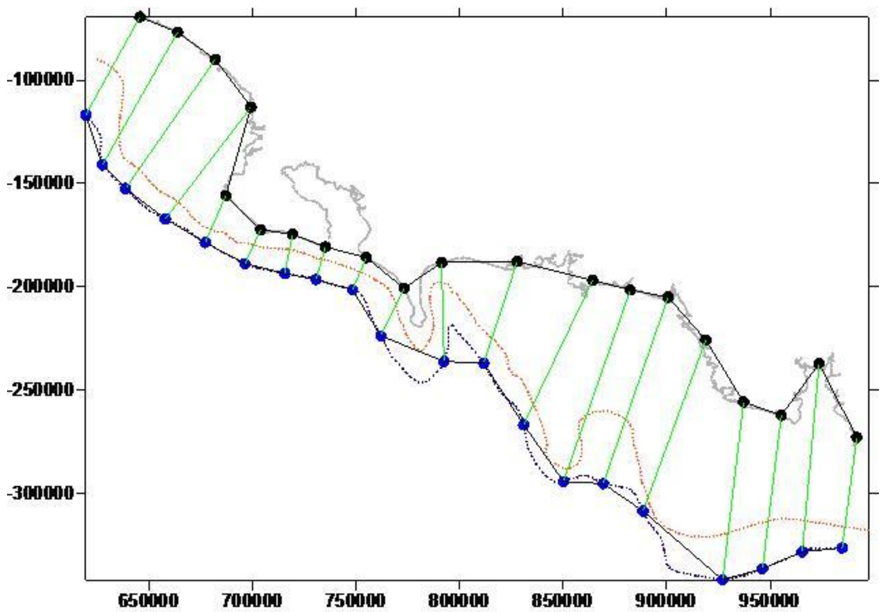

Figure 5.25: Profile Distribution along a segment of the Pacific Central American Coast.

e) Each profile is then related to one of the zones defined in the statistical analysis, therefore values of Gutenberg-Richter coefficients (a, b), M_{max} and slip (δ) are assigned to each profile.

- Then, the number of events N exceeding the maximum magnitude M_{max} can be estimated for a single profile.
- For each profile, given a magnitude value and u_z^{max}, the wave amplification at z2 can be estimated using the Green's law (equation 5.4), the value obtained is called u_z^{max}.

$$\frac{\eta_2}{\eta_1} = \left(\frac{H_1}{H_2}\right)^{1/4} \qquad \text{Eq. 5.4}$$

where η_1 and η_2 are the wave heights at depths H_1 e H_2, with $H_1 > H_2$.

- Finally, the run-up (R) at the coast (z1) can be estimated using the Synolakis (1987) equation (Eq. 5.5),.

$$R = 2.831H\sqrt{\cot \propto}\left(\frac{H}{d}\right)^{\frac{1}{4}} \qquad \text{Eq 5.5}$$

Where R is the run-up, H is the wave height offshore at depth d and $\propto$ is the slope of the seafloor.

At the end of the analysis, an output table with values of magnitude (M), annual number of events (N), run-up(R) is obtained. Then, the annual rate of events per year can be computed as 1/N. If the value 1/N is fixed, then the run-up distribution along the coast can be plotted. Otherwise, if the run-up values are fixed, then the corresponding annual rate of occurrence along the coast can be plotted.

5.4. DETERMINISTIC ANALYSIS

The deterministic approach will be performed using the code UBO-TSUFE MODEL, which is a finite element code developed by the Tsunami Research Team of the University of Bologna. The model solves linear and non linear shallow water equations in Cartesian coordinates on a fixed-boundary grid, the model will be described in section 5.4.1. The parameters of the historical events chosen as scenarios will be mentioned in section 5.4.2.

5.4.1 The UBO-TSUFE Model

The UBO-TSUFE Model has been created to compute the extreme water elevation along coastal regions. The model solves the Navier Stokes equations for shallow water (see Equation 5.6 a and b) considering an incompressible and non-viscous fluid, therefore the condition of wavelength much larger than the seafloor depth must be satisfied. Tsunami wavelengths are usually within tens or even hundreds of kilometres, whereas the seafloor depths are generally smaller than

10km. Seafloor depth at the Pacific basin in Central America is not greater than 3000 or 4000m, as mentioned in Chapter 3 therefore the previous condition is satisfied.

$$\partial_t \eta = \partial_t h_s - \nabla \cdot [(h+\eta)\, \vec{v}] \qquad \text{Eq. 5.6a}$$

$$\partial_t \eta = \partial_t h_s - \nabla \cdot [(h+\eta)\, \vec{v}] \qquad \text{Eq. 5.6b}$$

where η is the instant height of the sea water surface over the average level of equilibrium, $\boldsymbol{h}$ is the local depth, $\vec{v}$ is the vector of horizontal velocity and g is the acceleration of gravity. Effects of forced variable excitation is considered in equation 5.6a, with the term $\partial_t \boldsymbol{h}_s$. Equation 5.6a represents the continuity equation, whereas 5.6b is the moment conservation equation.

The boundary conditions are of full wave transmission at the open boundaries (open ocean) and of partial reflection at the coastal boundaries (Tinti et al, 1994). The open boundary conditions are described by equation 5.7 and this condition allows the tsunami waves propagating towards the open sea to leave the domain boundaries without reflective effects. In equation 5.7, $\vec{n}$ is the versor normal to the boundary and its direction is going outside the domain.

$$\vec{v} \cdot \vec{n} = \frac{g}{c}\eta \qquad \text{Eq. 5.7}$$

At the coast, the boundary conditions are of partial reflection, this condition is imposed through equation 5.8, where R is the reflexion coefficient that can vary between 0 and 1, R =1 is the condition of pure reflexion, whereas R <1 means a loss of energy at any interaction with the boundary, in this case the coast.

$$\vec{v} \cdot \vec{n} = \frac{g}{c}\eta(1-R) \qquad \text{Eq. 5.8}$$

The model assumes that the coast does not move with the waves, which means that is considered as a vertical wall. The previous assumption does not allow one to compute the inundation or run-up values, but technically the maximum water elevation in the prosimity of the shoreline on the sea (wet) side.

A further loss of energy can be included at the boundary conditions to the coast through the insertion of the term $\partial_t K_\alpha - (\vec{v} \cdot \vec{t})^2 (1 - C_t^2)$ where K is the spatial density of the kinetic energy of the tsunami, $\vec{t}$ is a versor tangent to the coast and C_t is a coefficient that takes values between 0 and 1. If C_t=1, then there is no friction at the boundary and therefore there is no loss of energy; whereas C_t=0 implies that the energy dissipation due to currents parallel to the coast is maximum.

In this study, the values of R and C_t are 0.99 and 0.95, respectively; this allows us to control the numerical instabilities during long-term simulations with heavy boundary irregularities, and also gives a modest loss of energy over the shore associated to the seafloor friction.

This system of equations is then solved over triangle-element grids with variable dimensions, these grids are built by using an isotropic algorithm. The dimension of each triangle depends on the depth of the seafloor, h . Generally speaking, the goal is to make as uniform as possible the crossing time of the elements when creating the grids, $t_e = \frac{l_e}{v_e}$. Given that the velocity is a function of the depth $v_e = \sqrt{gh}$, then keeping constant the crossing times means that the length of the elements l_e increases with h The elements near the coast, where the values of h are less deep, are smaller than those at the open sea, and this allows to define the coastline accurately, see figure 5.26.

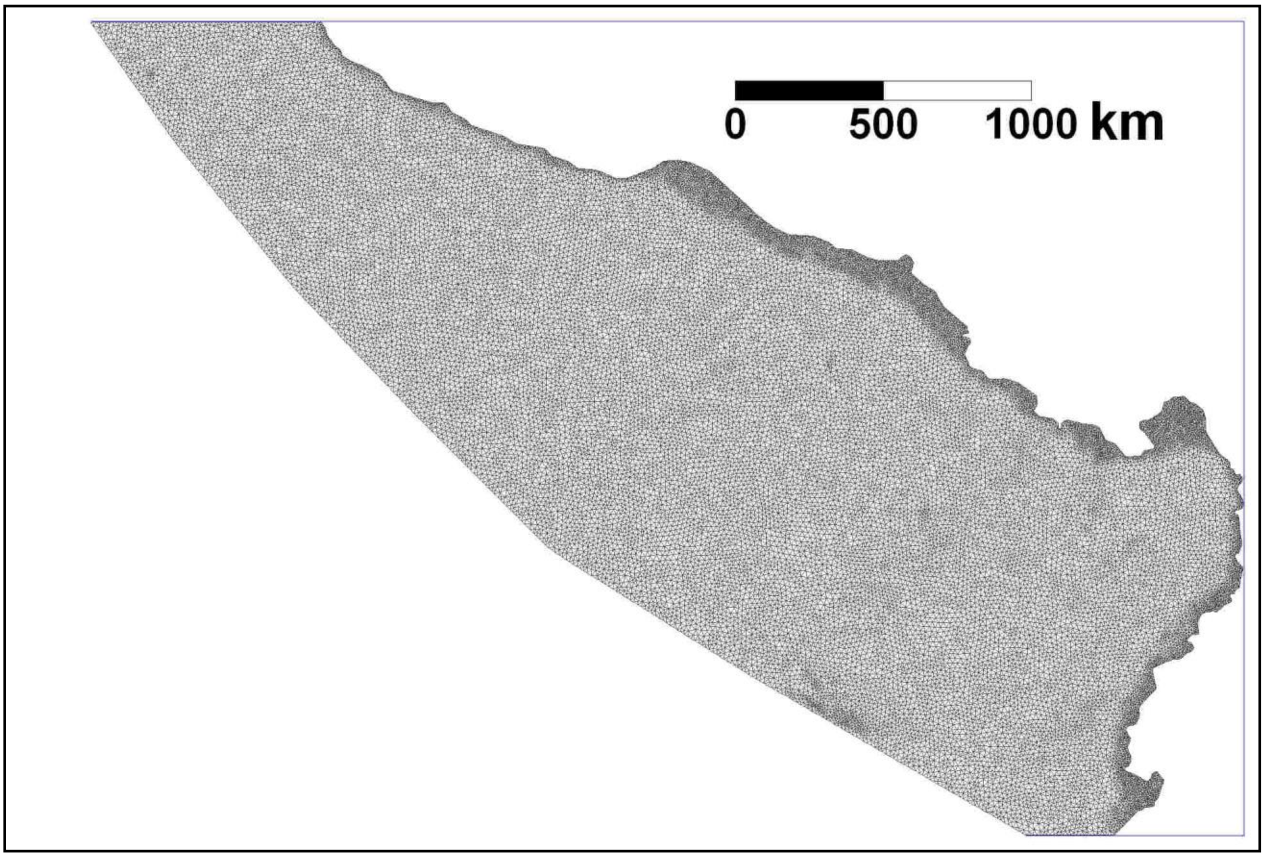

Figure 5.26: Triangular-element grid used for the simulation of the scenarios.

6. RESULTS

6.1. OVERVIEW

The results of the statistical and deterministic approaches are shown in this chapter. The results of the statistical analysis give the possibility of estimate the annual rate of occurrence. A hybrid analysis, probabilistic and deterministic, allows to estimate run-up values along the coast corresponding to a given annual rate of occurrence. The deterministic analysis thrown values of extreme water elevation and propagation fields for six historical scenarios.

6.2. STATISTICAL APPROACH

The Gutenberg-Richter coefficients that were compute for zones 1,2 and 4 (See the Section 5.2) are shown in table 6.1. Values of the annual rate of occurrence (N) and the corresponding return period (1/N) can be computed through the modified or truncated cumulative Gutenberg-Richter equation shown below.

$$\log N = a + \log\left(\frac{e^{-\beta M} - e^{-\beta M_{\max}}}{e^{-\beta M_{\min}} - e^{-\beta M_{\max}}}\right) \quad \text{with} \quad \beta = \frac{\mathbf{b}}{\log \mathbf{e}} \qquad \text{Eq.5.2}$$

where M_{min} is the lower bound of the magnitude interval where the GR coefficients are estimated and M_{max} is the maximum magnitude value expected for the zone studied.

Table 6.1 Gutenberg-Richter Coefficients and Boundary values.

Zone	Mmin	Mmax	a	b
1	7.3	8.5	0.001	1.91
2	6	8.7	0.737	0.68
4	7.4	8.7	-0.543	1.28

6.3. PROBABILISTIC AND DETERMINISTIC ANALYSIS

A hybrid analysis, probabilistic and deterministic, aiming at obtaining run-up values along the coast corresponding to a given annual rate of occurrence was performed. The results after the analysis are shown below.

The typical profile of the Central American Pacific seafloor led us to simplify its cross section as shown in figure 5.22. One hundred and thirty Bathymetric profiles were plotted in order to gain better insight of the seafloor shape, the region was divided into 4 sub regions based on the shape of the seafloor. The profiles considered in the analysis are shown in figures 6.1 to 6.4, where the isobaths chosen for each case are shown, the shallowest isobaths in all cases is 200m whereas the deepest isobaths vary from sub region with the values shown.

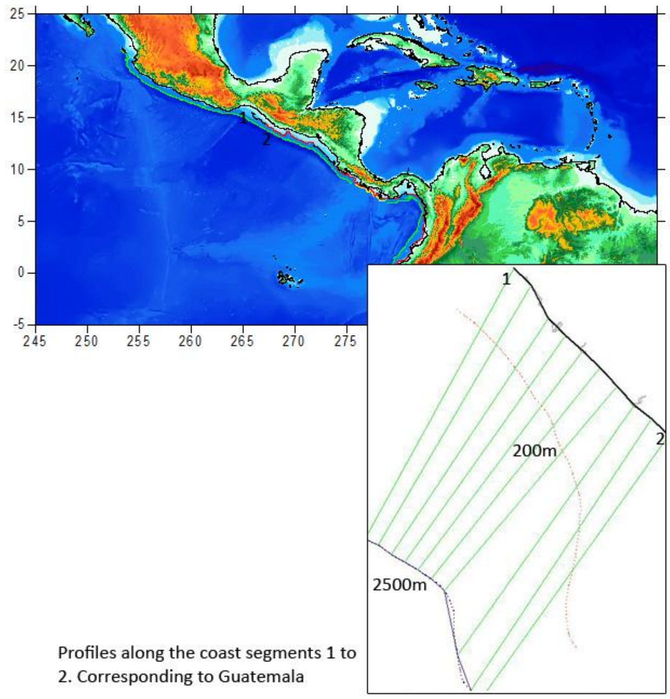

Figure 6.1: Profiles along the coast corresponding to Guatemala.

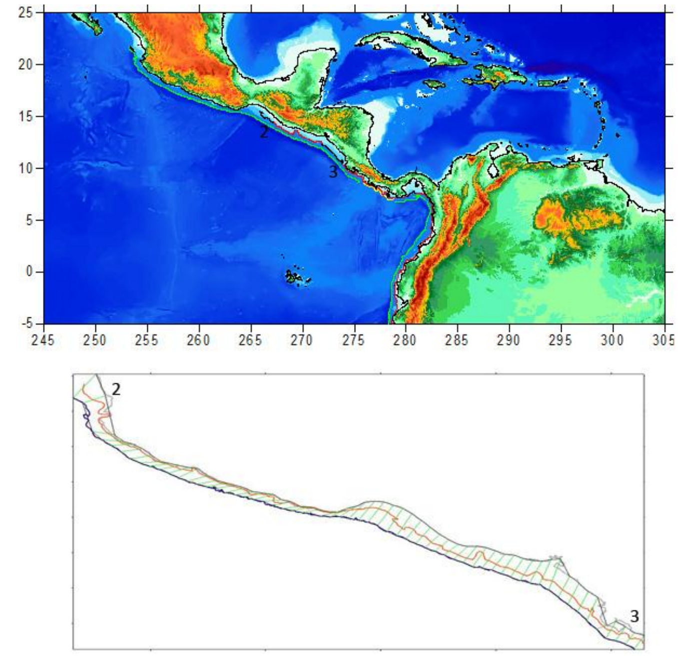

Profiles along the segment coast 2 to 3 from Guatemala to Nicaragua

Figure 6.2: Profiles along the coast from Guatemala to Nicaragua.

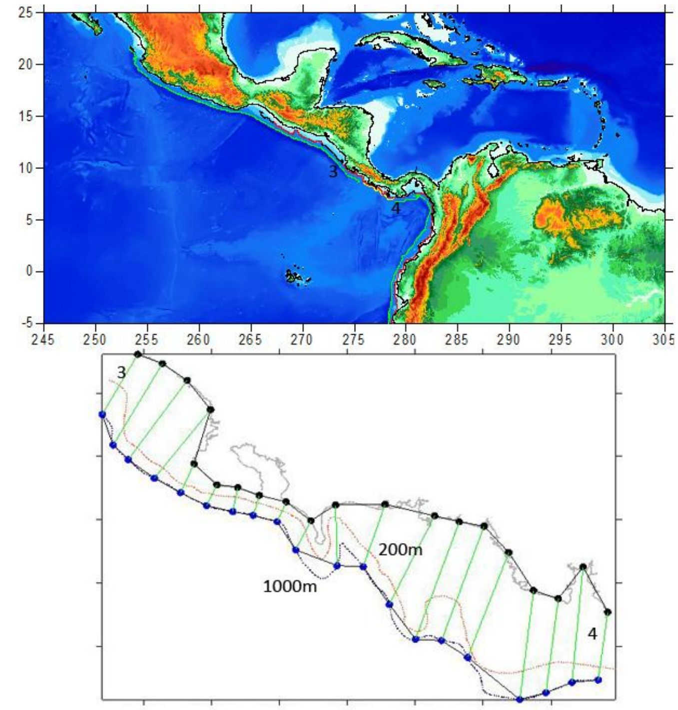

Profiles along the segment 3 to 4, from Costa Rica to Panama

Figure 6.3: Profiles along the coast from Costa Rica to Panama.

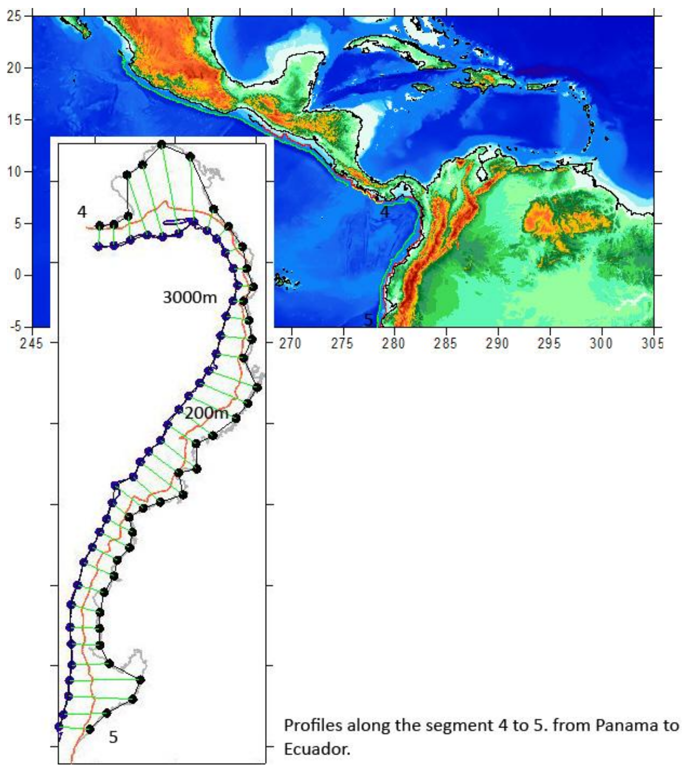

Figure 6.4: Profiles along the coast from Panama to Ecuador.

The methodology explained in Section 5.3 was followed for all the 130 profiles that described the Pacific Central American coast. At the end of the analysis, an output table with values of magnitude (M), run-up(R) was obtained. Then, the annual rate of events per year is 1/N. Examples of the output of this analysis are shown in table 6.2.

Table 6.2 Profile 1, Run-up estimation for variable Magnitude values.

Profile	Zone	M	1/N (years)	R (m)
1	1	7.3	6.9839	0.169591
1	1	7.4	10.88143	0.235711
1	1	7.5	16.97959	0.324412
1	1	7.6	26.55786	0.442614
1	1	7.7	41.69399	0.599217
1	1	7.8	65.84412	0.805643
1	1	7.9	104.974	1.076502
1	1	8	169.9843	1.430432
1	1	8.1	282.6233	1.891199
1	1	8.2	492.7555	2.488988
1	1	8.3	944.8483	3.262258
1	1	8.4	2306.995	4.259836
1	1	8.5	31941.77	5.543857

Where output values of 1/N (recurrence time in years), run-up in metres(R) are shown for profile 1 that belong to Zone 1.

Run-up estimation for profile 1, at its coastal point can be found by fixing the recurrence time, (1/N), the return period (T) values when doing so are shown in table 6.3. On the contrary, when fixing run-up values, estimated values of the Return Period (T), at the coastal point of profile 1, can be found. The values of Return period are shown in table 6.4. The x and y coordinates in table 6.2 and 6.3 are in the UTM system.

Table 6.3 Profile 1, Run-up estimation for fixed Return Periods.

Profile	x	y	R (m)	T year
1	-1821783	1499600	0.670214	50
1	-1821783	1499600	1.042072	100
1	-1821783	1499600	2.50138	500
1	-1821783	1499600	3.302649	1000

Table 6.4 Profile 1, Return Period estimation for fixed Run-up values.

Profile	x	y	T years	R (m)
1	-1821783	1499600	93.92205	1
1	-1821783	1499600	320.8687	2
1	-1821783	1499600	19389.74	5

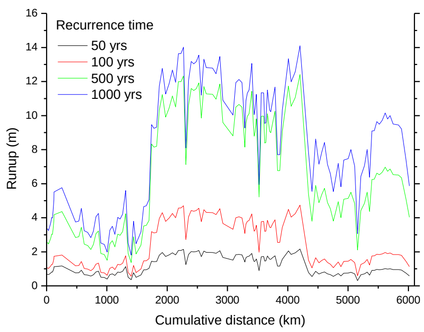

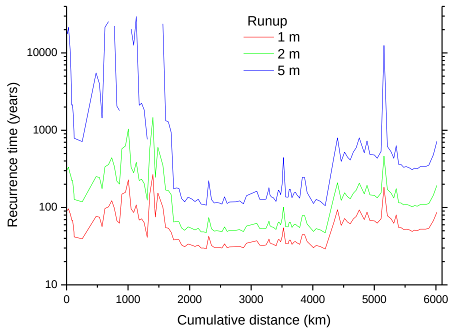

6.4. DETERMINISTIC ANALYSIS

The deterministic approach was performed by using the code UBO-TSUFE, which is a finite element code developed by the Tsunami Research Team of the University of Bologna, see chapter 5. The model solves linear and non linear shallow water equations in Cartesian coordinates on a fixed-boundary grid (see picture 5.26). The scenarios chosen for this analysis are six earthquakes occurred along the Middle American Thrench (see figure 6.4), the parameters of each earthquake have been established after technical papers or estimated as characteristic values of the area. The scenarios chosen and the results of the numerical simulations are shown below.

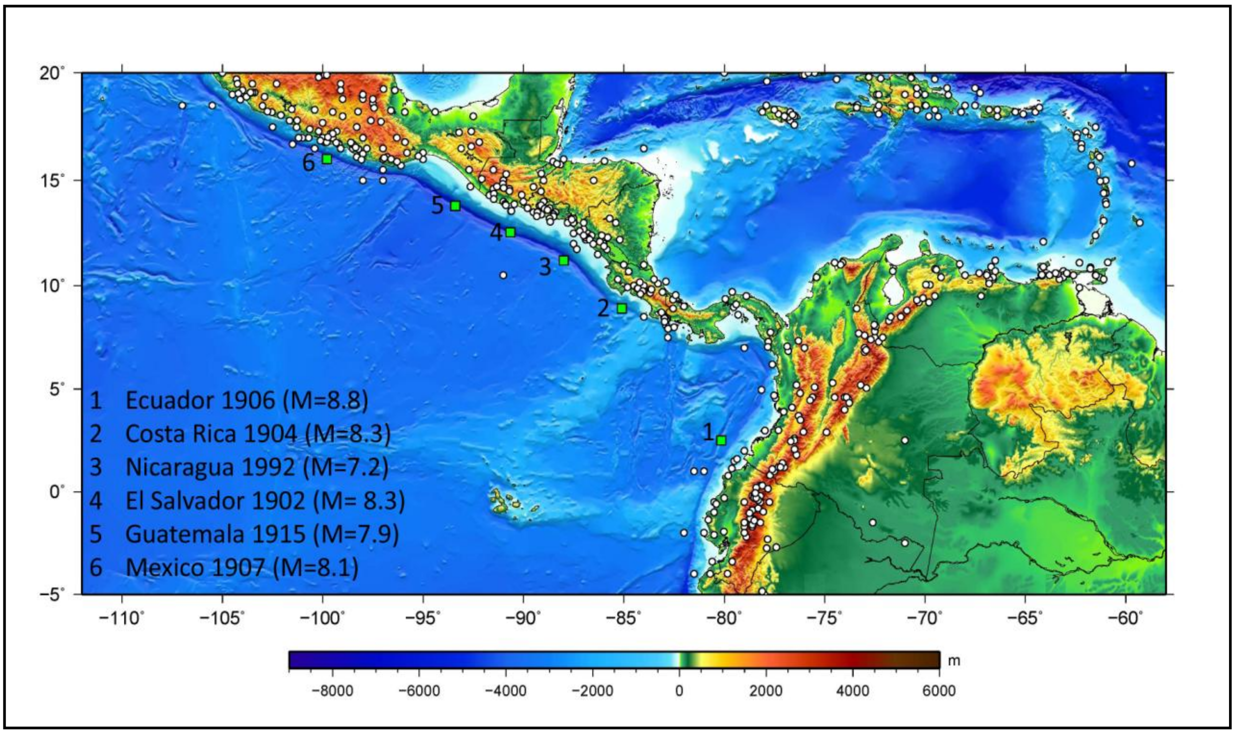

Figure 6.4: Scenarios along the Middle American Trench.

6.1.1 Ecuador 1906

The 31 January 1906 Ecuador earthquake had a M_w equal to 8.8 and an associated rupture of approximately 500 km along the Ecuador-Colombia Trench (Scott M., et al, [2003]). This event triggered a devastating tsunami that left more than 500 victims and propagated northern as far as Central America, San Diego and San Francisco and western as far as Japan. The tsunami waves reached at least 5 m that destroyed 49 houses and killed 500 people in Colombia. (Lander and Lockridge, [1989a and b]).

The parameters of the earthquake are shown in table 6.5, whereas the initial conditions for the UBO-TSUFE MODEL are shown in picture 6.5.

Table 6.5. Parametres of Scenario 1, Ecuador 1906 (M=8.8)

L (km)	631
W (km)	107
Strike (°)	30
Dip (°)	20
Rake (°)	90
Slip (m)	17.5
Position (longitude, latitude)	-80.15, 2.5

Depth (km)	5
Magnitude	9

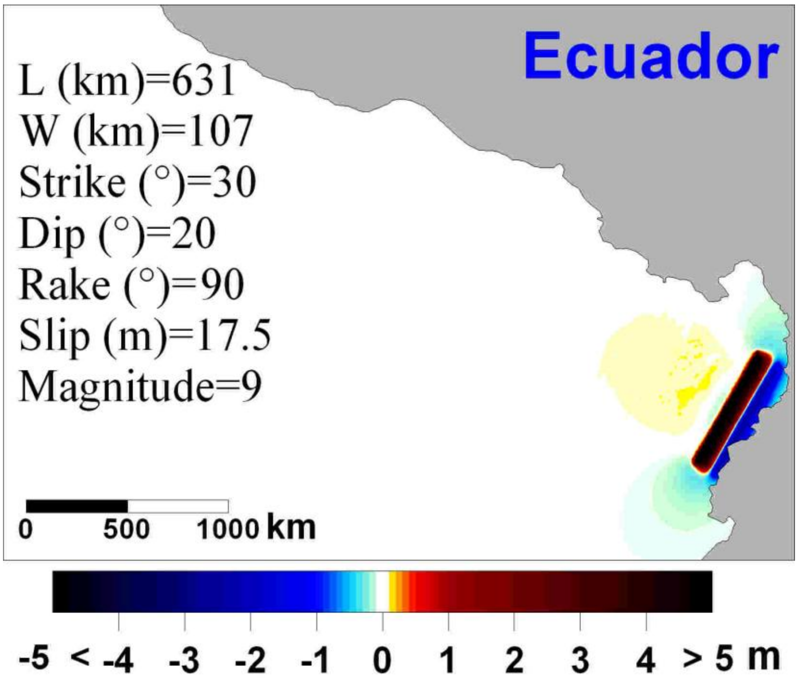

Figure 6.5: Initial Conditions of Scenario 1, Ecuador 1906.

The results obtained for the Ecuador 1906 event are the propagation of tsunami waves at different time intervals and the maximum and minimum water elevation levels. The propagation field is shown in figure 6.6, where it can be seen that tsunami waves propagated north-west, striking the coast within 30 minutes after the earthquake with wave heights exceeding 5 m. From figure 6.6 it can be also seen that after 5 hours the tsunami waves where not dissipated and continued travelling to the north-west. The maximum and minimum wave height for the Ecuador 1906 scenario are shown in figure 6.7. According to the results, the maximum wave height values occurred near the coast, and were higher than 10m; the waves propagated following the source shape pattern to the north-west. The minimum wave height values on the other hand, occurred almost exclusively near the coast, reaching depths of -3 m.

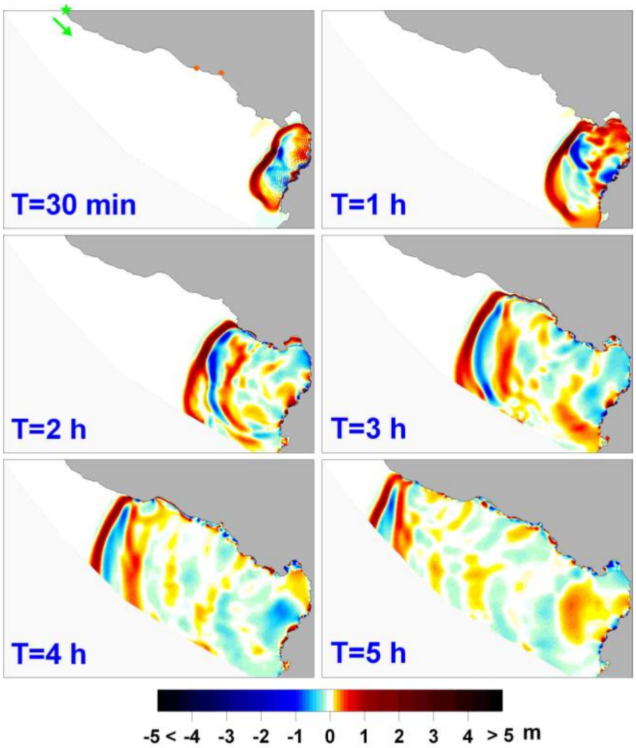

Figure 6.6: Propagation of the Tsunami waves for the Scenario 1, Ecuador 1906.

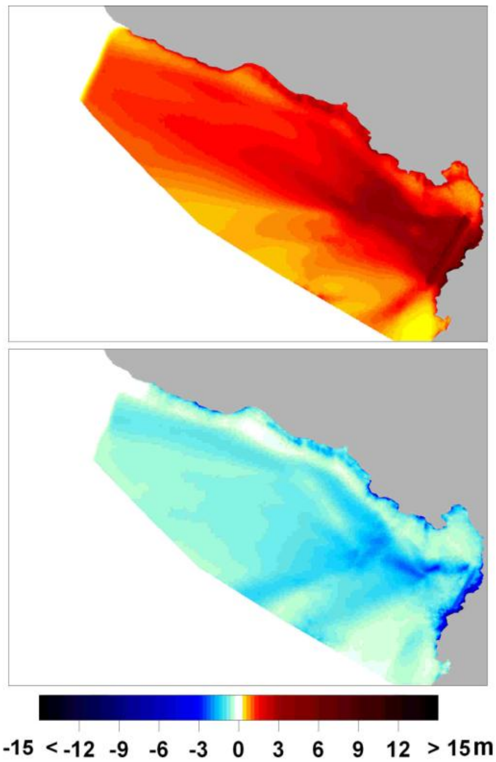

Figure 6.7: Maximum and minimum water elevations for the Scenario 1, Ecuador 1906.

6.1.2 Costa Rica 1904

The 20 January 1904 Costa Rica earthquake had a Ms equal to 7, the earthquake was felt also in Panama. Reports of a sailing ship crew near the Revilla Griego Island, in Panama, concerned observations of floating three-trunks and animal bodies and can be considered as evidence of tsunami (Molina, E., [1997]).

The parameters of the earthquake are shown in table 6.6, whereas the initial conditions for the UBO-TSUFE MODEL are shown in picture 6.8.

Table 6.6. Parametres of Scenario 2, Costa Rica 1904 (M=8.3)

L (km)	324
W (km)	68
Strike (°)	298
Dip (°)	16
Rake (°)	90
Slip (m)	9.6
Position (longitude, latitude)	-85.1, 8.9
Depth (km)	5
Magnitude	8.5

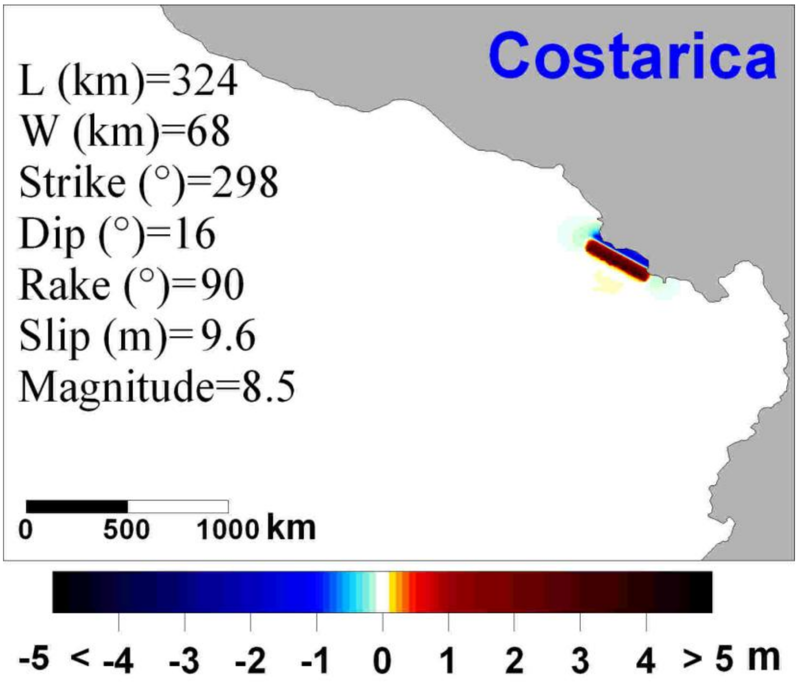

Figure 6.8: Initial Conditions of Scenario 2, Costa Rica 1904.

The propagation field shows that the tsunami waves travel south-west and, see figure 6.9. The event propagates locally and the wave heights do not exceed 1m. The waves are almost dissipated after 2 and a half hours from the earthquake occurrence. Maximum and minimum wave heights are shown in figure 6.10. According to the results, the maximum values occurred at the coast right in front of the source and at the south-eastern coast from the source, and the minimum elevations followed more or less the same pattern.

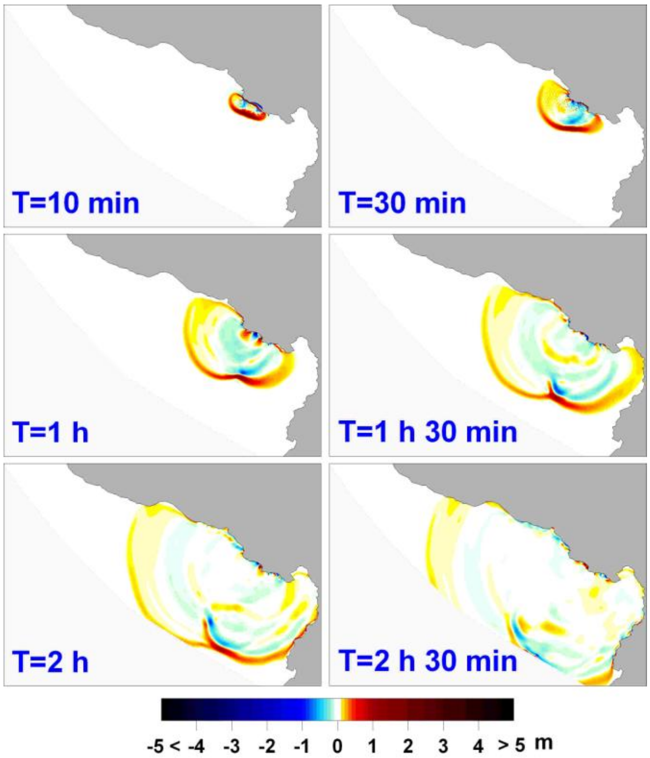

Figure 6.9: Propagation of the Tsunami waves for the Scenario 2, Costa Rica 1904.

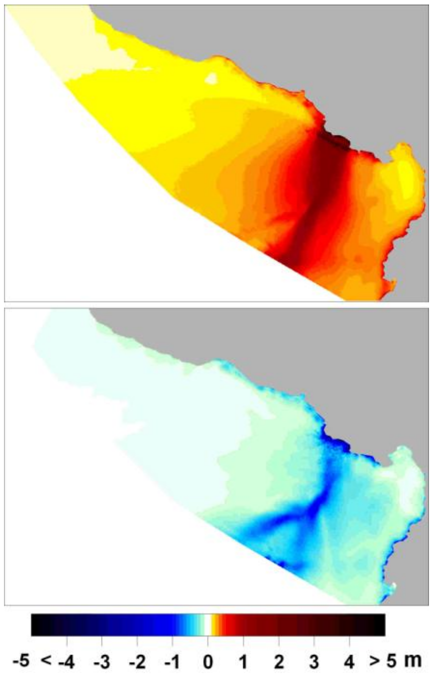

Figure 6.10: Maximum and minimum water elevations for the Scenario 2, Costa Rica 1904.

6.1.3 Nicaragua 1992

On 2 September 1992, an Ms 7.0, Mw 7.7, earthquake occurred 100 km offshore Nicaragua at 45 km depth within the Cocos-Caribbean Plate subduction zone in the Pacific Coast. The event lasted about 100 seconds; its rupture length was estimated as 100 km wide by 200 km long and the velocity of rupture of about 1 to 1.5 km/s. The earthquake was barely felt by the coastal inhabitants, but it generated a very destructive tsunami that hit the coast between 40 and 70 minutes later. Run-up heights measured at different points at Nicaraguan coast varied between 2 and 6 meters. The maximum run-ups recorded were about 10 meters. The tsunami struck mainly the Nicaraguan coast, other Central American countries recorded small tsunami waves. After this event 170 fatalities and about 13,000 homeless were reported. The direction of propagation was westwards and 10 cm-height waves were recorded in Japan and Hawaii (Bryant, E., [2001], Satake et al., [1993], Gonzalez, F., [1999]).

The parameters of the earthquake are shown in table 6.7, whereas the initial conditions for the UBO-TSUFE MODEL are shown in picture 6.11.

Table 6.7. Parametres of Scenario 3, Nicaragua 1992 (M=7.2)

L (km)	85
W (km)	27
Strike (°)	312
Dip (°)	16
Rake (°)	90
Slip (m)	2.9
Position (longitude, latitude)	-88.0, 11.2
Depth (km)	5
Magnitude	7.5

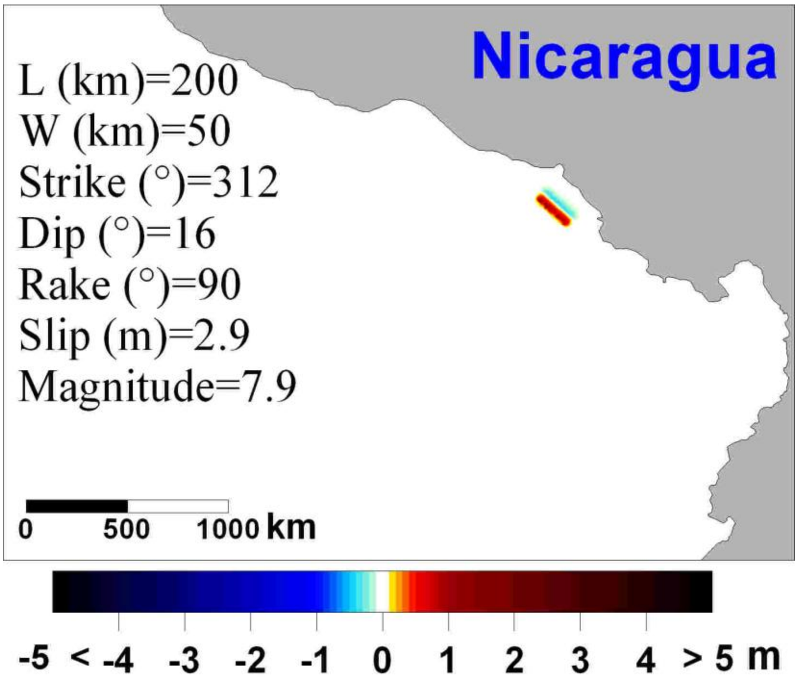

Figure 6.11: Initial Conditions of Scenario 3, Nicaragua 1992.

The 1992 Nicaraguan scenario propagated south-west from the source, according to the UBO-TSUFE MODEL. The front waves reached the coast within an hour from the earthquake occurrence. The tsunami propagated locally and its effects were over about 2 and a half hours from the earthquake, see figure 6.12. The maximum wave height values were concentrated near the source region and at the coast in front of it, the minimum wave height values were deeper than -1m, see figure 6.13.

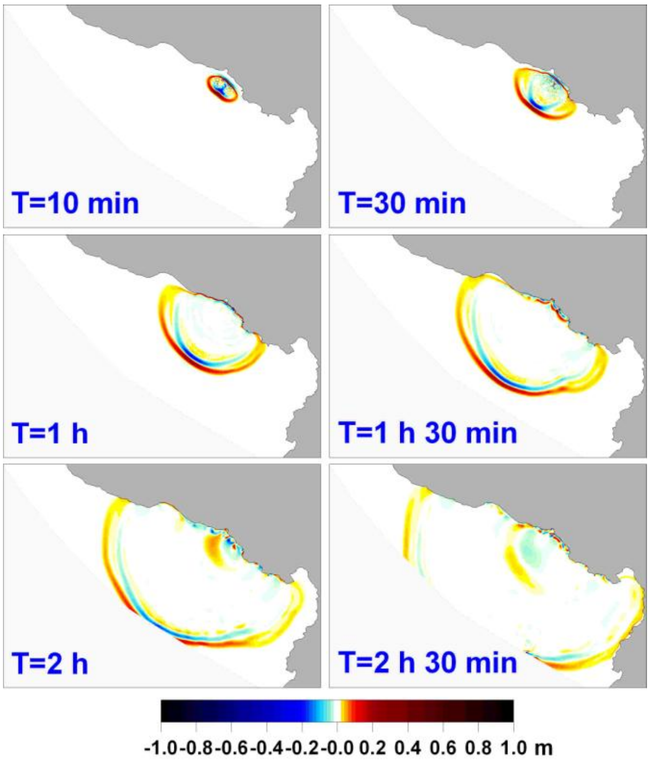

Figure 6.12: Propagation of the Tsunami waves for the Scenario 3, Nicaragua 1992.

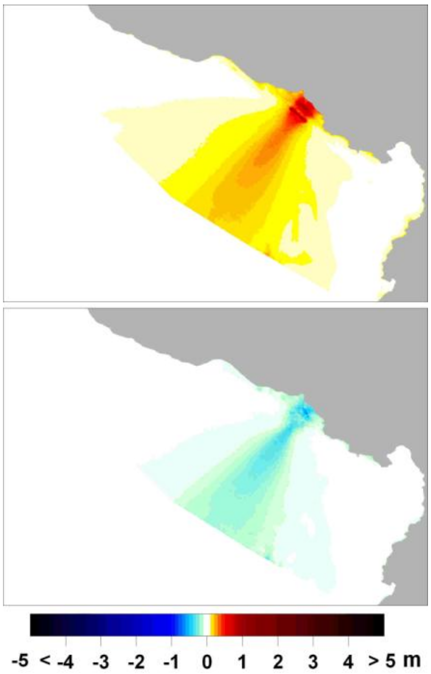

Figure 6.13: Maximum and minimum water elevations for the Scenario 3,Nicaragua 1992.

6.1.4 El Salvador 1902

The 26 February 1902 El Salvador earthquake had a M equal to 7 (Fernandez, et al, [2004]). The earthquake triggered a tsunami that flooded about 120 km of coast. There is no report of run-up values, but there were reports of about 185 victims and some damage (Molina, [1997]).

The parameters of the earthquake are shown in table 6.8, whereas the initial conditions for the UBO-TSUFE MODEL are shown in picture 6.14.

Table 6.8. Parametres of Scenario 4, El Salvador 1902 (M=8.3)

L (km)	324
W (km)	68
Strike (°)	298
Dip (°)	16
Rake (°)	90
Slip (m)	9.6
Position (longitude, latitude)	-90.65, 12.55
Depth (km)	5
Magnitude	8.5

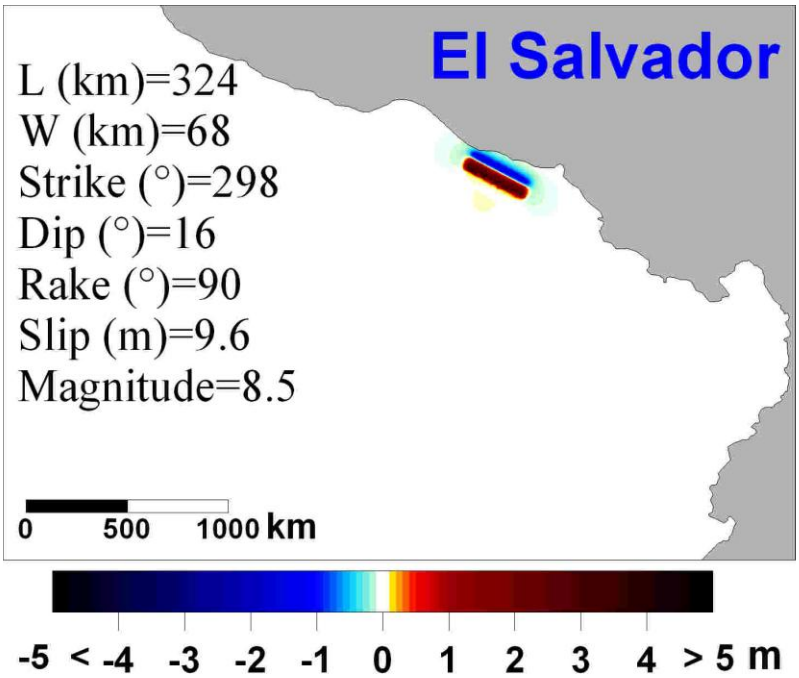

Figure 6.14: Initial Conditions of Scenario 4, El Salvador 1902.

Figure 6.15 shows the propagation field of the scenario of the El Salvador 1902 event. The figure shows that the tsunami waves reached the coast within 30 minutes, that the event propagated to the south-west and that its effects were almost dissipated after 2 and a half hours after the earthquake. Maximum wave height values, according to the model, occurred along the whole coast of the country, whereas the minimum wave height values were concentrated at the portion of coast nearest to the source, see figure 6.16

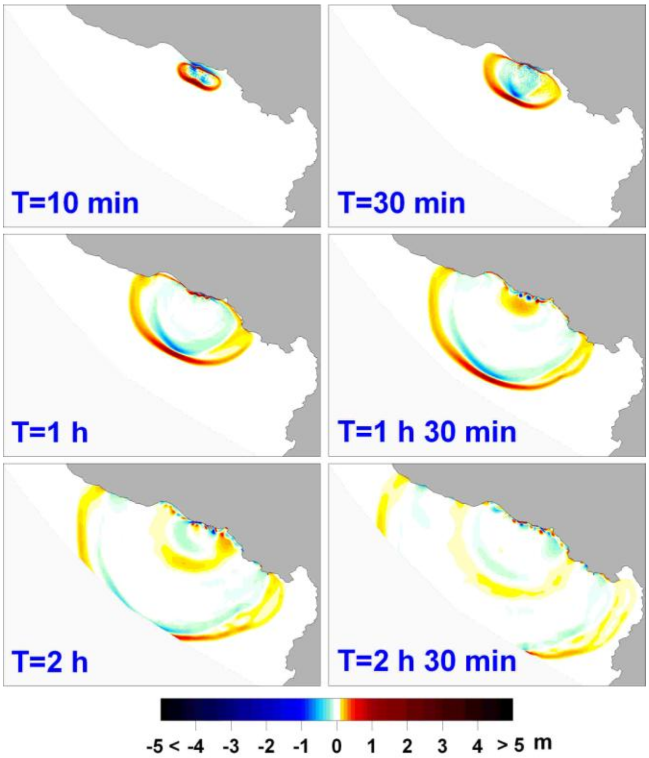

Figure 6.15: Propagation of the Tsunami waves for the Scenario 4, El Salvador 1902.

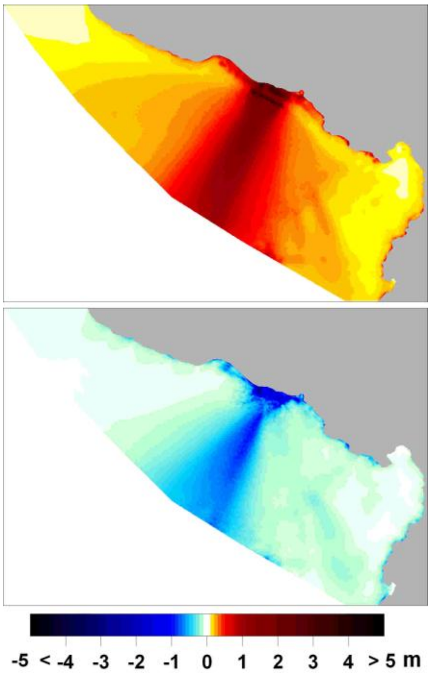

Figure 6.26: Maximum and minimum water elevations for the Scenario 4, El Salvador 1902.

6.1.5 Guatemala 1915

The 7 September 1915 Guatemala-El Salvador event, had a magnitude of Ms equal to 7.7 (Bommer J. And Rodriguez E., 2002) This was a major lower crustal earthquake with epicentre extending from southwestern El Salvador to southeastern Guatemala. Large waves were observed at La

Union, a southern Salvadorian port, but it is not clear if these waves were related to a storm (Molina, [1997]).

The parameters of the earthquake are shown in table 6.9, whereas the initial conditions for the UBO-TSUFE MODEL are shown in picture 6.17.

Table 6.9. Parametres of Scenario 5, Guatemala 1915 (M=7.9)

L (km)	190
W (km)	47
Strike (°)	298
Dip (°)	16
Rake (°)	90
Slip (m)	6.0
Position (longitude, latitude)	-93.4, 13.8
Depth (km)	5
Magnitude	8.1

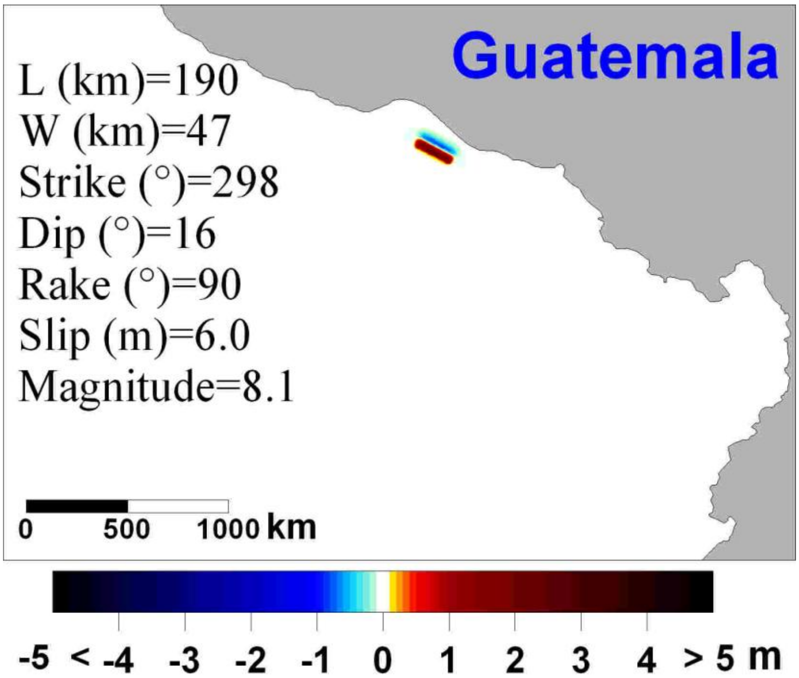

Figure 6.17: Initial Conditions of Scenario 5, Guatemala 1915.

The propagation field for the Scenario Guatemala 1915 is shown in figure 6.18. According to the model, the tsunami propagated locally to the south-west, and reached the coast within 30 minutes and dissipated within 2 and a half hours from the earthquake occurrence. Values of maximum and minimum wave height were concentrated near the source, as shown in figure 6.19.

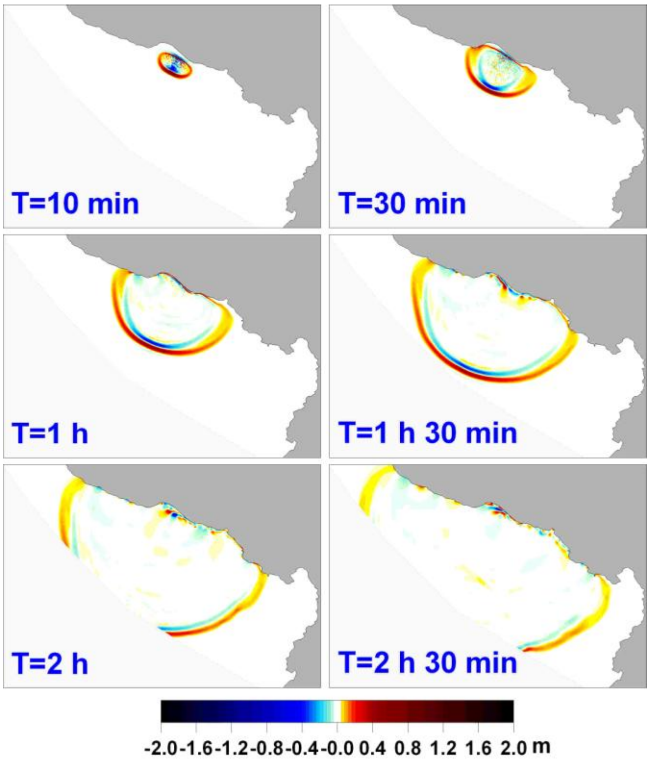

Figure 6.18: Propagation of the Tsunami waves for the Scenario 5, Guatemala 1915.

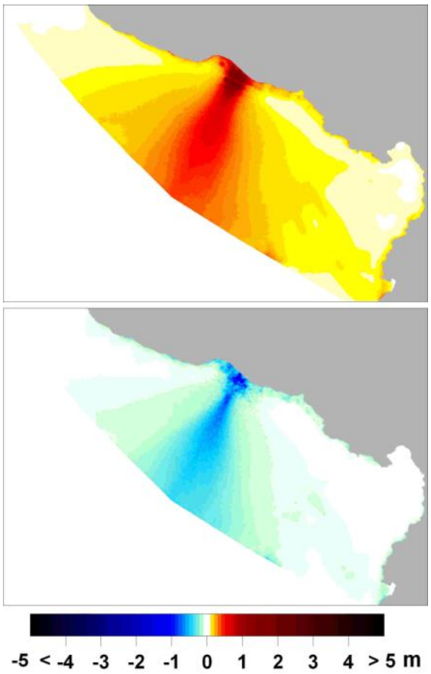

Figure 6.19: Maximum and minimum water elevations for the Scenario 5, Guatemala 1915.

6.1.6 Mexico 1907

The 15 April 1907 Mexican earthquake had a Ms equal to 8, its rupture has been estimated to be between 110 km and 140 km based on intensity data or aftershock location within 2 weeks after the main shock.

The parameters of the earthquake are shown in table 6.10, whereas the initial conditions for the UBO-TSUFE MODEL are shown in picture 6.20.

Table 6.10. Parametres of Scenario 6, Mexico 1907 (M=8.1)

L (km)	248
W (km)	56
Strike (°)	289
Dip (°)	16
Rake (°)	90
Slip (m)	7.6
Position (longitude, latitude)	-99.8, 16.0
Depth (km)	5
Magnitude	8.3

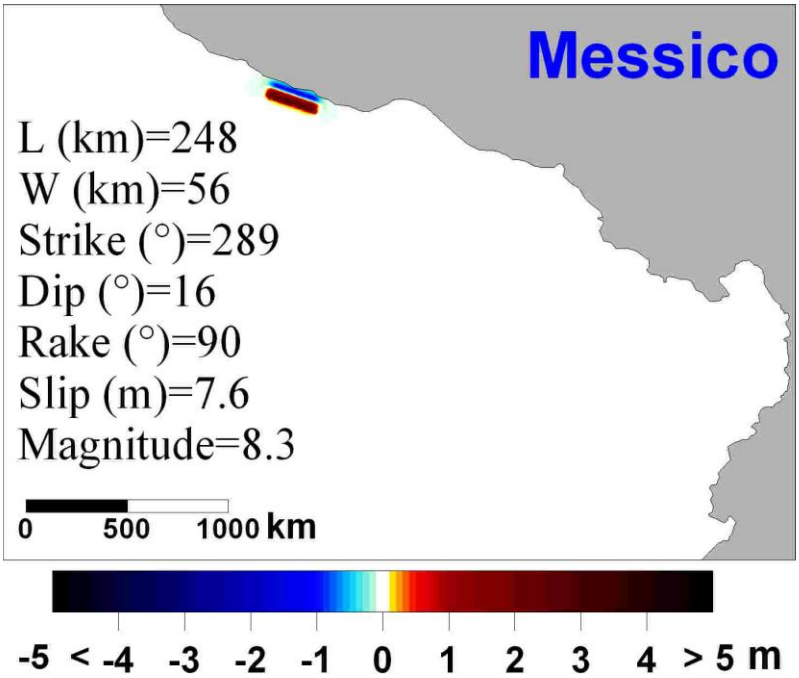

Figure 6.20: Initial Conditions of Scenario 6, Mexico 1907.

According to the UBO-TSUFE MODEL, the tsunami reached the coast after 10 minutes and propagated seaward to the south-west. The tsunami effects dissipated within 2 hours from the earthquake. See figure 6.21 Values of maximum and minimum wave height were concentrated near the source, as shown in figure 6.22.

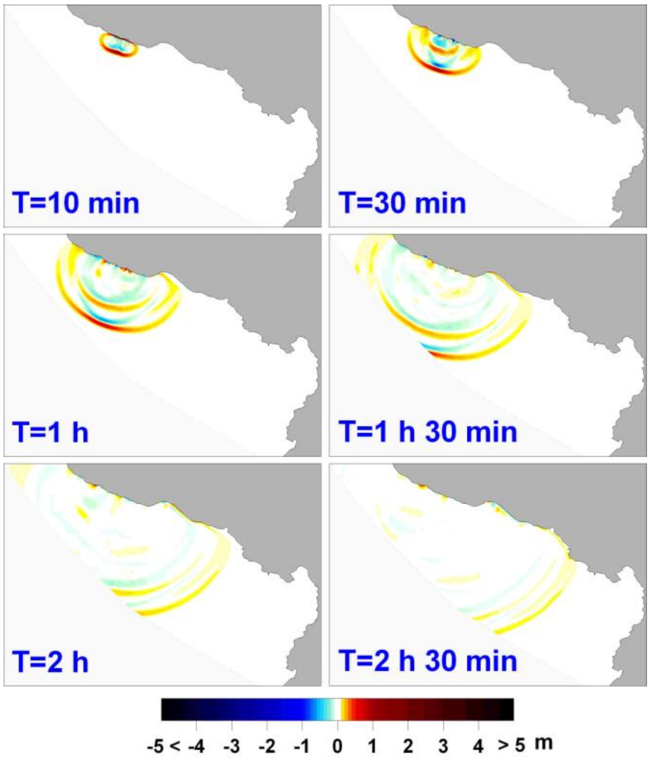

Figure 6.21: Propagation of the Tsunami waves for the Scenario 6, Mexico 1907.

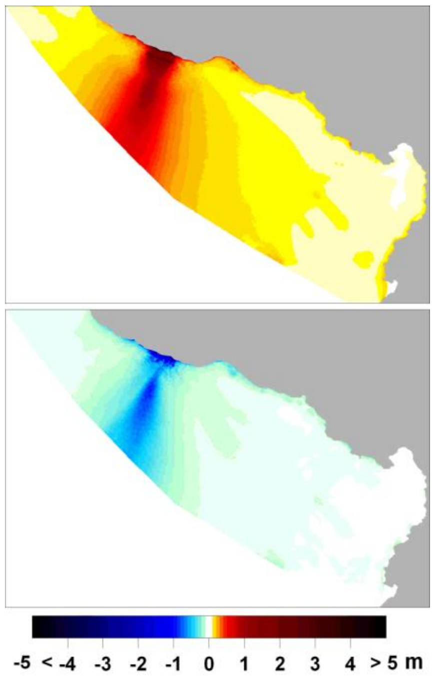

Figure 6.22: Maximum and minimum water elevations for the Scenario 6, Mexico 1907.

The UBO-TSUFE MODEL allows also to plot the extreme water elevation levels along the coast, these values for Scenarios 1, 2 and 4 (Ecuador 1906, Costa Rica 1904 and El Salvador 1902, respectively) are shown in figure 6.23. The figure shows that the Ecuador 1906 earthquake produced a much larger tsunami than the El Salvador 1902 and Costa Rica 1904, and also that the Ecuador event propagated regionally, whereas the other two events propagated only locally. Figure 6.24 shows a zoom along the Salvadorian coast. It can be seen that effects due to the Costa

Rica 1904 tsunami are small, whereas effects due to the Ecuador 1906 and El Salvador 1902 are considerable.

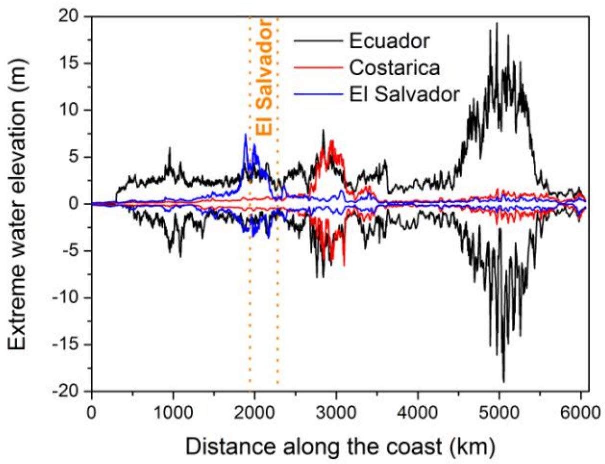

Figure 6.23: Extreme water levels for Scenarios 1, 2 and 4.

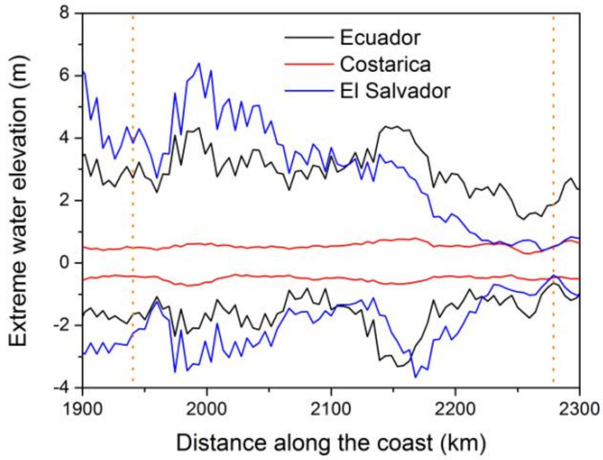

Figure 6.24: Extreme water levels for Scenarios 1, 2 and 4 at the Salvadorian coast.

Extreme water levels of Scenarios 3, 5 and 6 (Nicaragua 1992, Guatemala 1915 and Mexico 1907) are shown in figure 6.25. These events are less strong than the Ecuador 1907. The Mexico 1907 event propagated regionally and the other two events propagated locally, according to the UBO-TSUFE MODEL. The output shows that extreme water levels did not exceed 1 m at the Salvadorian coast, see figure 6.26

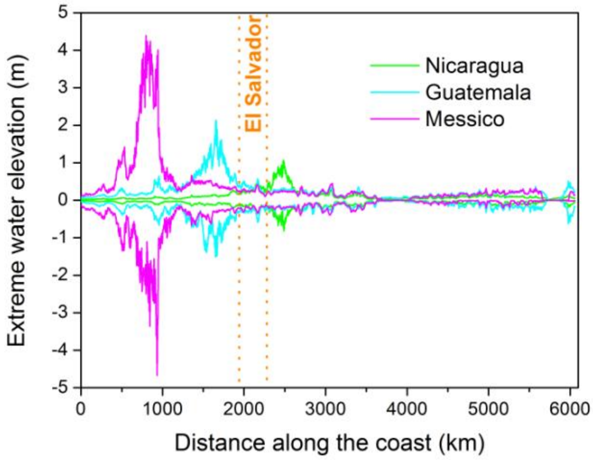

Figure 6.25: Extreme water levels for Scenarios 3, 5 and 6.

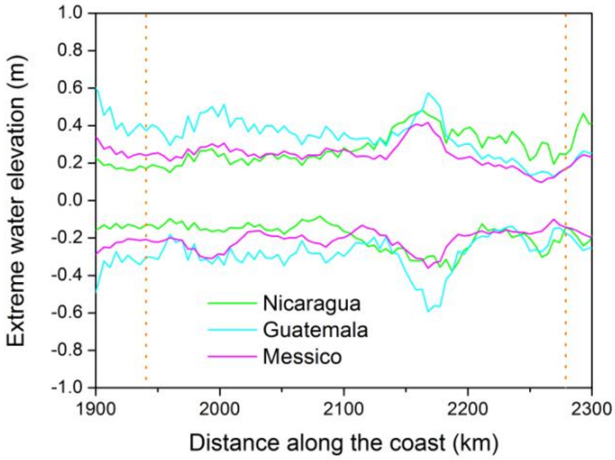

Figure 6.26: Extreme water levels for Scenarios 3, 5 and 6 at the Salvadorian coast.

7. CONCLUSIONS AND RECOMENDATIONS

- Central America is a potential tsunamigenic region that can be hit by local events, triggered by earthquakes at the Middle American Trench; and also by regional events, triggered at the South American subduction zone.
- Research on tsunamis should be carried out in order better understand the phenomena and also to find strategies to deal with the tsunami hazard.
- Research on historical and paleo-tsunamis should be done, in order to increase the number of tsunamis contained in the Central American Tsunami Catalogue.
- Tsunamis triggered by landslides in Central America should be studied in order to establish the hazard posed by landslides as tsunami triggering mechanism.
- Events like El Salvador 1902, Guatemala 1915, Mexico 1907 and Nicaragua 1992 could trigger local tsunamis that would propagate and reach the coast within 10 minutes in some cases and 30 minutes in others. This timing should be considered when establishing a Tsunami Warning System for the region.
- The numerical simulations results have shown that earthquakes along the Middle American Trench triggered local or regional tsunamis, and their effects could dissipate within 2 or 2 and a half hours; whereas the 1906 Ecuador earthquake related to the Ecuador-Colombian Thrench triggered a destructive regional tsunami whose effects did not dissipate 5 and a half hours after the shock.
- South American Sources, as the Ecuador 1906 earthquake, could produce tsunamis with water elevation levels higher than 1m.
- Awareness campaigns, that prepare the population in case they are involved in a tsunami, should be carried out.

REFERENCES

- Albarello D., Camassi R., and Rebez A., 2001, Detection of space and time heterogeneity in the completeness of a seismic catalogue by a statistical approach: an application to the Italian area, Bulletin of the Seismological Society of America Vol. 91, No. 6 pp. 1694-1703.
- Ambraseys N.N. and Adams R., 2000. The seismicity of Central America, Imperial College Press.
- Bommer, J.J., Rodrıguez, C.E., 2002, Earthquake-induced landslides in Central America, Engineering Geology 63 189–220
- Bryant, E., 2001. Tsunami the underrated hazard, Cambridge University Press.
- Fernández, M., Ortiz-Figueroa, M., Mora, R., 2004, Tsunami Hazards in El Salvador, Natural Hazards in El Salvador. Geological Society of America Special Paper 375, pp. 435-444.
- Fernández, M., Rojas, W., 2000, Geología de Costa Rica, Editorial Tecnológica de Costa Rica, pp. 287-301.
- Fisher, R., 1961, Middle America Trench: Topography and Structure, Scripps Institution of Oceanography, University of California, La Jolla, California.
- GEBCO website [http://www.gebco.net/USGS]
- González, F., 1999, Tsunami!, Scientific American, 280, pp. 56-65.
- Hanks T. C., Kanamori H., 1979, A moment-magnitude scale, Journal of Geophysical Research, 84, 2348-2350.
- Harr, M. E.,1996, Reliability-Based Design in Civil Engineering, Dover Publications INC.
- ITIC/UNESCO, [http://www.shoa.cl/oceano/itic/frontpage.html]
- Lander, James F. and Patricia A. Lockridge, 1989a, Tsunamis in Hawaii, Publication 41-2. U.S. Department of Commerce. August 1989.
- Lander, James F. and Patricia A. Lockridge, 1989b, Tsunami on west coast of United States, Publication 41-2. U.S. Department of Commerce. August 1989.
- Lardé y Larín, J., 2000, El Salvador, Inundaciones e Incendios, Erupciones y Terremotos; Dirección de Publicaciones e Impresos, Biblioteca de historia salvadoreña, V 5
- Leeds, J., 1974, Catalogue of Nicaraguan Earthquakes, Bulletin of the Seismological Society of America, Vol. 64, No. 4, pp. 1135 1158.
- Molina, E., 1997, Tsunami Catalogue for Central America 1539-1996, Reduction of Natural Disasters in Central America, Technical Report No. II 1-04 , Institute of Solid Earth Physics, University of Bergen.
- Nishenko S.P and Singh S.K., 1987, The Acapulco-Ometepec, Mexico, Earthquakes of 1907-1982: Evidence for a Variable Recurrence History, Bulletin of the Seismological Society of America, Vol. 77, no. 4, pp. 1359-1367.
- NOAA, [www.ngdc.noaa.gov/seg/hazard/tsuintro.shtml]
- Okada Y., 1992, Internal deformation due to shear and tensile faults in a half-space, Bulletin of the Seismological Society of America, 82, 1018-1040.

- Phipps Morgan, J.; Ranero, C. R.; Vannucchi, P., 2008, Intra-arc extension in Central America: Links between plate motions, tectonics, volcanism, and geochemistry, Earth and Planetary Science Letters, Volume 272, Issue 1-2, p. 365-371.
- Ranero, C.R., Weinrebe, W.,Grevemeyer, I., Morgan, J.P., Vannucchi, P., Von Huene,R. [2004], Tectonic Structure of the Middle America Pacific Margin and Incoming Cocos Plate from Costa Rica to Guatemala, Geophysical Research Abstracts, V 6, 05185, European Geosciences Union.
- Scott M. White, Robert Trenkamp, James N. Kellogg, 2003, Recent crustal deformation and the earthquake cycle along the Ecuador-Colombia subduction zone, Earth and Planetary Science Letters 216, pp. 231-242
- Singh, K., Rodriguez, M. and Espindola, J.M. [1984], A Catalog Of Shallow Earthquakes Of Mexico From 1900 To 1981, Bulletin of the Seismological Society of America, Vol. 74, No. 1, pp. 267-279.
- Synolakis C.E., 1987, The run-up of solitary waves, Journal of Fluid Mechanics 185, 523-545.
- Tinti S., Gavagni I. and Piatanesi A.,1994. A finite-element numerical approach for modelling tsunamis, Annali di Geofisica, 37, 1009-1026.
- Tinti, S., Maramai, A., Graziani, L., [2001], A new version of the European tsunami catalogue: updating and revision. Natural Hazards and Earth System Sciences, 1: 255–262.
- UNESCO, [1991], Tsunami Glossary: A Glossary of Terms and Acronyms used in the Tsunami Literature, Intergovernmental Oceanographic Comission, technical series 37, UNESCO.
- USGS [http://earthquake.usgs.gov/image_glossary/fault.html]
- Wells D. L. & Coppersmith K. J., 1994, New empirical relationships among magnitude, rupture length, rupture width, rupture area, and surface displacement, Bulletin of the Seismological Society of America, 84(4), 974-1002.